The Dissertation Committee for Leena Kumari Prasad Certifies that this is the approved version of the following dissertation:

Electrostatic Powder Deposition as a Dry Powder Process to Prepare Orodispersible Films

Committee:

Robert O. Williams III, Supervisor

James W. McGinity, Co-Supervisor

Hugh D.C. Smyth

Feng Zhang

Justin M. Keen

Electrostatic Powder Deposition as a Dry Powder Process to Prepare Orodispersible Films

by

Leena Kumari Prasad, B. S.

Dissertation

Presented to the Faculty of the Graduate School of

The University of Texas at Austin

in Partial Fulfillment

of the Requirements

for the Degree of

Doctor of Philosophy

The University of Texas at Austin

August 2016

Dedication

To my partner, Justin Scott LaFountaine - you are my constant source of motivation, inspiration, and happiness.

Acknowledgements

I would like to first thank my supervisors, Dr. James W. McGinity and Dr. Robert O. Williams III, for the opportunity to work under their guidance. I am grateful for their generous support and insightful conversations. I would like to thank my supervisors, Dr. James W. McGinity and Dr. Robert O. Williams III, and committee members, Dr. Hugh D.C. Smyth, Dr. Feng Zhang, and Dr. Justin M. Keen, for their time and thoughtful recommendations regarding my research. I am also thankful to the professors who were not on my committee, but who have contributed to my academic growth, including Dr. Salomon Stavchansky, Dr. Alan Watts, Dr. Greg Lyness, Dr. Zhengrong Cui, Dr. Rana Ghosh, and Dr. Benny Freeman. I would also like to thank Stephanie Crouch, Claudia McClelland, and Yolanda Camacho for their support.

I would like to thank my colleagues for their technical, and more importantly, emotional support. Thank you to Abbe Haser (nèe Miller), Hannah O'Mary, and Julien Maincent for providing me with support in bulk and with great frequency. To Dr. Matt Herpin, Solange Valdes, Daniel Moraga-Espinoza, Zach Warnken, Silvia Ferrati, Patricia Martins, Tamara Tarbox, Tania Bahamondez, Jasmim Leal, Siyuan Huang, Soraya Hengsawas, Kristina Jonsson-Schmunk, Chaeho Moon, Sophie Peng, Yajie Zhang, Irnela Bajrovic, Sachin Thakkar, Dan Ellenburger, Dr. Youssef Wahib Najuib, and Dr. Chris Brough, I appreciate the conversations we've had.

I am extremely grateful for my mentors and colleagues from my time at Abbvie and Abbott Laboratories. I am especially appreciative of Dr. Rajeev Gokhale and Dr. Jonathan Miller, who inspired me to invest in my academic and professional growth.

I would like to thank my sister, Dr. Suchitra Prasad, for being a source of inspiration and setting a high bar for me to live up to. Thank you to my mother, Shashi

Prasad, for sending me money for Starbucks every once in a while. I would like to thank my dear friend, Marc Maurice Frankson, for being my source of sanity. I am also thankful for my girls, Naana and Baaba Grant-Acquah, Yasmin Gorleku, Jaclyn Bivins, Ebonie Funnye, and Dr. Natasha Nichols (nèe Lloyd), for always keeping things interesting. Lastly, I would like to thank my partner, Justin Scott LaFountaine. I am grateful to have you by my side every day.

Electrostatic Powder Deposition as a Dry Powder Process to Prepare Orodispersible Films

Leena Kumari Prasad, Ph. D.

The University of Texas at Austin, 2016

Supervisor (s): Robert O. Williams III and James W. McGinity

Orodispersible films (ODFs) are an advantageous dosage form, particularly for pediatric and geriatric populations, due to their ease of administration. ODFs are predominantly manufactured by solvent casting using aqueous or organic solvents. However, this process may be limited by long drying times for aqueous systems, required solvent handling capabilities and residual solvent testing for organic solvents, or due to moisture or solvent sensitive active pharmaceutical ingredients (API). Additionally, solvent casting can produce non-uniform doses due to API aggregation in solution or during drying.

More recently, electrostatic powder coating has been adapted as a dry powder process for coating pharmaceutical dosage forms, such as tablets and pellets. Electrostatic powder coating is advantageous as it eliminates the need for solvents and exhibits greater transfer efficiencies than non-electrostatic dry powder coating. In this work, this technology was further modified to utilize electrostatic powder deposition (ESPD) as a dry powder process to prepare ODFs.

Low molecular weight polyethylene oxide (PEO) was investigated as the film-forming polymer for use with ESPD. The influence of processing parameters, such as charging voltage, curing conditions, and substrate roughness, on PEO deposition

behavior and film formation were investigated. The deposition behavior of PEO was significantly influenced by the environmental humidity during processing due to its impact on the particle resistivity. The PEO films prepared by ESPD exhibited favorable mechanical properties, a low degree of adhesion to the substrate, and rapid disintegration.

Drug-containing films were prepared using physical mixtures and composite particles of acetaminophen (APAP) and PEO. Films prepared using a physical mixture exhibited significantly higher drug content variability. The active films exhibited favorable mechanical properties due to the plasticizing effect of APAP on PEO. Additionally, the films exhibited rapid drug release *in vitro*, with greater than 85% drug release by two minutes.

Films with increasing drug load were prepared using ESPD utilizing both physical mixtures and composite particles of benzocaine (BNZ) and PEO. Films prepared using physical mixtures were superpotent due to preferential deposition of the charged BNZ particles during ESPD. The complex viscosity profile of the composite particles were shown to decrease with increasing drug loading, enabling lower cure temperatures for film formation. Films produced using the composite particles exhibited low adhesion to the substrate and rapid *in vitro* drug release. However, the composite particles of the highest drug load showed greater crystalline BNZ content than the lower drug loads, resulting in a decrease in its mechanical properties, as well as a slightly reduced dissolution rate.

Ultimately, this body of work demonstrated that ESPD could be utilized as a solvent-free process to prepare orodispersible films with favorable mechanical and drug release properties. Additionally, the use of composite particles has been shown to be advantageous to produce particles with favorable electrical properties, ensure film drug content uniformity, and enable reduced cure temperatures.

Table of Contents

List of Tables

List of Figures

Chapter 1: Electrostatic Powder Coating: Principles and Pharmaceutical Applications[1]

1.1 ABSTRACT

A majority of pharmaceutical powders are insulating materials that have a tendency to accumulate charge. This phenomenon has contributed to safety hazards and issues during powder handling and processing. However, increased understanding of this occurrence has led to greater understanding and control of processing and product performance. More recently, the charging of pharmaceutical powders has been employed to adopt electrostatic powder coating as a pharmaceutical process. Electrostatic powder coating is a mature technology used in the finishing industry and much of that knowledge applies to its use in pharmaceutical applications. This review will serve to summarize the principles of electrostatic powder coating and highlight some of the research conducted on its use for the preparation of pharmaceutical dosage forms.

1.2 INTRODUCTION

The concept of electrostatic coating was recognized in the 1930s and 1940s (Pugh, 1932; Ransburg and Green, 1941). Electrostatic coating involves the charging of particles, spraying or atomization of the charged particles, and the deposition of the charged particle onto a grounded substrate. The deposited particles are then cured, usually by heat, to produce a film. The benefits of electrostatic powder coating include the ability to coat without the use of solvents, organic or aqueous. The use of organics solvents is undesirable from an environmental and operating cost standpoint, as handling and collection systems must be in place to avoid exposure to operators and release of volatiles into the environment. The use of aqueous solutions or suspensions usually requires longer processing times and high-energy consumption due the slow drying rate

[1] This work has been published in Prasad, L.K., McGinity, J.W., Williams Iii, R.O., 2016. Electrostatic powder coating: Principles and pharmaceutical applications. International Journal of Pharmaceutics 505, 289-302.

of water (enthalpy of vaporization: 40.65 kJ/mol). Additionally, it was found that transfer efficiencies of the electrostatic powder coating process were greater than seen with conventional liquid spray coating or dry powder fluidized bed processes (Misev and van der Linde, 1998; Wicks et al., 2007). Electrostatic powder coating also yields higher transfer efficiencies when compared to dry powder coating without utilizing electrostatic charge (or nonelectrostatic powder coating); generally 20% higher transfer efficiencies are seen with the application of 40-100kV charging voltage, with these efficiencies increasing with decreasing particle size of coating material (Ratanatriwong and Barringer, 2007; Yousuf and Barringer, 2007). In addition to greater than 80-90% transfer efficiencies reported with electrostatic powder coating, recycling systems have allowed for 100% recovery of coating powder, further decreasing manufacturing waste (O'Neill and Bright, 1978; Sims et al., 2001). Increasingly strict environmental laws limiting volatile organic compound (VOC) emissions from coating solvents led to the rapid adoption of this technology by the metal finishing industry, both in Europe and the USA, in the 1960s and early 1970s (Castle, 2011; Wicks et al., 2007). Continued efforts for more environmentally friendly and energy efficient processes in other industries lead to use of this technology to treat electronics, plastic, and wood products and has even been adapted for use in food processing (Barringer and Sumonsiri, 2015).

More recently, electrostatic powder coating has been investigated for use in pharmaceutical manufacturing (Sauer et al., 2013). As many pharmaceutical powders are classified as insulating materials, they are amenable to charge accumulation with slow charge decay, making them suitable for use with electrostatic powder coating (Watanabe et al., 2007). Dry powder coating in pharmaceutical processing can be advantageous for manufacturing without the need for solvents, particularly when processing moisture sensitive active pharmaceutical ingredients (APIs) or biologics. It also eliminates the need for microbial testing of coating solutions/suspensions and reduces processing times and energy consumption, thus reducing operating costs. Electrostatic powder coating has also been shown to increase dry powder coating efficiencies, reported as higher coating levels obtained during tablet coating

when compared to dry powder coating without applied voltage (Qiao et al., 2010b). The higher transfer efficiencies of electrostatic powder coating make this technique attractive to move towards more environmentally friendly and energy efficient dry powder coating of pharmaceuticals. This review will summarize the principles of electrostatic powder coating and highlight some of the applications of electrostatic powder coating to prepare pharmaceutical dosage forms.

1.3 ELECTROSTATIC POWDER COATING

Coatings utilized by the finishing industry are primarily formulated to prevent corrosion of metals, especially in environments of extreme heat and/or moisture (Wicks et al., 2007). The cost savings due to the increased efficiency and reduced processing times, as well as the environmentally and regulatory friendly operation provided by electrostatic coating is invaluable. Over the last 40-50 years, development efforts continued to address other coating challenges, such as the ability to produce semi-conductive and corrosion resistant coatings for electronics (Radhakrishnan et al., 2009), improve temperature resistance (Kiefer, 2004), further increase efficiencies (Weiss, 1997), and enhance the appearance of the coating layer for aesthetic purposes (Meng, 2009). The technique was further advanced for the treatment of other substrates, such as wood, plastic and even paper (Barletta and Gisario, 2009; Cazaux, 2007; Mazumder et al., 2006). Due to the broad application of this technology, there is a significant amount of knowledge surrounding the utilization of electrostatic powder coating. This section will serve to summarize the principles of electrostatic powder coating, specifically the mechanisms of electrostatic charging, film formation, and adhesion of the film to the substrate.

1.3.1 Principles of Electrostatics

Particles can be charged by two mechanisms: triboelectric or corona charging. Triboelectric charging describes charge accumulation due to friction. “Tribo-“ is derived from

Greek meaning “to rub”. This mechanism of charging results from the contact or rubbing of two dissimilar surfaces, the transfer of electrons from one surface to the other followed by the separation of the two surfaces, resulting in oppositely charged surfaces or charge separation. Triboelectrification is the primary mechanism of electrostatic charge generation during powder handling, a phenomenon that is heavily studied in pharmaceutical manufacturing processes (DesRosiers Lachiver et al., 2006; Pu et al., 2009; Rowley, 2001). Triboelectric guns are designed to facilitate maximum particle to gun wall interactions or contacts and therefore increase the charge accumulation of the fluidized particles, as shown in Figure 1.1. The gun wall is usually composed of PTFE, which has a tendency to become negatively charged, leading to particles that are positively charged; however, this can be modified if negatively charged particles are desired (Bailey, 1998; Peart, 2001).

Tribocharging is highly complex and can be difficult to predict. Particle charge accumulation from triboelectric charging was initially approximated using a work function theory based on the contact charging between metals and iterations of the model were developed to better predict the charging of the insulating materials used in electrostatic coating processes (Bailey, 1998; Matsusaka et al., 2010). More recently, Matsusaka et al. provided a comprehensive review on the concepts and theories to better model the charge transfer during triboelectric charging; therefore, these theories will not be discussed further in this review (Matsusaka et al., 2010). Tribocharging is strongly influenced by numerous factors including environmental conditions (relative humidity, temperature), number of collisions and duration of contact, and particle properties such as electrical resistivity (greater than 10^{12} Ω m generally required) and surface roughness.

Corona charging describes the charging of particles by passing them through an electric field in the presence of free ions, also referred to as a corona discharge. A corona discharge is a process by which current flows, usually through a gas, from a point of high potential to a neutral or grounded substrate, generating free ions near the region of high potential in the process. A corona source, such as the corona gun shown in Figure 1.2, consists of an electrode, usually a

highly curved rod or a small diameter wire to create the greatest potential gradient, and a high applied voltage (usually 60-100kV) to strip electrons from the surrounding gas molecules to produce free ions. The area between the emitting electrode of high potential and the grounded substrate, usually a plate or cylinder, produces a strong electric field to facilitate the discharge phenomenon (Bailey, 1998; Giacometti and Oliveira Jr, 1992). Particles can be charged by two mechanisms in the presence of free ions: 1) field charging and 2) diffusion charging. Introducing a particle to the electric field alters the field, resulting in free ions being directed to and adsorbed by the particle as shown in the inset of Figure 1.2; this is referred to as field charging. Diffusion charging is induced by collisions between ions and particles due to the random motion of the ions in the gas. Diffusion charging tends to occur in the absence of an electric field and usually with very small particle sizes (less than 0.2 μm) (Lee, 2006; Meng, 2009). Due to the strong electric field produced by the corona discharge and the recommended particle size range (1-100 μm) for use with corona guns, field charging is the predominant charging mechanism for electrostatic coating processes using corona charging.

With field charging, Pauthenier's equation (equation 1) of particle charge accumulation through a corona field can be used to derive the maximum charge accumulation or charge limit (equation 2) for a given particle (Bailey, 1998). However, these equations assume the particle to be conductive and that the imparted charge can be distributed uniformly along its surface. Thus these equations may not be completely accurate when applied to the corona charging of insulating particles, particularly with respect to the maximum charge limit (Adamiak, 2003; Masuda and Washizu, 1979).

$$q(t) = 4\pi r^2 \varepsilon_0 E \left(\frac{t}{t+\tau}\right)\left[1 + 2\left(\frac{\varepsilon_r - 1}{\varepsilon_r + 1}\right)\right] \tag{1.1}$$

$$q_{max} = 12\pi r^2 \varepsilon_0 E \tag{1.2}$$

where r is the particle radius, ε_0 is the absolute permittivity, ε_r is the relative permittivity of the powder, E is the field strength, and τ is the charging time constant, which is a function of the absolute permittivity, number and mobility of ions, and the electronic charge.

Corona charging can be utilized with both insulating and conductive materials making it a more flexible charging process. Additionally, particle trajectories from corona charging, albeit a combination of electrostatic and aerodynamic forces, can be better modeled due to the presence of the electric field. Corona charging is considered to be a more robust charging process than tribocharging; however, the presence of excess free ions, with only about 10% of the ions carried by the charged particles (Bailey, 1998; Mazumder et al., 2006), can lead to a higher incidence of back ionization. Back ionization, also referred to as back corona, is a phenomenon where deposition of incoming charged particles is prevented due to a high repulsive charge from the already deposited particles or when ions of opposite polarity are formed that then neutralize the incoming particles as shown in Figure 1.3. Oppositely charged ions can also neutralize or oppositely charge particles already adhered to the substrate leading to the ejection of particles from the deposited powder surface, which can result in surface defects (Hoburg, 1982). Back corona occurs when the apparent field strength in the deposited powder layer is greater than its breakdown field strength, as described in equation 3. Thus, powders of high resistivity, usually greater than 10^{13} Ω m, are associated with a greater occurrence of back ionization (Masuda and Mizuno, 1977). McLean summarized three requirements for the formation of back ionization as follows: 1) a porous layer so that gaseous breakdown can take place, 2) a high electric field across the layer, and 3) a supply of incoming ions (McLean, 1988). All of these requirements are established during corona charging, making this process susceptible to back ionization.

$$E_d = \rho_d J > E_b \tag{1.3}$$

where E_d is the electrical field of the across the deposited powder layer, ϱ_d is the resistivity of the deposited powder, J is the current density, and E_b is the electrical breakdown field of the powder layer.

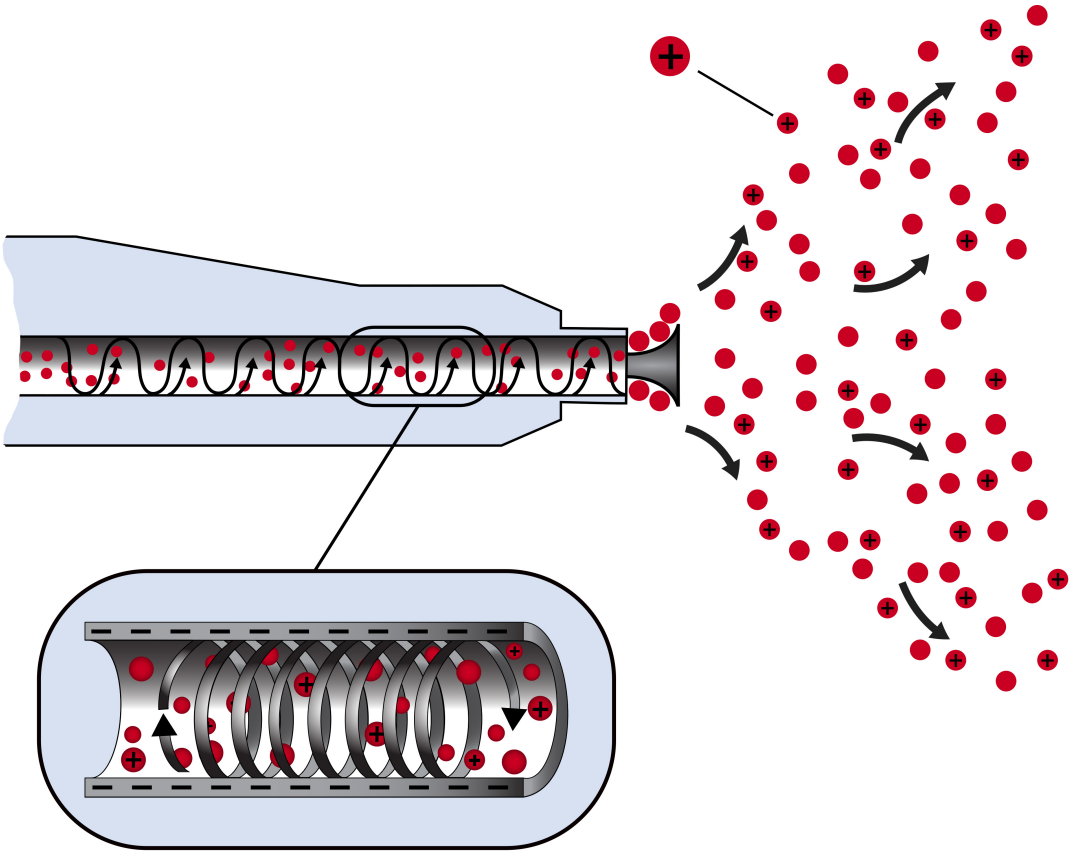

Figure 1.1 Schematic of triboelectric gun designed to facilitate maximum particle to gun wall collisions (shown in inset).

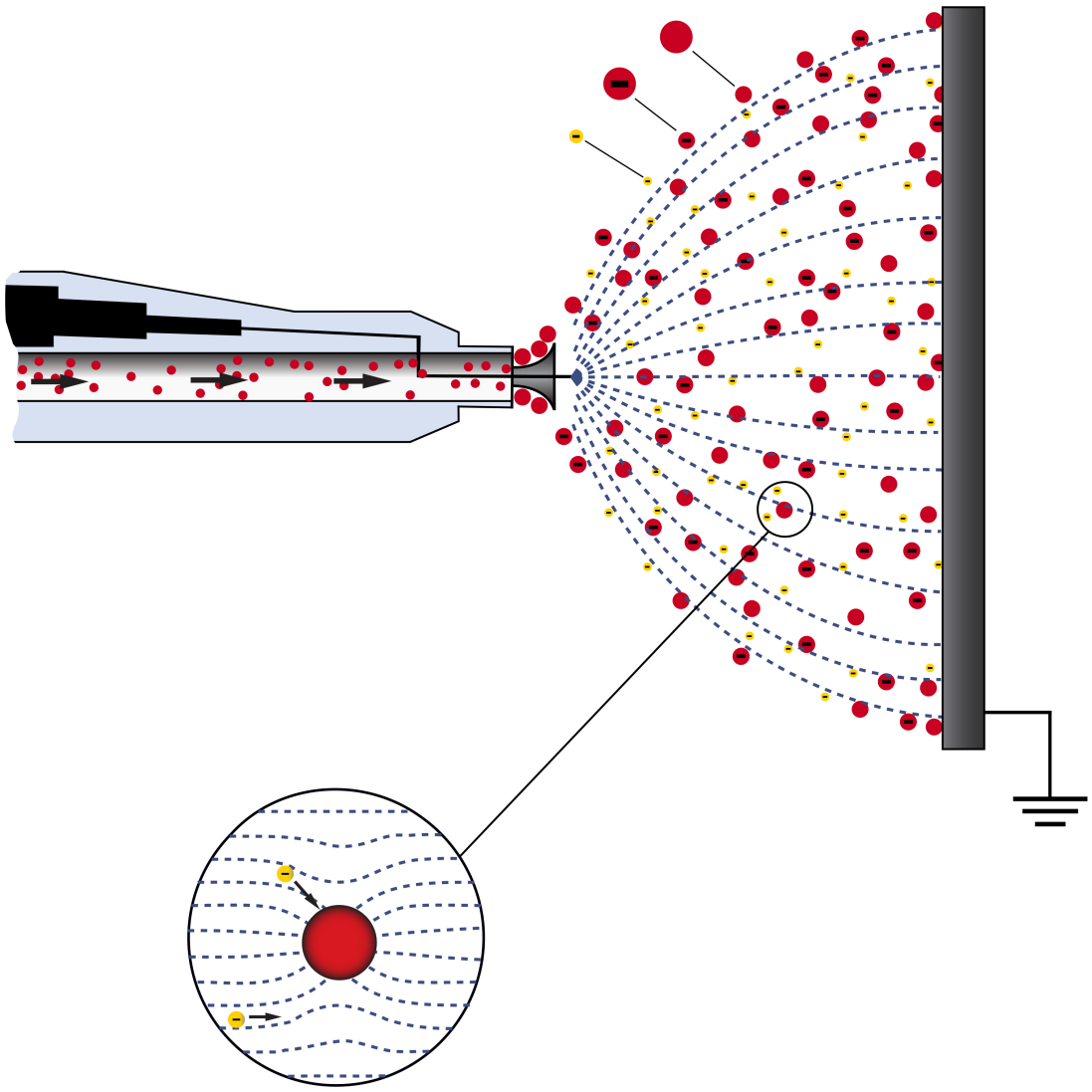

Figure 1.2 Schematic of corona gun, which applies high voltage to an electrode to produce corona discharge and electric field; particles undergo field charging (shown in inset) due to distorted electrical field and free ion adsorption.

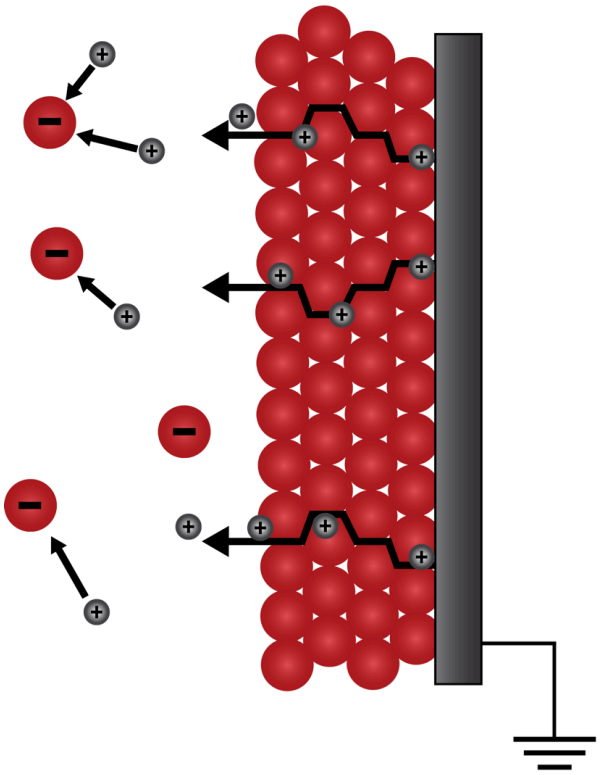

Figure 1.3 Back ionization caused by the formation oppositely charged ions.

The electrical properties of the coating powder, both intrinsic and during charging, allow for the characterization and optimization of the electrostatic coating process. The resistivity of a powder is generally reported as bulk or volume resistivity (Ω m) and can be measured using a resistivity meter. Per ASTM D-257, volume resistivity of insulating materials is measured by applying a voltage (usually 100-500V) to a sample for a period of time (usually 60s) and measuring the resulting current; volume resistivity can be calculated by simply applying Ohm's Law as shown in equation 1.4. Due to the low resultant current (nA to μA) from insulating materials, the electrometers used for these measurements must be equipped to apply a relatively high voltage and read low amperage. Additionally, standard resistivity meters require the use of a film or compacted sample; however, powder resistivity meters have been developed are now commercially available to measure properties of powder samples.

$$\rho_v = (A\,V)/(t\,I) \tag{1.4}$$

where A is the effective area of the guarded electrode, V is the applied voltage, t is the sample thickness or electrode spacing, and I is the measured current.

The charge accumulation on a particle is typically described by the charge to mass ratio (q/m). This measurement can be carried out using a simple Faraday cup, whereby a charged powder of known mass is placed in a grounded conductive metal cup shielded by an insulating wall. The cup is connected to an electrometer and the resulting current is measured and used to calculate the total charge on the sample mass. To enable measurements of in-flight particles, such as those being charged using a corona gun, a modified Faraday system using a vacuum has been utilized to collect samples for measurement (Meng et al., 2009), as shown in Figure 1.4. While the Faraday measurement can determine charge to mass ratio of a collected sample, the Electrical Single Particle Aerodynamic Relaxation Time or ESPART analyzer can measure the charge and aerodynamic particle size simultaneously and in real-time (Mazumder et al., 1991; Stark et al., 2008). For high resistivity materials, charge accumulation is a surface effect and thus can be significantly influenced by the particle size of the charged powder; thus, the simultaneous measurement can provide valuable information for a given powder formulation and/or charging process.

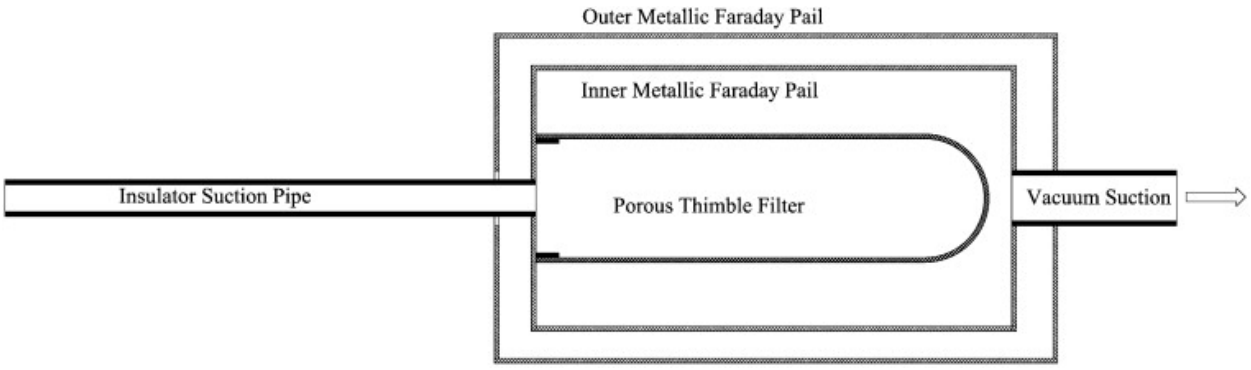

Figure 1.4 Modified Faraday system utilizing vacuum suction to collect samples in-flight (reprinted with permission from (Meng et al., 2009))

Other electrical parameters that can affect or be used to characterize the performance of the electrostatic coating operation include the gun potential (kV) and current (μA), which are typically tunable by the corona gun controller, as well as the electrical field (V/m) and space permittivity (F/m) (Hughes, 1984).

Factors that influence particle charging include particle electrical resistivity, size distribution and shape and flow properties (Bailey, 1998; Mazumder et al., 1997). The majority of powders used with electrostatic powder coating have resistivity values of greater than 10^{10} Ω m. Lower resistivity values can lead to quicker charge dissipation and loss of electrostatic forces holding particles to the substrate. Higher resistivities allow for charge accumulation with slow charge dissipation, which facilitates adhesion to the substrate through the curing process. However, very high resistivity can lead to a high charge accumulation and the induction of back ionization; this often results in a self-limiting layer thickness (Hughes, 1989; Mazumder et al., 2006). Particle size also influences charge accumulation. Smaller particles sizes generally acquire higher charge-to-mass ratios, which can induce back ionization and result in relatively thin powder layer deposition; however, smaller particles also produce more consistent and uniform deposition, as well as smoother films upon curing. Larger (also referred to as coarse) particles sizes, usually defined as having a d_{50} greater than 30-40 μm, can produce final film with a rough surface. This appearance can be attributed to a slower or incomplete coalescence and leveling of the film during curing (discussed in the next section), but can also be due to reduced deposition uniformity as larger particles have a tendency to lose charge faster than smaller particles (Shah et al., 2006a). Particle size distribution can also affect deposition behavior (Barmuta and Cywiński, 2001). Meng et al. showed that using coarse particles electroseparation occurred such that the smaller particles preferentially deposited onto the substrate (Meng et al., 2009). Alternatively, in ultrafine particle size distributions, defined as having d_{90} less than 30-40 μm, the finer particles are lost to overspray with preferential deposition of the large particles in the distribution.

As mentioned earlier, the deposition behavior of charged particles is a function of electrostatic and aerodynamic forces. Finer particles sizes tend to have poor fluidization behavior, as they tend to be more cohesive in nature. Low airflow rates may be insufficient to break up agglomerates and/or provide good fluidization, but conversely, high airflow rates can lead to overspray of fine particles, resulting in poor transfer efficiencies (Mazumder et al., 1997). Coarse particles are more likely to follow the electrostatic field towards the substrate as opposed to the airflow; however, if the distance between the gun and the substrate is too far, they can be affected by drag and gravitational forces (Shah et al., 2006b). Overall, electrostatic charging is a complex, but well studied phenomenon that is widely utilized due to the high transfer efficiencies achieved when compared with non-electrostatic powder coating (Shah et al., 2006b; Yousuf and Barringer, 2007).

1.3.2 Principles of Film Formation

In conventional solvent-based coating processes, the solvent and evaporation of solvent, respectively act to as a temporary plasticizer and to provide capillary forces to aid in film formation. In the absence of solvent, film formation is primarily driven by the coalescence of discrete powder particles and leveling of the coalesced particles to produce smooth and even film layer, as shown in Figure 1.5. The deposited dry powder is subject to heat to promote particle deformation and fusion with surrounding particles. As more and more particles coalesce, there is a reduction of void spaces leading to an overall reduction in free volume in the film layer; this is referred to as the leveling process. The leveling or spreading process will determine the final thickness of the film, as well as the smoothness of the surface of the film layer. When the heat is removed, the coalesced and leveled film layer will harden to produce the final, dry film. Polymers that are cured by application of heat and coalescence of particles as described above are classified as thermoplastic polymers (Sauer et al., 2013; Wicks et al., 2007). There are many other polymers types that are cured by different modes in addition to or in place of heat. For

example, thermosetting polymers are predominantly used in the finishing industry. These polymer particles coalesce, but additionally undergo chemical crosslinking to form the final film. Many of these thermosetting polymers allow for shorter processing times, making them desirable for high throughput industries, including automotive and electronics. Additionally, there are polymers that can form films through free radical or UV polymerization (Wicks et al., 2007). However, as many of these chemically reacting polymers are not applicable for pharmaceutical applications, they will not be discussed further in this review.

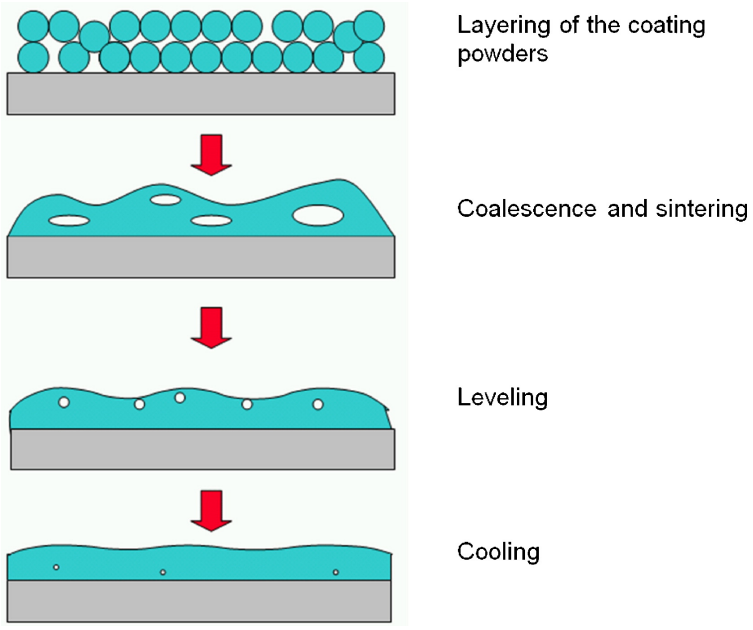

Figure 1.5 Mechanism of film formation of dry powder coating particles (reprinted with permission from (Sauer et al., 2013)).

For thermoplastic polymers, particle deformation occurs at temperatures at or above the melting point of a polymer, where the material transitions from solid to liquid, or above the glass transition of a polymer, where there is increased molecular mobility of the solid. The majority of polymers used for coating processes are synthetic or semi-synthetic and are relatively large

molecular structures, which are more likely to be semi-crystalline or amorphous in nature (Wicks et al., 2007). Thus, the glass transition temperature, T_g, is often considered when determining conditions for the curing process. At temperatures above T_g, the viscosity of the polymer decreases allowing for particle deformation. High molecular weight polymers tend to be highly viscous and may require temperatures markedly higher than the T_g to facilitate particle deformation and coalescence. Alternatively, a plasticizer may be incorporated to decrease the T_g to enable lower curing temperatures. In addition to adequate viscosity for particle deformation, increased surface energy is needed to facilitate particle coalescence and leveling (Andrei et al., 2000; Mazur et al., 1997). As with the use of plasticizers to promote melt flow, additives can be incorporated into the coating material to reduce surface tension, if needed.

The polymer viscosity, surface tension, and particle size has been shown to influence the time needed for film coalescence, as shown in equation 1.5 (Sauer et al., 2013). The viscosity of the polymer is a factor of the polymer molecular weight and the temperature used for curing of the film; temperature can also influence the surface energy of the polymer.

$$t = k\mu r/\gamma \tag{1.5}$$

where k is a constant, μ is the polymer viscosity, r is the radius of the powder particle, and γ is the surface tension.

1.3.2 Principles of Adhesion

Much of finishing industry involves the electrostatic powder coating for the treatment of metal surfaces; however, this has expanded to include surface treatments of substrates such as wood and plastic. To limit the scope and length of this discussion, this section will focus on the mechanisms of polymer adhesion to metal substrates. A later section will discuss mechanisms of adhesion of coating to pharmaceutically relevant substrates. Adhesion describes the tendency or degree to which two dissimilar surfaces are held together. For this review, adhesion pertains to

the permanent or semi-permanent adhesion of the coating layer to the substrate, for example post-curing. Mechanisms of polymer to metal adhesion include mechanical interlocking, chemical bonding, boundary layer forces, and electrostatic interactions (Ramarathnam et al., 1992; Wicks et al., 2007). Mechanical interlocking occurs due to the penetration of coating into macroscopic pores on the metal surface; upon hardening, this interlocking along the surface of the metal increases the adhesive strength of the coating layer. To facilitate mechanical interlocking, most metals must undergo abrasive blasting to create the rough surface needed for this type of adhesion.

Chemical pretreatment of metals are conducted to mildly etch and precipitate functional groups onto the surface of the metal (Ramarathnam et al., 1992; Wicks et al., 2007). These functional groups are then available to form chemical bonds with the coating material to strengthen adhesion. These chemical treatments can be done using zinc phosphates, chromium, silanes or other chemicals (Gray and Luan, 2002; Puig et al., 2014). Although, chemical pretreatments have been utilized since the early years of metal coating, development efforts continue to identify pretreatments that are environmentally compliant and less hazardous to operators (Puig et al., 2014; Subramanian and van Ooij, 1999). The latter two mechanisms of adhesion, boundary layer and electrostatic interactions, are relatively weak and though usually present, are not the primary mechanisms for long-term or permanent adhesion.

Measuring adhesive strength can be very difficult and there are various methods of measurement utilized across the industry. Early direct measurement techniques to evaluate adhesive strength included peel tests and tape peel tests. The peel test is simply measuring the force, quantitatively or qualitatively, to peel the coating from the substrate. This test can be done at varying angles and speeds; however, the film must be strong enough to remain intact with the applied force in order to make a robust measurement. This test method has been more recently developed for use in conjunction with a tensile test apparatus (Kim et al., 2002). The tape peel test, sometimes referred to as the “scotch tape” test, is a variant of the peel test that utilizes an adhesive tape applied to the coating layer. This applied tape is then peeled off and observations

of the test surface are made. This test has numerous factors than can affect the results, including the properties of the adhesive tape and its ability to reproducibly adhere to the coating layer, making this test more qualitative in nature (Awaja et al., 2009; Lacombe, 2005). A pull test was developed to quantitatively measure adhesive strength, whereby a test stud is attached to the coating layer. The test stud is then pulled off under very controlled conditions using a tensile test instrument and the force to failure is measured.

Many surface characterization techniques have been developed to measure adhesive strength, particularly with thin film coatings. Awaja et al. summarized many of these methods in a relatively recent review on polymer adhesion (Awaja et al., 2009). The methods summarized include time-of-flight secondary ion mass spectrometry (ToF-SIMS), X-ray photoelectron spectroscopy (XPS), atomic force microscopy (AFM), secondary electron microscopy (SEM), attenuated total reflectance infrared spectroscopy (ATR-IR) and other microscopy techniques. A comprehensive list of methods used to test adhesive strength of coatings can also be found in the Paint and Coating Testing Manual: 15 edition (Koleske, 2012) and Adhesion Measurements Methods: Theory and Practice (Lacombe, 2005).

1.4 Application of Electrostatic Powder Coating in Pharmaceuticals

A majority of pharmaceutical powders have high resistivity values (greater than 10^8 Ω m) making them susceptible to charge accumulation with slow charge decay (Blythe, 1984; Grosvenor and Staniforth, 1996). The industrial implications of this include combustion potential, poor flow properties and powder adhesion to equipment walls (Bailey, 1984; Wong et al., 2015). Powder ignition requires multiple steps including charge generation, charge accumulation, electrostatic discharge, and an ignition source (Glor, 1985; Glor, 2003). Knowing these steps, as well as the tendency of a given powder to accumulate charge, the operations that said powder will undergo, and the minimum ignition energy (MIE) of the powder allow one to take necessary precautions to prevent dust explosions during powder processing operations

(Gibson, 1997; Paasi et al., 2001). Issues of blend and dosage form homogeneity can be an issue if powder-equipment surface adhesion and/or poor flow properties result of charge accumulation. Pu et al. studied the effects of charging on homogeneity of binary mixtures using blending procedures with and without charge control (Pu et al., 2009). Interestingly, neutralizing the blend showed a decrease in blend homogeneity compared to the uncontrolled blend, indicating charge accumulation in powder can benefit the blending process. Blending with corona charging showed that when the API, caffeine, was negatively charged with lactose or microcrystalline cellulose positively charged, blend homogeneity improved when compared to the uncharged control, showing that attractive forces between API and excipient can be advantageous to produce homogeneous mixtures. Hao et al. measured the charge of an uncontrolled (no applied charged) blending process and showed that there was a cyclical pattern of charge distribution, with periods of less disparity in measured charge correlating with periods of greater blend homogeneity, demonstrating the measurement of charge can be used as a tool for process development or even as an in-process control (Hao et al., 2013).

Powders with large surface area to volume ratios have a tendency for high charge accumulation (Murtomaa et al., 2004; Rowley, 2001); therefore, micronized or micron-sized powders are especially prone to the effects of electrostatic charging. Considering the particle size ranges used for pulmonary delivery, less than 10 μm, the formulation and performance of aerosols and dry powder inhalers can be influenced by electrostatic charge accumulation. Chang et al. showed that increased charge accumulation of micron sized particles led to increased deposition efficiencies (Chang et al., 2012), consistent with what was seen from a study by Xi et al. (Xi et al., 2014). However, Xi additionally showed that this charge accumulation had less of an effect on ultrafine particles (defined as 40nm of smaller), which exhibited a less discernible effect on deposition efficiencies. Many studies and reviews address the implications of electrostatics for pulmonary delivery systems (Byron et al., 1997; Carter et al., 1998; Glover and Chan, 2004; Karner and Urbanetz, 2011; Wong et al., 2013; Yurteri et al., 2002), as well as the factors that can influence charging of pharmaceutical powders, such as crystalline nature (Wong

et al., 2014), relative humidity (Chow et al., 2008), and kinetics with respect to tribocharging (Chow et al., 2008; Watanabe et al., 2007). The remainder of this section will highlight the application of charge to pharmaceutical powders for the manufacture of dosage forms and drug delivery devices.

1.4.1 Solid Dosage Form Coating

Pharmaceutical coatings are now predominantly aqueous based; however, the solids loading can still be relatively low and require long processing and drying times which equate to higher energy inputs and cost. Thus, the drivers to move towards dry powder coating in the pharmaceutical industry are similar to those in the finishing industry, namely to move towards more energy efficient processing, but also to enable processing of moisture sensitive drugs. Solvent-free coating processes developed to address these aims include compression coating, hot-melt coating, dry powder coating and electrostatic dry powder coating (Bose and Bogner, 2007; Luo et al., 2008; Sauer et al., 2013); however, the latter two techniques have proved to be the most promising. Dry powder coating involves the feeding of dry powder either in parallel or subsequent to the application of a plasticizer to the tablet cores. The plasticizer, usually a liquid, is the primary facilitator to enable the dry powder coating material to adhere to the tablet surface. Electrostatic coating utilizes electrostatic forces either in place of or in addition to a liquid plasticizer to enable adhesion to the tablet until curing, allowing for more efficient utilization of the coating material. Phoqus Pharmaceuticals, a spin-off company of Colorcon and now part of Diurnal, was the first to utilize electrostatic dry powder coating on a larger scale, including for the preparation of clinical test supplies of Chronocort, a hydrocortisone tablet for the treatment of adrenal insufficiency (Mallappa et al., 2014; Whiteman et al., 2006). Their equipment was custom designed to allow the coating of one side/face of the tablet at a time (Whiteman et al., 2006).

More recently, researchers at the University of Western Ontario have modified a conventional pan coater to incorporate a corona gun and to electrically ground the coating pan to use for electrostatic powder coating, as shown in Figure 1.6 (Qiao et al., 2010b; Zhu et al., 2007). Electrostatic powder deposition onto a tablet as the substrate can be especially challenging due to the high resistivity of the pharmaceutical excipients used in the tablet core. Initial work to develop electrostatic coating processes for tablets incorporated treatment of the tablet core to increase conductivity, usually by adsorbed moisture (Grosvenor, 1991; Grosvenor and Staniforth, 1996; Staniforth and Grosvenor, 1992). Qiao et al. found that the resistivity of the tablet core could be significantly reduced with the application of a small amount liquid plasticizer. In one study a tablet core resistivity of 10^{13} Ω m was reduced to less than 10^{9} Ω m after an application of a small amount of plasticizer (~ 0.4% coating level); higher levels of plasticizer did not further decrease the resistivity of the tablet (Qiao et al., 2010b). The application of the liquid plasticizer for the electrostatic coating process is multifunctional as it increases the conductivity of the tablet core to facilitate electrostatic deposition of the charged coating powder, provides liquid bridges to further ensure good adhesion, as well as to reduces the T_g of the coating polymer to aid in the film formation process. Qiao et al. showed the applicability of their technology to prepare tablets with immediate (Qiao et al., 2010b), enteric (Qiao et al., 2013), and sustained release (Qiao et al., 2010a) coatings, and more recently to coat pellets (Yang et al., 2015).

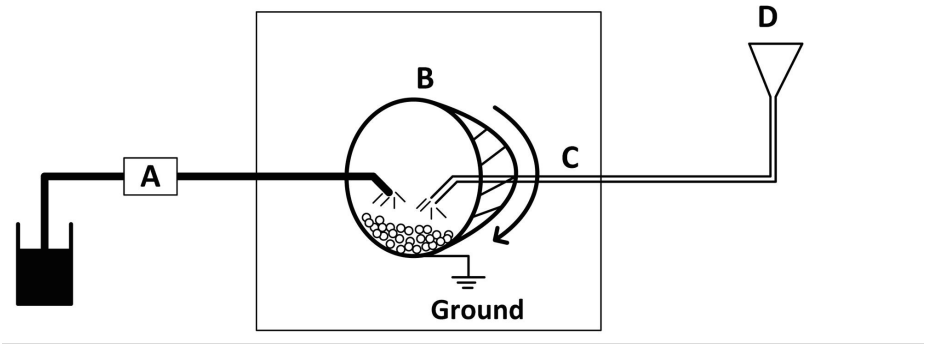

Figure 1.6 Schematic of electrostatic powder coating system designed by researchers at the University of Western Ontario comprised of (A) liquid plasticizer spray system, (B) coating pan, (C) electrostatic spray gun, and (D) powder feeder. (Reprinted with permission from (Yang et al., 2015))

Qiao et al. conducted control experiments without the application of charge on the coating materials which exhibited decreased coating efficiencies; one study showed a 33% coating efficiency from dry powder coating alone compared to 70-72% efficiency when utilizing 60kV electrostatic charging (Qiao et al., 2013). In another study, Qiao et al. showed that the coating thickness was limited when using dry powder coating alone, with only 1.6% coating level obtained compared to 3% with electrostatic coating, showing the ability of the electrostatic forces to improve adhesion to the tablet core and enable powder layering (Qiao et al., 2010a). The influence of charging voltage showed that increased coating levels were achieved when increasing voltage from 0 to 60 kV, showing the ability to control coating thickness by applied voltage. However, a decrease in coating level was seen when particles were charged at 90 kV (Qiao et al., 2010b). This was attributed to the development of back ionization with higher voltage application.

As described earlier, the mechanism of film formation in dry powder coating is by the coalescence and leveling of discrete powder particles, promoted by the application of heat. Thermoplastic polymers or composite/pre-plasticized coating compositions with low Tg, preferably 40-60°C, are favored such that curing for film formation can be conducted at relatively low temperatures, as certain APIs may be thermally labile (Grosvenor, 1991; Herling

and Bill, 2000). The influence of plasticizers on reducing T_g to enhance film formation of dry powder has been investigated specifically for use in dry powder coating of tablets (Sauer and McGinity, 2009; Sauer et al., 2007; Smikalla et al., 2011). When applying a plasticizer directly on the tablet core, the spreading behavior of the plasticizer is critical to ensure coverage of the tablet surface in order to increase coating efficiency, and in the case of electrostatic coating to reduce tablet resistivity prior to application of the charged particles. During film formation, the degree of plasticization or reduction in T_g plays a larger role in the ability of the particles to coalesce. The properties of polymer-plasticizer systems that have been characterized for dry powder coating are summarized in Table 1.1. Lastly, due to the small particle size particles utilized for electrostatic powder coating, Qiao et al. observed a very smooth appearance of the cured coating layer, comparable to that of a conventional aqueous-based film coated tablet (Qiao et al., 2010b).

As with dry powder coating in the metal finishing industry, adhesion of the coating to the tablet core can be crucial to the integrity and functionality of the coating, such as with enteric or sustained release tablet coatings. However, measuring adhesive strength of a coating on tablet core can be difficult, especially given the range of geometries used for tablet compression. Many qualitative methods have been used similar to the peel and tape peel tests described earlier. More quantitative methods have also been developed, such as butt adhesion tests (Felton and McGinity, 1996) and modified pull tests using a magnetic probe (Missaghi and Fassihi, 2004). As electrostatic powder coating and dry powder coating in general are still in the developmental stage, there is limited data available on the adhesive strength of these coatings; however, observations and physical stability studies are reported to characterize the integrity of coating. For example, Qiao et al. noted that even though TEC exhibited a small contact angle, which generally yield of better coating efficiencies, the resulting coating layer detached from the tablet core (Qiao et al., 2013). TEC was shown to be more readily absorbed into the tablet core leading to reduced contact area and liquid bridges to promote adhesion of the applied dry powder (Felton and McGinity, 1997).

Also consistent with the finishing industry, the mechanisms of adhesion for dry powder coating to a tablet are primarily from mechanical interlocking and via chemical bond formation. Rougher surfaces of a tablet core allow for greater interfacial contact between the coating and tablet core, leading to greater penetration of the coating material into the tablet core for greater adhesion. This phenomenon has been studied extensively for solvent-based coating processes, showing that increased tablet compression forces and resulting lower porosity can yield decreased adhesion of the coating to the tablet core (Felton and McGinity, 1996; Nadkarni et al., 1975). Dry powder coating studies have incorporated a primer coat to allow for liquid bridges to enhance the penetration of the dry coating material into the pores of the tablet surface, as seen with the incorporation of a PEG 3350 primer coat in studies conducted with Eudragit® L100-55 (Sauer and McGinity, 2009; Sauer et al., 2009; Sauer et al., 2007). With electrostatic coating, the liquid plasticizers applied to reduce conductivity of the tablet core also aid in enhancing adhesion.

Many solvent -based coating materials such as HPMC and PVA are amenable to hydrogen bonding with the tablet core excipients. These interactions may be facilitated by the wetting of the tablet surface by the coating solution in solvent-based coatings (Rowe, 1988); thus, may be a less prominent mechanism in dry power coating adhesion unless a liquid plasticizer or primer is applied prior to dry powder coating (Sauer et al., 2013).

Table 1.1 Polymer-plasticizer systems characterized for use in dry powder coating

Polymer	Plasticizer	Plasticizer level (% relative to polymer)	T_g (°C)[a]	Contact angle (°)[a]	Notes and observations	Ref.
Immediate Release Coatings						
Opadry® AMB	None	--	79.6	--	Plasticizer reported as spray rate, 0.4 and 0.3g/min for glycerol: water and PEG, respectively. Plasticizer reduced resistivity of tablet core from 10^{13} to less than 10^{9} Ω m.	(Qiao et al., 2010b)
	Glycerol: Water (1:1)	~13	53.3			
		~13	53.3			
Eudragit® EPO	PEG 400	--	53.1	--		
	None	~13	31.1			
	Glycerol: Water (1:1)	~13	31.1			
	PEG 400					
Eudragit® EPO (+ 8-9% talc +8% GMS or HPMC K4M or PVP K90 or PEG 3350)	None	--	50	--	Low melting point GMS and PEG 3350 lead to enhanced adhesion to tablet core. HPMC decreased release in acidic media, most probably due to gelling effect.	(Cerea et al., 2004)
Enteric Release Coatings						
Eudragit ® L100-55	None	--	126	--	Talc was incorporated at nearly 1:1 with L100-55 due to tackiness of high amount of plasticizer needed to decrease polymer T_g. TEC applied to tablet core did not	(Qiao et al., 2013)
	Triethyl citrate (TEC)	10	112	0.5[b]		
		25	96			
		50	90			
		100	66			
		10	102	20.5[b]		

Table 1.1 (Cont.)

Polymer	Plasticizer	Plasticizer level (% relative to polymer)	T_g (°C)[a]	Contact angle (°)[a]	Notes and observations	Ref.
	PEG 400	25 50 100	86 74 56		enhance adhesion due to absorption of liquid into core. 4% coating level achieved with 0 kV.	
Eudragit® L100-55 (+ talc)	Triethyl citrate (TEC)	None 20 30 40 10	126 -- 61 -- 122	63[c] 59[c] 59[c] -- 60[c]	L100-55 was pre-plasticized with TEC to reduce viscosity and increase surface free energy (10% TEC insufficient to reduce viscosity for extrusion). PEG improved spreading and adhesion without affecting surface energy.	(Sauer and McGinity, 2009b; Sauer et al., 2009; Sauer et al., 2007)
	+ PEG 3350	20TEC +10 30TEC +10 40TEC +10	47 29 11	49[c] 21[c] --		
HMPC AS	None	--	≥ 120	--	Showed a high correlation of increased coating efficiency with decreasing contact angle, than with T_g or viscosity.	(Smikalla et al., 2011)
	PEG 200	30	52	34		
	Triacetin	30	68	15		
	Cocoyl caprylocaprate	30	115	7		
		30	85	10		
	Myvacet	30	108	4		
	Isopropyl myristate	30	92	60		
	Glycerol					
HPMC AS	TEC/Myvacet (7:3)	33	52	nd	Enteric resistance from complete film formation could be achieved by curing at 55°C for 45 min. but could	(Kablitz and Urbanetz, 2007)

Table 1.1 (Cont.)

Polymer	Plasticizer	Plasticizer level (% relative to polymer)	T_g (°C)[a]	Contact angle (°)[a]	Notes and observations	Ref.
					also be achieved at 45°C (under T_g) for 12h due to the migration of plasticizer over time.	
Sustained Release Coatings						
Eudragit® RL	None	--	62.5		Plasticizer was applied at a 1:3 ratio to coating polymer. 3% coating level achieved with 60 kV versus 1.6% with 0 kV. RS/RL ratios evaluated from 0/1, 1/2, 1/1, and 2/1 showing ability to tailor release profile from 97% to 6% release in 4h.	(Qiao et al., 2010a)
	Triethyl citrate (TEC)	15	~46			
		30	40			
		> 40	< 30			
Eudragit® RS			58			
	None	--	45			
	Triethyl citrate (TEC)	15	38			
		30	< 30			
		> 40				
Ethylcellulose (EC)	None	--	127	--	Coating efficiencies increased with decreasing contact angles, T_g, and viscosities. Isopropyl myristate exhibited best spreading behavior, due to low contact angle, and showed highest coating efficiency; however, even	(Smikalla et al., 2011)
	Triacetin	20	84	43[d]		
		40	72			
	Diethyl phthalate	20	79	nd		
		40	42			
	Triethyl citrate (TEC)	20	70	30[d]		
		40	40-42			
	Acetyltributyl	20	68	21[d]		
		40	40			

Table 1.1 (Cont.)

Polymer	Plasticizer	Plasticizer level (% relative to polymer)	T_g (°C)[a]	Contact angle (°)[a]	Notes and observations	Ref.
	citrate	20	58	nd	with T_g in the 40-60°C range, 80°C cure temperature was needed for film formation.	
		40	32			
	Dynacet 285	20	57	22[c]		
		40	27			
	Dibutyl sebacate	20	56	31[c]		
		40	25			
	Myvacet	30	60	8[c]		
		40	51			
	Isopropyl myristate	50	46			
		nd	nd	73[c]		
	Glycerol					
Eudragit® L100-55 (pre-plasticized) + Eudragit® EPO + 10% talc + 2% PEG 3350 (subcoat)	Triethyl citrate (TEC)	30	65	nd	2% PEG 3350 applied as a primer layer to facilitate adhesion, required for L100-55 adhesion to tablet. Ratios of 7:3, 1:1, 3:7 of L100-55 (pre-plasticized with 30% TEC): EPO studied, with 7:3 unable to form complete film leading to 100% drug release in 2h.	(Sauer and McGinity, 2009a; Sauer et al., 2009)
	None	--	43 (varies with polymer ratios)			
	PEG 3350	10				

nd – not determined; [a] Values were approximated if data was reported in figures; [b] Contact angle measured on lightly compacted powder layer; [c] Contact angle measured using water dropped onto compacts of coating material; [d] Contact angle measured on polymer films

1.4.2 Drug Delivery Device Coating

The application of a coating for protective purposes, such as to prevent corrosion, is a primary driver in the finishing industry, but is also advantageous for coating of stents and/or other implants. In addition to corrosion protection, coatings applied to stents can improve biocompatibility and enhance surface properties such as surface energy and texture (Mani et al., 2007). These coatings can be applied using electrostatic powder deposition (Callol and Yan, 2001; Tseng et al., 2002). Coating for stents has expanded to include active coating and can also be applied using electrostatic coating techniques (Fulton et al., 2011; Malik and Hossainy, 2005; Myers, 2008). Drug eluting stents have become more commonly utilized for local drug delivery of immunosuppressive, anti-inflammatory, or anti-proliferation agents for the treatment of coronary disease and reducing the reoccurrence of stenosis (Katz et al., 2015; Khan et al., 2012; Tzafriri et al., 2012). Nukala et al. utilized electrostatic dry powder coating to coat a stent with sirolimus encapsulated polymeric microspheres (Nukala et al., 2010). In this study, sirolimus microparticles were prepared using supercritical aerosol solvent extraction to produce spherical particles with an average particle size of 3 μm. The microparticles were then electrostatically deposited onto grounded metal stents and subsequently cured for 60 seconds using IR elements held between 80-100°C. The low glass transition temperature of the polymeric components, poly(ethylene-co-vinyl acetate) and poly(n-butyl methacrylate), allowed for complete coalescence with short cure times and relatively low curing temperatures. The use of electrostatics allowed for efficient coating with complete coverage of the complex geometry of the stent, shown in Figure 1.7 (a), and producing a smooth coating layer, shown in Figure 1.7 (b). Furthermore, the in-vitro studies of the electrostatic dry powder coated stent showed reproducible drug release without

substantial burst effect and comparable deterrence of platelet adhesion when compared to the commercially available sirolimus-eluting stent, Cypher ®. The short processing times and reduced residual solvents in the final dosage form are promising aspects of the application of electrostatic dry powder coating of drug delivery devices.

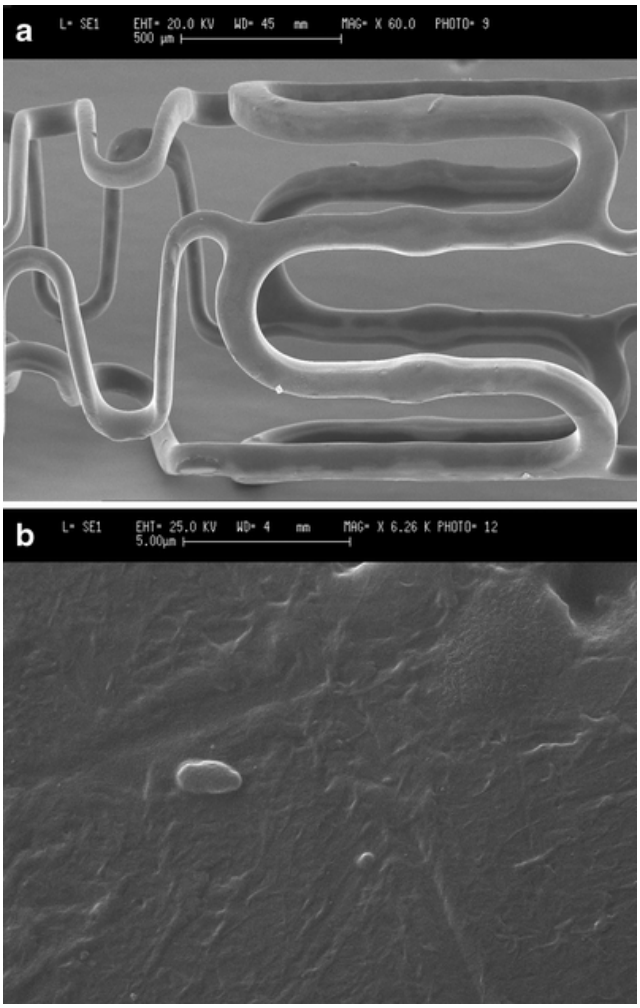

Figure 1.7 SEM images of (a) stent and (b) surface of stent coated with sirolimus-polymer microspheres by electrostatic powder coating (Reprinted with permission from (Nukala et al., 2010)) and fused at 80°C to produce continuous film coat.

1.4.3 Free Film Preparation

While tablets and capsules remain the most preferred oral dosage forms, difficulty swallowing or dysphagia can significantly limit their use in certain populations, such as pediatric and geriatric patients (Stegemann et al., 2010; Stegemann et al., 2012). Because of this, oral films are emerging as a promising dosage form for oral drug delivery (Borges et al., 2015; Dixit and Puthli, 2009). Oral films can be formulated to (1) rapidly dissolve or (2) adhere to the oral mucosa, allowing for rapid or controlled drug release, respectively. A mucoadhesive film also provides a distinct advantage of enabling transmucosal absorption, thus bypassing hepatic first-pass metabolism and the harsh and variable pH conditions of the GI tract (Patel et al., 2011; Shakya et al., 2011; Sudhakar et al., 2006; Zhang et al., 2002). Oral films are predominantly manufactured by solvent casting (2015; Borges et al., 2015; Dixit and Puthli, 2009; Morales and McConville, 2011). Solvent casting involves the preparation of a solution or suspension of the API, polymer carrier, and optionally a plasticizer and/or other excipients. The subsequent evaporation of the solvent produces a film, which is then cut into discrete shapes to produce the final unit doses. As with other solvent based coating processes, solvent casting is mainly limited by the need for a solvent, aqueous or organic, long drying times, and therefore high energy needs (Kianfar et al., 2012; Shen et al., 2013; Sievens-Figueroa et al., 2012; Visser et al., 2015).

Prasad et al. showed that electrostatic powder coating could be utilized as a dry powder coating process to prepare free films for drug delivery, provided the substrate does not significantly adhere with the coating material post curing (Prasad et al., 2015). Powder was electrostatically deposited onto a stainless steel substrate and subsequently cured; however, without mechanical or chemical pretreatment of the metal, the films were readily removed as only electrostatic and/or weak boundary layer forces held them

to the substrate. In this study, the deposition behavior of binary mixtures of acetaminophen (APAP) and polyethylene oxide (PEO) was compared to that of composite, co-processed particles by measuring the content uniformity of prepared films. At a 10% drug load, the content uniformity of the films prepared using the physical mixture was highly variable with an RSD of 11.9% compared to 1.8% of the films prepared using composite particles. This variability can be attributed to a number of factors, such as differences in particle morphology and charge accumulation of the APAP and PEO within the physical mixture. As this is one of the first studies to evaluate the deposition uniformity using a physical mixture incorporating an API, additional studies are needed to identify the causes and potential remedies to this variability.

The films produced using EPSD exhibited favorable mechanical properties, particularly when compared to the brittle break seen with a commercially available Listerine® strip, with ~4% elongation of the PEO film and > 14% elongation with the APAP containing films. PEO is a self-plasticizing, semi-crystalline polymer, with a T_g reported around -50 °C and a melting point around 61°C (Crowley et al., 2002; Prasad et al., 2015). No plasticizer was needed to enable the deposited PEO particles to coalesce for film formation. APAP further plasticized the PEO, confirmed by the reduced melting point of PEO seen in the DSC thermograms. The greater extent of displacement or elongation of the active films prior to break, as shown in Figure 1.8, illustrates the increased plasticity of the APAP containing films. This study shows electrostatic powder to be a viable, dry powder manufacturing process to prepare films for drug delivery; however, future studies are needed to evaluate the range of capabilities of this promising technique.

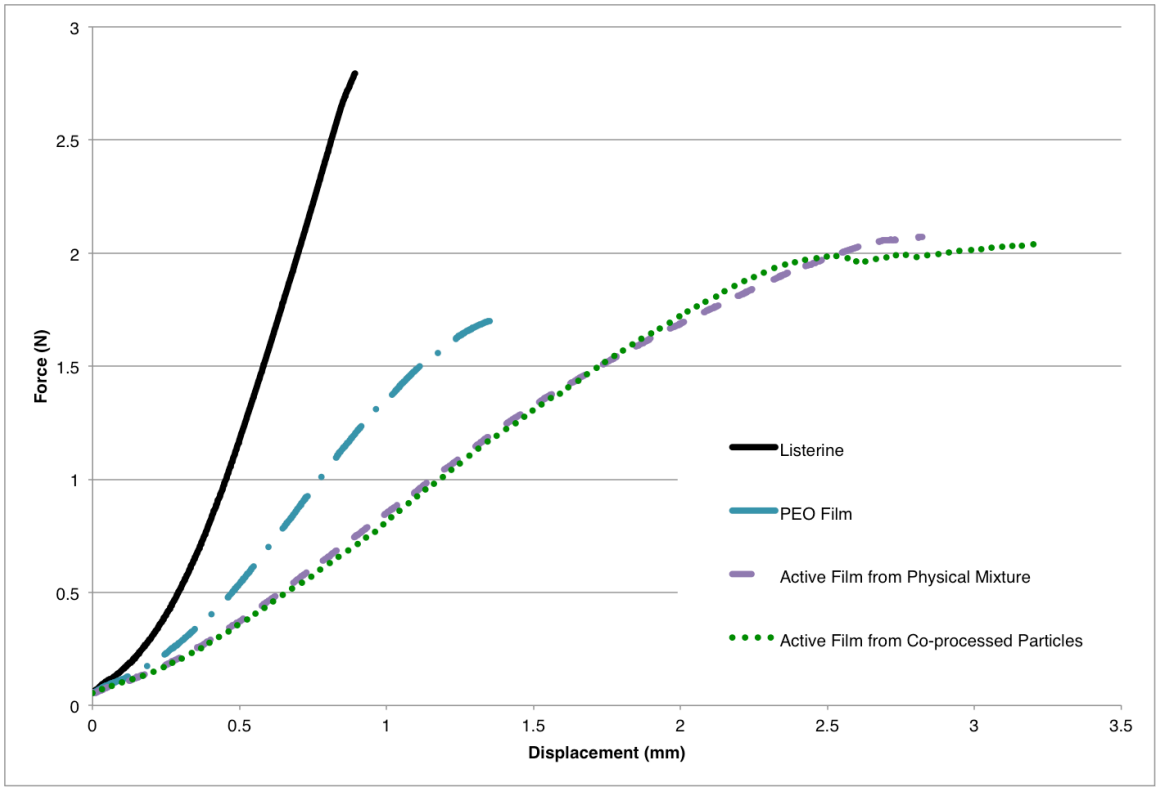

Figure 1.8 Representative force-displacement curves from puncture testing of films prepared using electrostatic powder deposition of PEO and using physical mixture and co-processed APAP: PEO, as well as of Listerine® breath strip as reference. (Adapted with permission from (Prasad et al., 2015))

1.5 CONCLUSION

Electrostatic powder coating provides a unique advantage to utilize the innate charging ability of pharmaceutical powders to develop solvent-free processes with increased manufacturing efficiencies. As this is a mature technology, much of the existing knowledge can and has been applied to its use in pharmaceutical manufacturing, including particle size and resistivity guidelines. The adoption of electrostatic powder coating of tablets and other solid dosage forms as a pharmaceutical operation is particularly promising due to the ability to utilize a modified pan coater and the

significant data collected around film formation behavior of dry powder pharmaceutical coatings, as highlighted in this review. The utility of electrostatic coating for drug delivery devices and for the preparation of free films for drug delivery has also been demonstrated using API-containing coating materials.

1.6 REFERENCES

2015. The United States Pharmacopeial Convention. General Chapter: 1151 Pharmaceutical Dosage Forms. USP 38–NF 33 Rockville, MD: The United States Pharmacopeial Convention, The United States Pharmacopeia and The National Formulary.

Adamiak, K., 2003. Analysis of charge transport in high resistivity conductors under different conduction models. Journal of Electrostatics 57, 325-335.

Andrei, D.C., Hay, J.N., Keddie, J.L., Sear, R.P., Yeates, S.G., 2000. Surface levelling of thermosetting powder coatings: theory and experiment. Journal of Physics D: Applied Physics 33, 1975.

Awaja, F., Gilbert, M., Kelly, G., Fox, B., Pigram, P.J., 2009. Adhesion of polymers. Progress in Polymer Science 34, 948-968.

Bailey, A.G., 1984. Electrostatic phenomena during powder handling. Powder Technology 37, 71-85.

Bailey, A.G., 1998. The science and technology of electrostatic powder spraying, transport and coating1. Journal of Electrostatics 45, 85-120.

Barletta, M., Gisario, A., 2009. Electrostatic spray painting of carbon fibre-reinforced epoxy composites. Progress in Organic Coatings 64, 339-349.

Barmuta, P., Cywiński, K., 2001. Electroseparation and efficiency of deposition during electrostatic powder coating. Journal of Electrostatics 51–52, 239-244.

Barringer, S.A., Sumonsiri, N., 2015. Electrostatic Coating Technologies for Food Processing. Annual Review of Food Science and Technology 6, 157-169.

Blythe, A., 1984. Electrical resistivity measurements of polymer materials. Polymer testing 4, 195-209.

Borges, A.F., Silva, C., Coelho, J.F.J., Simões, S., 2015. Oral films: Current status and future perspectives: I — Galenical development and quality attributes. Journal of Controlled Release 206, 1-19.

Bose, S., Bogner, R.H., 2007. Solventless pharmaceutical coating processes: a review. Pharmaceutical development and technology 12, 115-131.

Byron, P., Peart, J., Staniforth, J., 1997. Aerosol Electrostatics I: Properties of Fine Powders Before and After Aerosolization by Dry Powder Inhalers. Pharmaceutical research 14, 698-705.

Callol, J.R., Yan, J.Y., 2001. Protective coating for a stent with intermediate radiopaque coating. US6174329.

Carter, P.A., Rowley, G., Fletcher, E.J., Stylianopoulos, V., 1998. Measurement of Electrostatic Charge Decay in Pharmaceutical Powders and Polymer Materials Used in Dry Powder Inhaler Devices. Drug Development and Industrial Pharmacy 24, 1083-1088.

Castle, G.P., 2011. A century of development in applied electrostatics; nothing static here. Dielectrics and Electrical Insulation, IEEE Transactions on 18, 1361-1365.

Cazaux, J., 2007. Critical thicknesses of electrostatic powder coatings from inside. Journal of Electrostatics 65, 764-774.

Chang, K.-N., Chen, Y.-K., Huang, S.-H., Chen, C.-W., Lai, C.-Y., Chen, C.-C., 2012. Penetration of charged particles through metallic tubes. Journal of Aerosol Science 48, 10-17.

Chow, K., Zhu, K., Tan, R.H., Heng, P.S., 2008. Investigation of Electrostatic Behavior of a Lactose Carrier for Dry Powder Inhalers. Pharmaceutical research 25, 2822-2834.

Crowley, M.M., Zhang, F., Koleng, J.J., McGinity, J.W., 2002. Stability of polyethylene oxide in matrix tablets prepared by hot-melt extrusion. Biomaterials 23, 4241-4248.

DesRosiers Lachiver, E., Abatzoglou, N., Cartilier, L., Simard, J.-S., 2006. Insights into the Role of Electrostatic Forces on the Behavior of Dry Pharmaceutical Particulate Systems. Pharmaceutical research 23, 997-1007.

Dixit, R.P., Puthli, S.P., 2009. Oral strip technology: Overview and future potential. Journal of Controlled Release 139, 94-107.

Felton, L.A., McGinity, J.W., 1996. Influence of tablet hardness and hydrophobicity on the adhesive properties of an acrylic resin copolymer. Pharmaceutical development and technology 1, 381-389.

Felton, L.A., McGinity, J.W., 1997. Influence of plasticizers on the adhesive properties of an acrylic resin copolymer to hydrophilic and hydrophobic tablet compacts. International Journal of Pharmaceutics 154, 167-178.

Fulton, J.L., Deverman, G.S., Matson, D.W., Yonker, C.R., Taylor, C.D., McClain, J.B., Crowley, J.M., 2011. System and method for enhanced electrostatic deposition and surface coatings. US20110238161.

Giacometti, J., Oliveira Jr, O.N., 1992. Corona charging of polymers. Electrical Insulation, IEEE Transactions on 27, 924-943.

Gibson, N., 1997. Static electricity — an industrial hazard under control? Journal of Electrostatics 40–41, 21-30.

Glor, M., 1985. Hazards due to electrostatic charging of powders. Journal of Electrostatics 16, 175-191.

Glor, M., 2003. Ignition hazard due to static electricity in particulate processes. Powder Technology 135–136, 223-233.

Glover, W., Chan, H.-K., 2004. Electrostatic charge characterization of pharmaceutical aerosols using electrical low-pressure impaction (ELPI). Journal of Aerosol Science 35, 755-764.

Gray, J.E., Luan, B., 2002. Protective coatings on magnesium and its alloys — a critical review. Journal of Alloys and Compounds 336, 88-113.

Grosvenor, M.P., 1991. The physico-mechanical properties of electrostatically deposited polymers for use in pharmaceutical powder coating. University of Bath.

Grosvenor, M.P., Staniforth, J.N., 1996. The Influence of Water on Electrostatic Charge Retention and Dissipation in Pharmaceutical Compacts for Powder Coating. Pharmaceutical research 13, 1725-1729.

Hao, T., Tukianen, J., Nivorozhkin, A., Landrau, N., 2013. Probing pharmaceutical powder blending uniformity with electrostatic charge measurements. Powder Technology 245, 64-69.

Herling, U., Bill, W.S., 2000. Polyethylene glycol coating for electrostatic dry deposition of pharmaceuticals. WO2000035424.

Hoburg, J.F., 1982. Charge density, electric field, and particle charging in electrostatic precipitation with back ionization. Industry Applications, IEEE Transactions on, 666-672.

Hughes, J., 1989. Powder coating technology. Journal of Electrostatics 23, 3-23.

Hughes, J.F., 1984. Electrostatic Powder Coating. DTIC Document.

Karner, S., Urbanetz, N.A., 2011. The impact of electrostatic charge in pharmaceutical powders with specific focus on inhalation-powders. Journal of Aerosol Science 42, 428-445.

Katz, G., Harchandani, B., Shah, B., 2015. Drug-Eluting Stents: the Past, Present, and Future. Curr Atheroscler Rep 17, 1-11.

Khan, W., Farah, S., Domb, A.J., 2012. Drug eluting stents: Developments and current status. Journal of Controlled Release 161, 703-712.

Kianfar, F., Chowdhry, B.Z., Antonijevic, M.D., Boateng, J.S., 2012. Novel films for drug delivery via the buccal mucosa using model soluble and insoluble drugs. Drug Dev Ind Pharm 38, 1207-1220.

Kiefer, S.L., 2004. Powder coating material developments promise new opportunities for finishers. Metal Finishing 102, 35-37.

Kim, J.K., Kim, W.H., Lee, D.H., 2002. Adhesion properties of UV crosslinked polystyrene-block-polybutadiene-block-polystyrene copolymer and tackifier mixture. Polymer 43, 5005-5010.

Koleske, J.V., 2012. Paint and Coating Testing Manual: 15th Edition of the Gardner-Sward Handbook. ASTM International.

Lacombe, R., 2005. Adhesion measurement methods: theory and practice. CRC Press.

Lee, S., 2006. Encyclopedia of chemical processing. Taylor & Francis, New York.

Luo, Y., Zhu, J., Ma, Y., Zhang, H., 2008. Dry coating, a novel coating technology for solid pharmaceutical dosage forms. International Journal of Pharmaceutics 358, 16-22.

Malik, S., Hossainy, S., 2005. Electrostatic loading of drugs on implantable medical devices. US20050273161.

Mallappa, A., Sinaii, N., Kumar, P., Whitaker, M.J., Daley, L.-A., Digweed, D., Eckland, D.J.A., Van Ryzin, C., Nieman, L.K., Arlt, W., Ross, R.J., Merke, D.P., 2014. A Phase 2 Study of Chronocort, a Modified-Release Formulation of Hydrocortisone, in the Treatment of Adults With Classic Congenital Adrenal Hyperplasia. The Journal of Clinical Endocrinology & Metabolism 100, 1137-1145.

Mani, G., Feldman, M.D., Patel, D., Agrawal, C.M., 2007. Coronary stents: A materials perspective. Biomaterials 28, 1689-1710.

Masuda, S., Mizuno, A., 1977. Initiation condition and mode of back discharge. Journal of Electrostatics 4, 35-52.

Masuda, S., Washizu, M., 1979. Ionic charging of a very high resistivity spherical particle. Journal of Electrostatics 6, 57-67.

Matsusaka, S., Maruyama, H., Matsuyama, T., Ghadiri, M., 2010. Triboelectric charging of powders: A review. Chemical Engineering Science 65, 5781-5807.

Mazumder, M.K., Sims, R.A., Biris, A.S., Srirama, P.K., Saini, D., Yurteri, C.U., Trigwell, S., De, S., Sharma, R., 2006. Twenty-first century research needs in electrostatic processes applied to industry and medicine. Chemical Engineering Science 61, 2192-2211.

Mazumder, M.K., Wankum, D.L., Sims, R.A., Mountain, J.R., Chen, H., Pettit, P., Chaser, T., 1997. Influence of powder properties on the performance of electrostatic coating process. Journal of Electrostatics 40–41, 369-374.

Mazumder, M.K., Ware, R.E., Yokoyama, T., Rubin, B.J., Kamp, D., 1991. Measurement of particle size and electrostatic charge distributions on toners using E-SPART analyzer. Industry Applications, IEEE Transactions on 27, 611-619.

Mazur, S., Beckerbauer, R., Buckholz, J., 1997. Particle Size Limits for Sintering Polymer Colloids without Viscous Flow. Langmuir 13, 4287-4294.

McLean, K., 1988. Electrostatic precipitators. Physical Science, Measurement and Instrumentation, Management and Education-Reviews, IEE Proceedings A 135, 347-361.

Meng, X., 2009. Study on corona discharge and corona charging in electrostatic powder coating process. The University of Western Ontario (Canada), Ann Arbor, p. 347.

Meng, X., Zhang, H., Zhu, J., 2009. Characterization of particle size evolution of the deposited layer during electrostatic powder coating processes. Powder Technology 195, 264-270.

Misev, T.A., van der Linde, R., 1998. Powder coatings technology: new developments at the turn of the century. Progress in Organic Coatings 34, 160-168.

Missaghi, S., Fassihi, R., 2004. A novel approach in the assessment of polymeric film formation and film adhesion on different pharmaceutical solid substrates. AAPS PharmSciTech 5, 32-39.

Morales, J.O., McConville, J.T., 2011. Manufacture and characterization of mucoadhesive buccal films. European Journal of Pharmaceutics and Biopharmaceutics 77, 187-199.

Murtomaa, M., Savolainen, M., Christiansen, L., Rantanen, J., Laine, E., Yliruusi, J., 2004. Static electrification of powders during spray drying. Journal of Electrostatics 62, 63-72.

Myers, R., 2008. Process of Electrostatically Coating A Stent On a Catheter. US20080113084.

Nadkarni, P.D., Kildsig, D.O., Kramer, P.A., Banker, G.S., 1975. Effect of surface roughness and coating solvent on film adhesion to tablets. Journal of Pharmaceutical Sciences 64, 1554-1557.

Nukala, R., Boyapally, H., Slipper, I., Mendham, A., Douroumis, D., 2010. The Application of Electrostatic Dry Powder Deposition Technology to Coat Drug-Eluting Stents. Pharmaceutical research 27, 72-81.

O'Neill, B., Bright, A., 1978. A parametric study of electrostatic powder coating. Journal of Electrostatics 4, 325-334.

Paasi, J., Nurmi, S., Vuorinen, R., Strengell, S., Maijala, P., 2001. Performance of ESD protective materials at low relative humidity. Journal of Electrostatics 51–52, 429-434.

Patel, V.F., Liu, F., Brown, M.B., 2011. Advances in oral transmucosal drug delivery. Journal of Controlled Release 153, 106-116.

Peart, J., 2001. Powder electrostatics: theory, techniques and applications. KONA Powder and Particle Journal 19, 34-45.

Prasad, L.K., Keen, J.M., LaFountaine, J.S., Maincent, J., Williams Iii, R.O., McGinity, J.W., 2015. Electrostatic powder deposition to prepare films for drug delivery. Journal of Drug Delivery Science and Technology 30, Part B, 501-510.

Pu, Y., Mazumder, M., Cooney, C., 2009. Effects of electrostatic charging on pharmaceutical powder blending homogeneity. Journal of Pharmaceutical Sciences 98, 2412-2421.

Pugh, E., 1932. Method of and apparatus for coating articles. US1855869.

Puig, M., Cabedo, L., Gracenea, J.J., Jiménez-Morales, A., Gámez-Pérez, J., Suay, J.J., 2014. Adhesion enhancement of powder coatings on galvanised steel by addition of organo-modified silica particles. Progress in Organic Coatings 77, 1309-1315.

Qiao, M., Luo, Y., Zhang, L., Ma, Y., Stephenson, T.S., Zhu, J., 2010a. Sustained release coating of tablets with Eudragit® RS/RL using a novel electrostatic dry powder coating process. International Journal of Pharmaceutics 399, 37-43.

Qiao, M., Zhang, L., Ma, Y., Zhu, J., Chow, K., 2010b. A novel electrostatic dry powder coating process for pharmaceutical dosage forms: Immediate release coatings for tablets. European Journal of Pharmaceutics and Biopharmaceutics 76, 304-310.

Qiao, M., Zhang, L., Ma, Y., Zhu, J., Xiao, W., 2013. A novel electrostatic dry coating process for enteric coating of tablets with Eudragit® L100-55. European Journal of Pharmaceutics and Biopharmaceutics 83, 293-300.

Radhakrishnan, S., Sonawane, N., Siju, C.R., 2009. Epoxy powder coatings containing polyaniline for enhanced corrosion protection. Progress in Organic Coatings 64, 383-386.

Ramarathnam, G., Libertucci, M., Sadowski, M., North, T., 1992. Joining of polymers to metal. Welding Journal New York 71, 483-s.

Ransburg, H.P., Green, H.J., 1941. Apparatus for spray coating articles. US2247963.

Ratanatriwong, P., Barringer, S., 2007. Particle size, cohesiveness and charging effects on electrostatic and nonelectrostatic powder coating. Journal of Electrostatics 65, 704-708.

Rowe, R.C., 1988. Adhesion of film coatings to tablet surfaces —a theoretical approach based on solubility parameters. International Journal of Pharmaceutics 41, 219-222.

Rowley, G., 2001. Quantifying electrostatic interactions in pharmaceutical solid systems. International Journal of Pharmaceutics 227, 47-55.

Sauer, D., Cerea, M., DiNunzio, J., McGinity, J., 2013. Dry powder coating of pharmaceuticals: A review. International Journal of Pharmaceutics 457, 488-502.

Sauer, D., McGinity, J.W., 2009. Influence of additives on melt viscosity, surface tension, and film formation of dry powder coatings. Drug development and industrial pharmacy 35, 646-654.

Sauer, D., Watts, A.B., Coots, L.B., Zheng, W.C., McGinity, J.W., 2009. Influence of polymeric subcoats on the drug release properties of tablets powder-coated with pre-plasticized Eudragit® L 100-55. International journal of pharmaceutics 367, 20-28.

Sauer, D., Zheng, W., Coots, L.B., McGinity, J.W., 2007. Influence of processing parameters and formulation factors on the drug release from tablets powder-coated with Eudragit® L 100-55. European Journal of Pharmaceutics and Biopharmaceutics 67, 464-475.

Shah, U., Zhang, C., Zhu, J., 2006a. Comparison of electrostatic fine powder coating and coarse powder coating by numerical simulations. Journal of electrostatics 64, 345-354.

Shah, U., Zhu, J., Zhang, C., Nother, J., 2006b. Numerical investigation of coarse powder and air flow in an electrostatic powder coating process. Powder technology 164, 22-32.

Shakya, P., Madhav, N.V.S., Shakya, A.K., Singh, K., 2011. Palatal mucosa as a route for systemic drug delivery: A review. Journal of Controlled Release 151, 2-9.

Shen, B.d., Shen, C.y., Yuan, X.d., Bai, J.x., Lv, Q.y., Xu, H., Dai, L., Yu, C., Han, J., Yuan, H.l., 2013. Development and characterization of an orodispersible film containing drug nanoparticles. European Journal of Pharmaceutics and Biopharmaceutics 85, 1348-1356.

Sievens-Figueroa, L., Bhakay, A., Jerez-Rozo, J.I., Pandya, N., Romañach, R.J., Michniak-Kohn, B., Iqbal, Z., Bilgili, E., Davé, R.N., 2012. Preparation and characterization of hydroxypropyl methyl cellulose films containing stable BCS Class II drug nanoparticles for pharmaceutical applications. International Journal of Pharmaceutics 423, 496-508.

Sims, R., Mazumder, M., Liu, X., Chok, W., Mountain, J., Wankum, D., Pettit, P., Chasser, T., 2001. Electrostatic effects on first pass transfer efficiency in the application of powder coatings. Industry Applications, IEEE Transactions 37, 1610-1617.

Smikalla, M., Mescher, A., Walzel, P., Urbanetz, N.A., 2011. Impact of excipients on coating efficiency in dry powder coating. International Journal of Pharmaceutics 405, 122-131.

Staniforth, J.N., Grosvenor, M.P., 1992. Improvements in or relating to electrostatic coating of substrates of medicinal products. WO1992014451.

Stark, J., Zhang, J., Sharma, R., Adams, A., Mazumder, M., 2008. Measurement of Electrostatic Charge and Aero-dynamic Diameter of Sub-Micron Particles by the ESPART Analyzer, Proc. ESA Annual Meeting on Electrostatics, pp. 1-6.

Stegemann, S., Ecker, F., Maio, M., Kraahs, P., Wohlfart, R., Breitkreutz, J., Zimmer, A., Bar-Shalom, D., Hettrich, P., Broegmann, B., 2010. Geriatric drug therapy: Neglecting the inevitable majority. Ageing Research Reviews 9, 384-398.

Stegemann, S., Gosch, M., Breitkreutz, J., 2012. Swallowing dysfunction and dysphagia is an unrecognized challenge for oral drug therapy. International Journal of Pharmaceutics 430, 197-206.

Subramanian, V., van Ooij, W.J., 1999. Silane based metal pretreatments as alternatives to chromating: Shortlisted. Surface Engineering 15, 168-172.

Sudhakar, Y., Kuotsu, K., Bandyopadhyay, A.K., 2006. Buccal bioadhesive drug delivery — A promising option for orally less efficient drugs. Journal of Controlled Release 114, 15-40.

Tseng, D., Donahue, W., Parsons, B.A., 2002. Polymer coated stent. US6364903.

Tzafriri, A.R., Groothuis, A., Price, G.S., Edelman, E.R., 2012. Stent elution rate determines drug deposition and receptor-mediated effects. Journal of Controlled Release 161, 918-926.

Visser, J.C., Dohmen, W.M.C., Hinrichs, W.L.J., Breitkreutz, J., Frijlink, H.W., Woerdenbag, H.J., 2015. Quality by design approach for optimizing the formulation and physical properties of extemporaneously prepared orodispersible films. International Journal of Pharmaceutics 485, 70-76.

Watanabe, H., Ghadiri, M., Matsuyama, T., Ding, Y.L., Pitt, K.G., Maruyama, H., Matsusaka, S., Masuda, H., 2007. Triboelectrification of pharmaceutical powders by particle impact. International Journal of Pharmaceutics 334, 149-155.

Weiss, K.D., 1997. Paint and coatings: A mature industry in transition. Progress in Polymer Science 22, 203-245.

Whiteman, M., Hallett, M.D., Feather, D.H., Nelson, D.H., Gazza, J.M., 2006. Electrostatic application of powder material to solid dosage forms utilizing an electrically conductive shield. US7144597.

Wicks, Z.W., Jones, F.N., Pappas, S.P., Wicks, D.A., 2007. Organic coatings: science and technology, 3rd ed. Wiley-Interscience, Hoboken, N.J.

Wong, J., Chan, H.-K., Kwok, P.C.L., 2013. Electrostatics in pharmaceutical aerosols for inhalation. Therapeutic Delivery 4, 981-1002.

Wong, J., Kwok, P., Noakes, T., Fathi, A., Dehghani, F., Chan, H.-K., 2014. Effect of Crystallinity on Electrostatic Charging in Dry Powder Inhaler Formulations. Pharmaceutical research 31, 1656-1664.

Wong, J., Kwok, P.C.L., Chan, H.-K., 2015. Electrostatics in pharmaceutical solids. Chemical Engineering Science 125, 225-237.

Xi, J., Si, X., Longest, W., 2014. Electrostatic Charge Effects on Pharmaceutical Aerosol Deposition in Human Nasal–Laryngeal Airways. Pharmaceutics 6, 26-35.

Yang, Q., Ma, Y., Zhu, J., 2015. Applying a novel electrostatic dry powder coating technology to pellets. European Journal of Pharmaceutics and Biopharmaceutics 97, Part A, 118-124.

Yousuf, S., Barringer, S.A., 2007. Modeling nonelectrostatic and electrostatic powder coating. Journal of Food Engineering 83, 550-561.

Yurteri, C.U., Mazumder, M.K., Grable, N., Ahuja, G., Trigwell, S., Biris, A.S., Sharma, R., Sims, R.A., 2002. Electrostatic Effects on Dispersion, Transport, and Deposition of Fine Pharmaceutical Powders: Development of an Experimental Method of Quantitative Analysis. Particulate Science & Technology 20, 59.

Zhang, H., Zhang, J., Streisand, J., 2002. Oral Mucosal Drug Delivery. Clin Pharmacokinet 41, 661-680.

Zhu, J., Luo, Y., Ma, Y., Zhang, H., 2007. Direct coating solid dosage forms using powdered materials. US20070128274.

Chapter 2: Research Objectives

2.1 Overall Objectives

The objective of this work was to investigate the application of electrostatic powder deposition for the preparation of orodispersible films. Low molecular weight polyethylene oxide was utilized as the hydrophilic, film forming polymer. The impact of process parameters on deposition behavior, film formation, and film to substrate adhesion was investigated. The influence of an active pharmaceutical ingredient on the properties of and drug release form polyethylene oxide based orodispersible film was studied. Lastly, the physicochemical, electrical, and thermal properties of composite particles prepared for use with ESPD were investigated as a function of increasing drug load.

2.2 Supporting Objectives

2.2.1 Investigate the Influence of Process Parameters and Substrate Properties on the Properties of Films Prepared by Electrostatic Powder Deposition

Electrostatic powder deposition involves the (1) charging, (2) spraying, and (3) deposition of charged particles on a grounded substrate. The deposited powder is then placed under heat for film formation. The final film is then removed or peeled from the substrate. The influence of charging voltage, gun-to-substrate distance, and environmental humidity on deposition behavior of polyethylene oxide was investigated. Film formation as a function of cure temperature and time was characterized using scanning electron microscopy. The impact of curing conditions on mechanical properties and film to substrate adhesion was also investigated. Finally, the film to substrate adhesive strength was evaluated using substrates of varying surface roughness.

2.2.2 Investigate the Impact of Acetaminophen on the Properties and Performance of Polyethylene Oxide Orodispersible Films Prepared by Electrostatic Powder Deposition

Physical mixtures and composite particles containing acetaminophen and polyethylene oxide were prepared to investigate the impact of each on the drug content uniformity of films prepared using electrostatic powder deposition. The influence of acetaminophen on the mechanical properties, namely tensile strength and percent elongation, of the orodispersible film was investigated. The films were characterized using differential scanning calorimetry, powder x-ray diffraction, and scanning electron microscopy. Lastly, the films produced using physical mixtures and those using composite particles were characterized for drug release using *in vitro* dissolution testing.

2.2.3 Investigate the Influence of Benzocaine Loading on the Properties and Performance of Polyethylene Oxide Orodispersible Films Prepared by Electrostatic Powder Deposition

Physical mixtures and composite particles containing benzocaine and polyethylene oxide were prepared to investigate the impact of drug loading on the drug content uniformity of films prepared using electrostatic powder deposition. Raw materials were characterized for their particle size distribution and electrical properties, namely their resistive character. The influence of drug load on electrical, solid state, and thermal properties of the composite particles was investigated. The complex viscosity as a function of temperature was determined for the composite particles to identify appropriate curing conditions. Finally, the impact of benzocaine loading on mechanical strength and drug release from films prepared using composite particles was studied.

Chapter 3: Influence of process parameters on the preparation of pharmaceutical films by electrostatic powder deposition[1]

3.1 ABSTRACT

Electrostatic powder deposition (ESPD) has been developed as a solvent-free method to prepare pharmaceutical films. The aim of this work was to investigate the influence of process parameters during (1) electrostatic powder deposition, (2) curing, and (3) removal of the film from the substrate on the properties of the film. Polyethylene oxide (PEO) was used as the model polymer and stainless steel 316 as the substrate. Deposition efficiency was measured with varying charging voltage, gun tip to substrate distance, and environmental humidity. Scanning electron microscopy was utilized to assess film formation, and adhesive and mechanical strength of films were measured with varying cure temperature and time. Adhesive strength was measured for films prepared on substrates of varying surface roughness. At 25 %RH, process parameters did not significantly affect deposition behavior. At 40 %RH, increasing deposition efficiency with decreasing gun tip to substrate distance and increasing voltage (up to 60kV) was observed. Complete film formation was seen by 30 minutes at 80°C. All films were readily removed from the substrates. The results show the ESPD process can be optimized to produce films with good mechanical properties, suggesting it is a promising dry powder process for preparing pharmaceutical films.

[1] This work has been submitted for publication in the International Journal of Pharmaceutics.

3.2 INTRODUCTION

Oral solid dosage forms, specifically tablets and capsules, remain the most preferred dosage form and route of administration for drug delivery (Sastry et al., 2000). However, difficulty in swallowing or dysphagia can significantly limit the use of tablets and capsules, particularly in pediatric and geriatric populations, as well as patients with central nervous system or musculoskeletal disorders (Stegemann et al., 2010; Stegemann et al., 2012). Due to these potential problems, oral films are emerging as a promising dosage form for oral drug delivery (Borges et al., 2015; Dixit and Puthli, 2009). One of the advantages of oral films is the ability to either rapidly dissolve or adhere to the oral mucosa, allowing for rapid or controlled drug release for local and/or systemic absorption. A mucoadhesive film also provides a distinct advantage of enabling transmucosal absorption and thus bypassing hepatic first-pass metabolism and the harsh and variable pH conditions in GI tract (Patel et al., 2011; Shakya et al., 2011; Sudhakar et al., 2006; Zhang et al., 2002).

Oral films are predominantly manufactured by solvent casting (2015; Borges et al., 2015; Dixit and Puthli, 2009; Morales and McConville, 2011). Solvent casting involves the preparation of a solution of the active pharmaceutical ingredient (API), polymer carrier, and optionally a plasticizer and/or other excipients. The subsequent evaporation of the solvent produces a film, which can then be cut into discrete shapes to produce the final unit doses. Solvent casting is mainly limited by the need for a solvent, aqueous or organic. Given the high heat of vaporization of water, aqueous solutions can require long drying times, up to 24 hours (Kianfar et al., 2012; Shen et al., 2013; Sievens-Figueroa et al., 2012; Visser et al., 2015). The use of organic solvents is particularly undesirable from an environmental perspective and requires the manufacturing facility to incorporate solvent handling (i.e. explosion proof equipment and rooms) and collection

capabilities (Constable et al., 2007; Grodowska and Parczewski, 2010). Additionally, testing is required on the final drug product to ensure residual solvent levels are below ICH requirements. Formulation development activities for solvent casting, with both aqueous and organic solvent systems, involve optimizing solution rheology for casting (Preis et al., 2014) and ensuring physical stability upon storage (Gutierrez-Rocca and Mcginity, 1993).

More recently, electrostatic powder deposition (ESPD) has been shown as an alternative, solvent-free method to prepare free films for drug delivery (Prasad et al., 2015). ESPD involves the (1) charging, (2) spraying or transport, and (3) deposition of the charged particles onto a grounded substrate; this is typically done using a corona electrostatic gun. The deposited powder is then cured using heat and subsequently removed from the substrate. Prasad et al. showed that an active physical mixture or co-processed composite-particles could be electrostatically charged and deposited onto a stainless steel substrate and subsequently cured to prepare a drug-loaded film. The films were readily removed from the substrate, as they were only adhered by weak electrostatic and/or Van der Waals forces. The results of this study also illustrated that composite particles of acetaminophen (APAP): polyethylene oxide (PEO) (10:90) prepared by extrusion in this study, produced films of significantly less variability of APAP content (1.8% versus 11.9% RSD in films from composite particles versus from physical mixture, respectively) (Prasad et al., 2015). This finding correlates well with typical manufacturing methods for dry powder coating compositions which consists of pre-mixing the polymer, pigments and/or other additives, melt extrusion (alternatively spray-drying, granulation, or co-grinding techniques have also been utilized), followed by milling/micronization to obtain composite particles of acceptable particle size for electrostatic powder coating (Harmuth, 1982; Hogan et al., 2002; Noonan, 1977; Wicks

et al., 2007). These composite particles yield more efficient and uniform deposition, particularly for the deposition of components that may not exhibit ideal resistivity for processing. Additionally, uniform distribution of additives such as liquid plasticizers can be critical to film-forming properties of the coating material. Sauer et al. showed this to be advantageous for dry powder coating of tablets using pre-plasticized Eudragit L100-55 to promote film formation and obtain a functional, delayed-release tablet coating (Sauer et al., 2007).

The aim of this current work was to investigate the influence of the process parameters of electrostatic powder deposition (ESPD) including: (1) the impact of applied voltage, distance from the substrate, and environmental humidity on the deposition efficiency and uniformity; (2) the impact of cure temperature and time on film formation, peel strength and mechanical properties; and (3) the impact of substrate properties on adhesion of the film to the substrate. Polyethylene oxide (PEO) was utilized as a model thermoplastic polymer and stainless steel 316 was utilized as the substrate.

3.3 MATERIAL AND METHODS

3.3.1 Materials

POLYOX™ WSR N10 NF was generously donated by Colorcon® (West Point, PA, USA). Bulk material was sieved and material between 25 μm (500 mesh) and 90 μm (170 mesh) was collected for use.

Sheets of stainless steel 316 (SS 316), 0.060" (1.524 mm) thickness, were used as received from McMaster Carr (McMaster Carr, Atlanta, GA, USA) in the following finishes: unpolished, mirror finish #8, brush finish #4. Additional sheets of unpolished stainless steel 316 were subject to abrasive surface treatments as described below. The

bulk composition of the unpolished SS 316 was reported as follows: (wt. %): C (0.28) Cr (16.58), Ni (10.08), Mo (2.04), Mn (1.46), Si (0.29), P (0.03), S (≤ 0.01) and Fe (balance).

3.3.2 Substrate Abrasive Treatments

Sheets of unpolished SS316 were mechanically roughened by sand blasting using 70/100 (150-212 μm) beads. After abrasive treatment, samples were cleaned by isopropyl alcohol rinse, 10 minute sonication in a 1% Contrex® solution, followed by a thorough rinse using de-ionized water. After cleaning, the samples were passivated by soaking in a 50% HNO_3 solution at 50°C for a minimum of 30 minutes to reform the protective chromium oxide surface layer per ASTM A380/A380M Standard Practice for Cleaning, Descaling, and Passivation of Stainless Steel Parts, Equipment, and Systems (ASTM, 2013). Immediately after removal from the passivating solution, the substrates were thoroughly rinsed using de-ionized water and allowed to dry overnight in a desiccator at 50°C. Substrates were wiped with isopropyl alcohol prior to use or analysis, as needed (ASTM, 2013).

3.3.3 Surface Analysis

Surface imaging and roughness calculations were conducted using a non-contact, optical profilometry using a Wyko NT9100 profiling system (Veeco, Plainview, NY, USA). Imaging was conducted using the following settings: 20x objective lens, 2x field of view (FOV), scan size of 120 x 160 μm, and a vertical resolution of 4 μm (12 μm for the sandblasted substrate).. Surface roughness was calculated using WYKO Vision 4.2 software (Veeco, Plainview, NY, USA). The average roughness, R_a, root mean squared

roughness, R_q, and the maximum height of the profile, R_t, were calculated as shown in equations 3.1, 3.2, and 3.3, respectively (per ASME B46.1-2009). Note that n=3 samples were analyzed; however, due to no discernable difference between the measurements, data and images from one representative sample is reported.

$$R_a = \frac{1}{L}\int_0^L |Z(x)|dx \tag{3.1}$$

$$R_q = \sqrt{\frac{1}{L}\int_0^L Z(x)^2 dx} \tag{3.2}$$

$$R_t = R_p + R_v \tag{3.3}$$

where L is the evaluation length, Z(x) is the distance from the reference mean line, R_p is the distance between the highest point of the profile from the mean reference line, and R_v is the lowest point of the profile from the mean reference line.

XPS analyses were performed on an Axis Ultra DLD photoelectron spectrometer (Kratos, Manchester, U.K.) utilizing a monochromated Al Kα anode X-ray source ($h\nu$ = 1486.5 eV), hybrid optics (magnetic/electrostatic), and a multi-channel plate coupled to a hemispherical photoelectron kinetic analyzer. The spectrometer was calibrated by using Ag 3d 5/2 (368.3 eV) peak. All spectra were recorded in an analysis chamber at 10^{-9} Torr base pressure using an aperture slot of 300 x 700 μm^2 and pass energy of 80 eV. The photoelectrons takeoff angle was normal to the surface of the sample and 45° with respect to the X-ray beam. Casa XPS analysis software was used for peak analysis and

the stoichiometry of samples was determined from corrected peak areas and employing Kratos sensitivity factors for each element of interest.

Surface energies were calculated based on contact angle measurements using water, formamide, and diiodomethane. Contact angles were measured using a FTA200 goniometer (First Ten Angstroms, Inc., Portsmouth, VA, USA). Solid surface energies were calculated using equation 3.4, derived from Young's equation (Young, 1805), showing the relationship between contact angle, surface energy and interfacial energy, and the relationship of interfacial energy as a combination of dispersive and polar forces proposed by Owens and Wendt (Owens and Wendt, 1969).

$$\frac{1}{2}\gamma_l(1+\cos\theta) = \sqrt{\gamma_s^d \gamma_l^d} + \sqrt{\gamma_s^p \gamma_l^p} \tag{3.4}$$

where γ_l represents the surface energy of the liquid, γ_s represents the surface energy of the solid, and the superscripts of *d* and *p* indicate the dispersive/apolar and polar components, respectively, of the total free energy. Values for surface e nergies, including dispersive and polar components, of test liquids were taken from Good (Good, 1992).

3.3.3 Electrostatic Powder Deposition

The ESPD process consists of the following steps: powder charging, spraying and deposition. The deposited material is then cured and the final film is removed from the metallic substrate. In this study, the substrate was covered with a stencil such that the powder deposited only on the exposed metal, a 25 x 63 mm strip along the center of the substrate. For each sample preparation, a fixed amount of powder was fed to a Nordson Vantage® Manual corona gun (Nordson Corporation, Westlake, OH, USA) using a

volumetric feeder (Schenk AccuRate, Whitewater, WI, USA); thus, a fixed feed rate and spray time was utilized for each sample preparation. The powder was then sprayed using compressed air (0.5 bar pressure) through a conical deflector and charged by passing through the corona discharge produced by the high applied voltage (Prasad et al., 2016). After powder deposition, the substrate was then placed in an infrared oven. The resulting film was peeled from the substrate and film weight and thickness were measured. Thickness was measured using a Mitutoyo digital micrometer (Mitutoyo, Kawasaki, Japan) and the average of n=3 values was reported. Statistical analysis was conducted using JMP software (JMP Pro 12.0).

To study the impact of process parameters during ESPD on deposition efficiency, the charging voltage and gun tip to substrate distance were varied, as shown in Figure 3.1. Additionally, experiments were conducted at two environmental humidity conditions: 25 and 40 %RH. The humidity was controlled using humidifiers or dehumidifiers, as needed and monitored using a Fisher Scientific Traceable™ Humidity/Temperature Pen (Pittsburgh, PA, USA). The samples form this study were prepared using unpolished SS 316 as the substrate and cured at 80°C for 60 minutes.

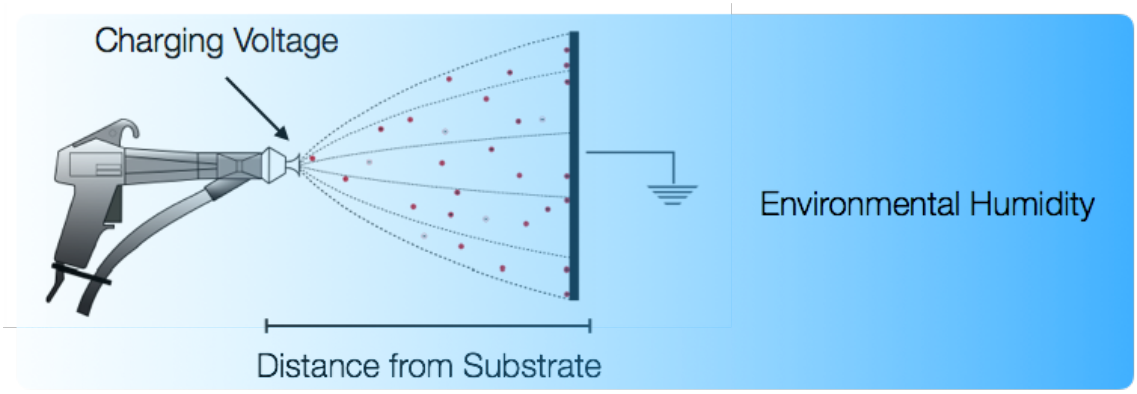

Factor	Low	Mid	High
Voltage (kV)	40	60	80
Distance (cm)	10	20	30
Humidity (%RH)	25	-	40

Figure 3.1. Schematic of electrostatic powder deposition and process parameters including charging voltage, distance from substrate, and environmental relative humidity.

To study the impact of process parameters during curing on film formation, the cure temperature and time was varied as follows: 70, 80 and 90°C for 15, 30 and 60 minutes. These samples were prepared using 60 kV charging voltage, 20 cm gun tip to substrate distance, and using unpolished SS 316 as the substrate. Environmental humidity was measured at 40-44 %RH during these preparations. Films (n=3 for each condition) were removed from the substrate using the texture analyzer to measure peel energy for removal, characterized for film formation using SEM, and tested for mechanical strength by puncture testing.

To study the impact of substrate properties on peel energy for film removal, substrates of varying surface finish including mirror finish #8, unpolished, brush finish #4, and sandblasted 70/100 were utilized as substrates for ESPD. Substrates were characterized by surface analysis techniques described above. Films (n=3 for each substrate) were prepared using were 80 kV charging voltage, 30 cm gun tip to substrate distance, and cured at 80°C for 60 minutes. The resulting films were removed from the substrate using the texture analyzer to measure peel energy for removal.

3.3.4 Adhesive Strength Testing

Samples for adhesion testing were equilibrated for at least 24 hours at room temperature. Scotch tape was applied to substrates and equilibrated for at least 24 hours at room temperature as a positive control for adhesion testing. Adhesive testing was carried out using a 90° peel test fixture (TA-305A) on a Texture Analyzer (Stable Micro System TA-XTplus) equipped with a 5 kg load cell. The test was conducted with a crosshead speed of 0.2 mm/s. Exponent software (Stable Microsystems, Godalming, Surrey, UK) was used to process data. The peel energy was calculated by equation 3.5.

$$G_a = \frac{F_{avg}}{b}(1 - \cos\theta) \tag{3.5}$$

where F_{avg} is the average force of removal, b is the width of the sample, and θ is the angle of peel force; θ=90° for the test fixture used in this study.

3.3.5 Mechanical Strength Testing

Mechanical properties of films were tested on a Texture Analyzer TA-XTplus (Stable Microsystems, Godalming, Surrey, UK) using 5 kg load cell. Samples were mounted on a TA-108s-5 fixture (Texture Technologies, Hamilton, MA, USA) and were punctured using a ¼" spherical probe moving at 1 mm/s. Exponent software (Stable Microsystems, Godalming, Surrey, UK) was used to process data. Tensile strength was calculated as shown in equation 3.6, as defined by Radebaugh et al. (Radebaugh et al., 1988).

$$\sigma_{TS} = \frac{F}{A_{cs}} \tag{3.6}$$

where F is the force at rupture (N) and A_{cs} is the cross sectional area of the film in the film holder (mm^2).

3.3.6 Scanning Electron Microscopy (SEM)

Samples were mounted onto pin stubs using conductive carbon adhesive tape and sputter coated with a 12 nm thickness of palladium/platinum under argon using a Cressington 208HR sputter coater (Cressington, Watford, UK). The Zeiss Supra field emission SEM (Zeiss, Oberkochen, Germany) was operated at an accelerating voltage of 5 kV to obtain images.

3.3.7 Disintegration Testing

Disintegration time was determined using a petri dish method. A petri dish containing 25 mL of Sørensen's buffer, pH 6.8 at 37 °C was placed in an incubating

shaker also held at 37 °C. The film sample, 25 x 25 mm, was gently placed on top of the media and the incubator shaker was set at 50 rpm to provide agitation. The time at which disintegration starts and the time for complete disintegration were recorded for n=3 samples.

3.4 RESULTS

3.4.1 Impact of applied voltage, distance from substrate, and environmental humidity on the deposition efficiency during ESPD

Films (n=3) were prepared using the conditions outlined in Figure 3.1. The weights of the film were used an indicator of deposition efficiency, whereby higher weights indicate increased deposition efficiency. The resulting film weights and corresponding standard deviations from these preparations are shown in Figure 3.2.

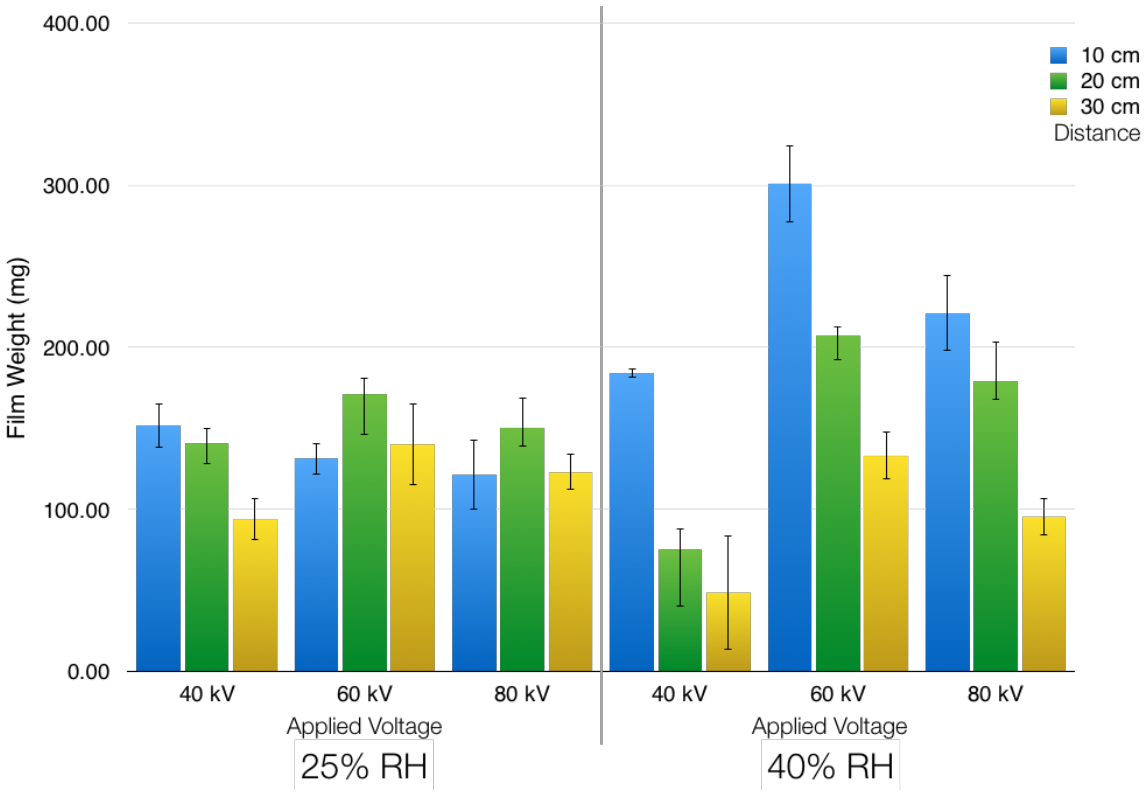

Figure 3.2. Weights and standard deviations from films (n=3) prepared using varying voltage (40, 60 and 80kV), distance from substrate (10, 20, and 30 cm), and at different environmental humidity conditions (25 and 40% RH).

The films prepared at 25 %RH showed less influence on deposition efficiency with changing voltage and distance from substrate than seen with films prepared at 40 %RH. One-way ANOVA using Tukey-Kramer HSD ($\alpha = 0.05$) to compare means of film weights produced at 25 %RH indicated only the mean weights of films prepared at 20 vs. 30 cm distances showed a significant difference ($p = 0.0046$). Films prepared at 40 %RH exhibited a more significant impact from processing parameters, with one-way ANOVA using Tukey-Kramer HSD ($\alpha = 0.05$) confirming significant differences in mean weights of films produced at 40 vs. 60 kV ($p=0.0042$), and 10 vs. 30 cm ($p<0.0001$) and vs. 20

cm (p=0.0090). The effect summary of the environmental humidity, applied voltage, and distance from substrate is shown in Figure 3.3; note that LogWorth is equal to -$\log_{10}$ (p value). This chart illustrates the significance of interactions of environmental humidity with voltage (p<0.0001), distance (p<0.0001) and voltage*distance (0.0071). Distance was also classified as a significant factor (p=0.0007).

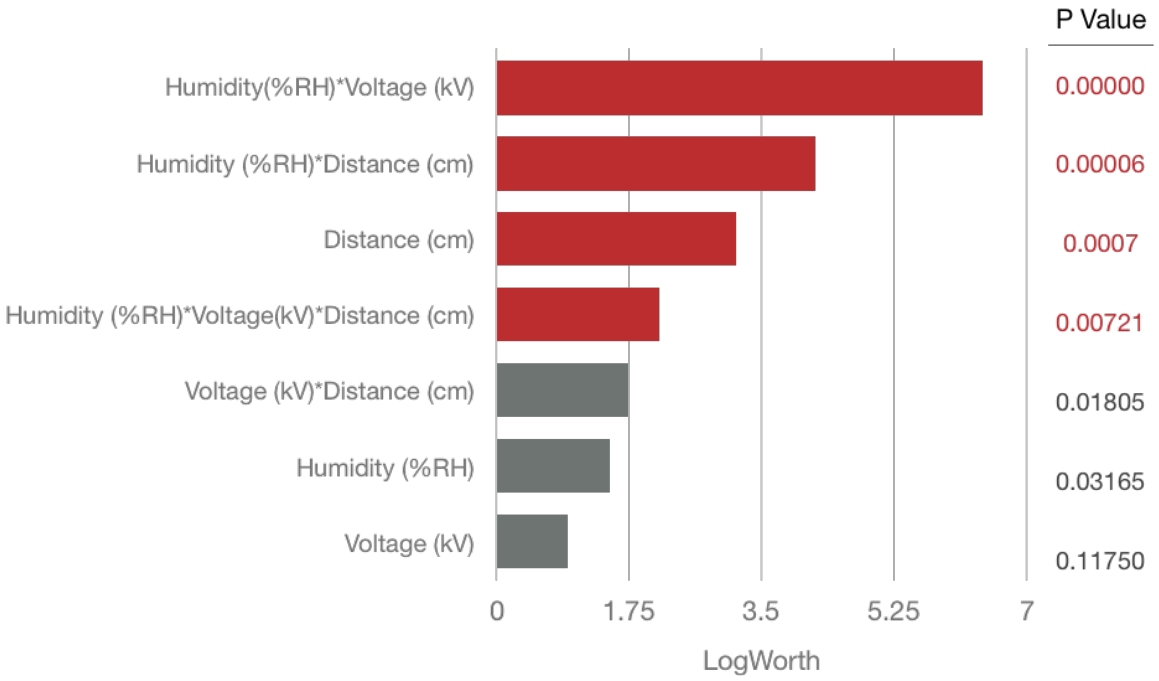

Figure 3.3. Summary of factors that significantly influenced deposition efficiency (shown in red) and factors that did not significantly affect deposition efficiency (shown in grey) and corresponding p-values.

At 40 %RH, the influence of the processing parameters on film weight was more marked than seen with the 25 %RH condition. A trend of decreasing deposition efficiency was seen with increasing distance from the substrate, illustrated in Figure 3.2. Additionally, deposition efficiency increased when charging voltage was increased from

40 to 60kV; however, a drop in weight was seen when voltage was increased from 60 to 80kV.

3.4.2 Impact of cure temperature and time on film formation, peel strength and mechanical properties

SEM micrographs obtained from the surface of the films cured at the varying temperature and time conditions are shown in Figure 3.4. After 15 minutes at 70°C particles were still undergoing deformation; however, after 60 minutes the particles edges and small voids can still be seen indicating incomplete coalescence. At 80 and 90°C after 15 minutes, much of the particle deformation and coalescence has taken place with some small voids visible and after 30 minutes complete coalescence is achieved.

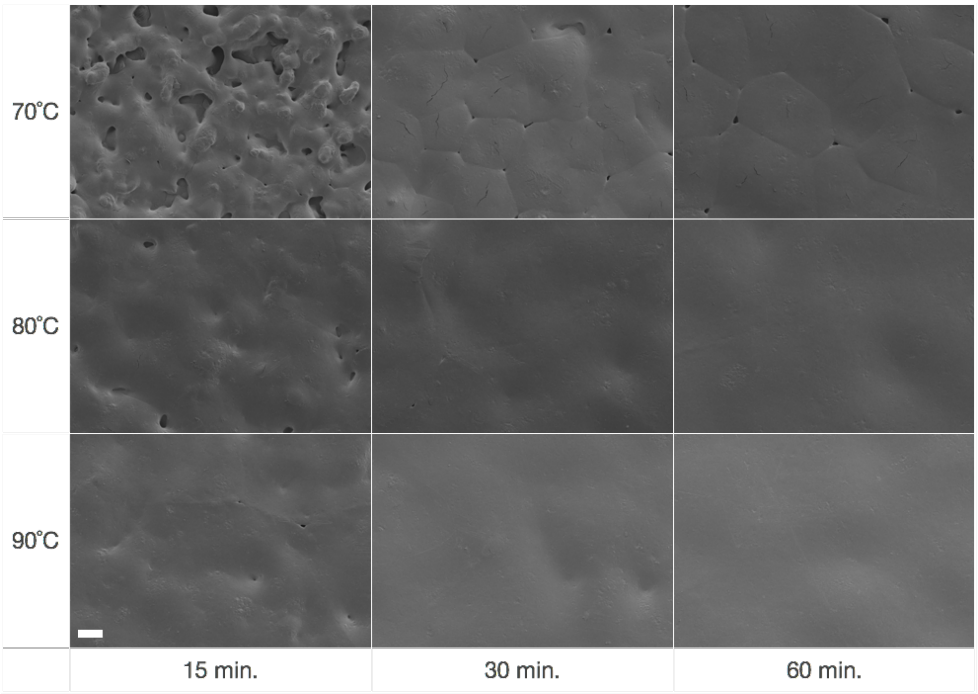

Figure 3.4. SEM micrographs of surface of PEO N10 films cured at varying temperatures (70, 80, and 90°C) and times (15, 30, or 60 minutes). White bar (lower left) represents 100 μm.

The peel energies to remove the cured films from the unpolished SS316 substrate are shown in Figure 3.5. All films required low peel energy for removal, with mean values of 21 J/m^2 or lower, corresponding to mean peel forces of 0.36N or lower. Cure temperature exhibited the most significant effect on peel energy (p=0.0107), with samples cured at 90°C for all time conditions requiring mean peel energies greater than 15 J/m^2.

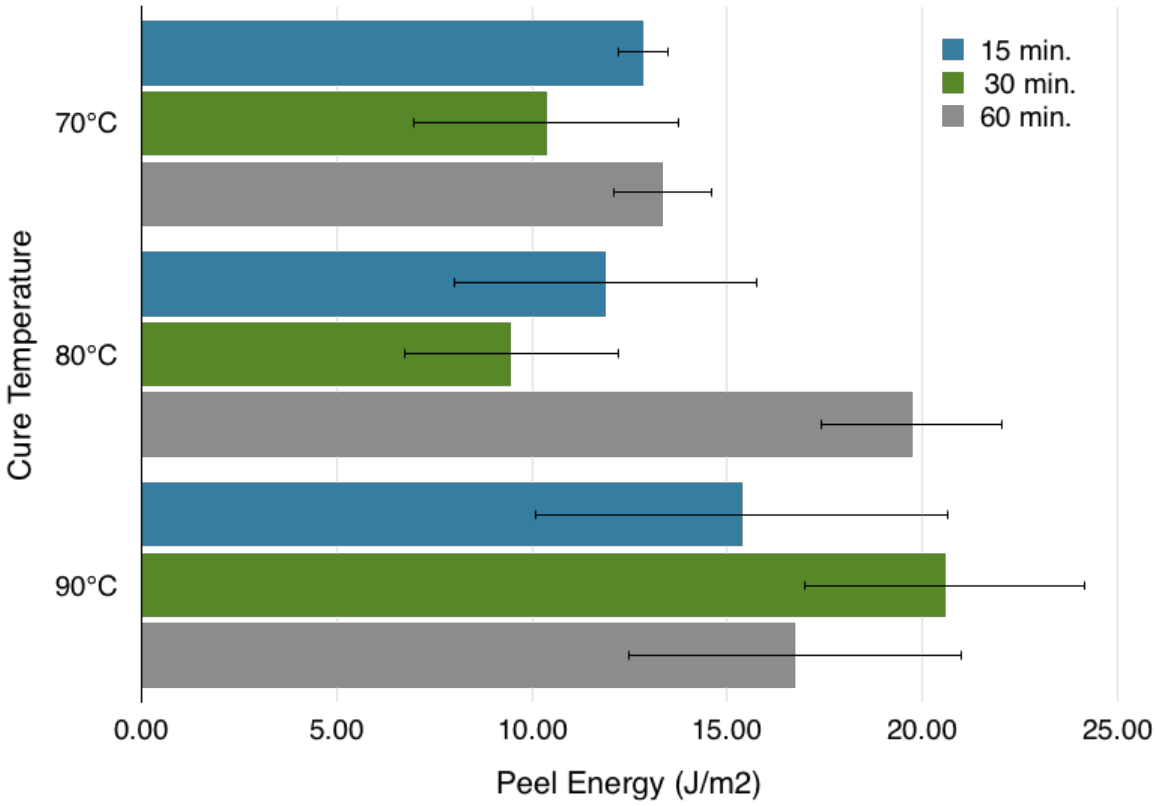

Figure 3.5. Peel energies measured to remove PEO N10 films (n=3) prepared at varying cure temperatures (70, 80, and 90°C) and times (15, 30, or 60 minutes) from unpolished, SS316 substrate.

Puncture testing was conducted to determine the mechanical properties of the films prepared from the varying cure conditions. The calculated tensile strengths of these films are shown in Figure 3.6. One-way ANOVA using Tukey-Kramer HSD ($\alpha = 0.05$) to compare means of the tensile strength determined that the 70°C cure temperature showed a somewhat significant difference from the means from the 80 and 90°C conditions, specifically due to the high mean tensile strength, 1.57 MPa, of the film from the 70°C, 15 minute curing condition. Excluding this value, the mean tensile strengths of the cured films ranged from 0.60-0.89 MPa.

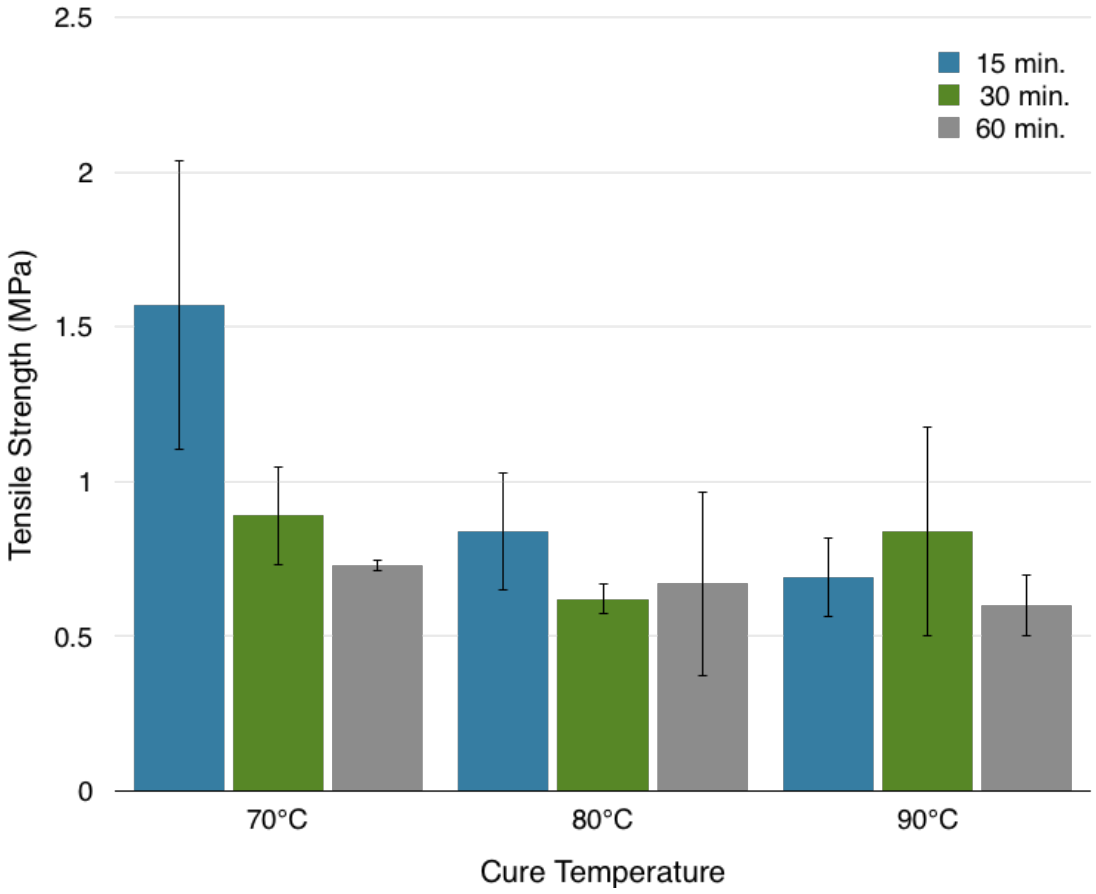

Figure 3.6. Tensile strength of PEO N10 films (n=3) prepared with varying cure temperatures (70, 80, 90°C) and time (15, 30, 60 minutes).

With comparable mechanical properties and complete film formation seen with 80°C and 90°C samples after 15 minutes, films from the 80°C, 60 minute cure condition were chosen to evaluate disintegration behavior. Initial disintegration of the films was observed by 10-12 s, as shown in Figure 3.7. A very thin film edge can still be seen by 30 s and complete disintegration was observed by 40-55 s.

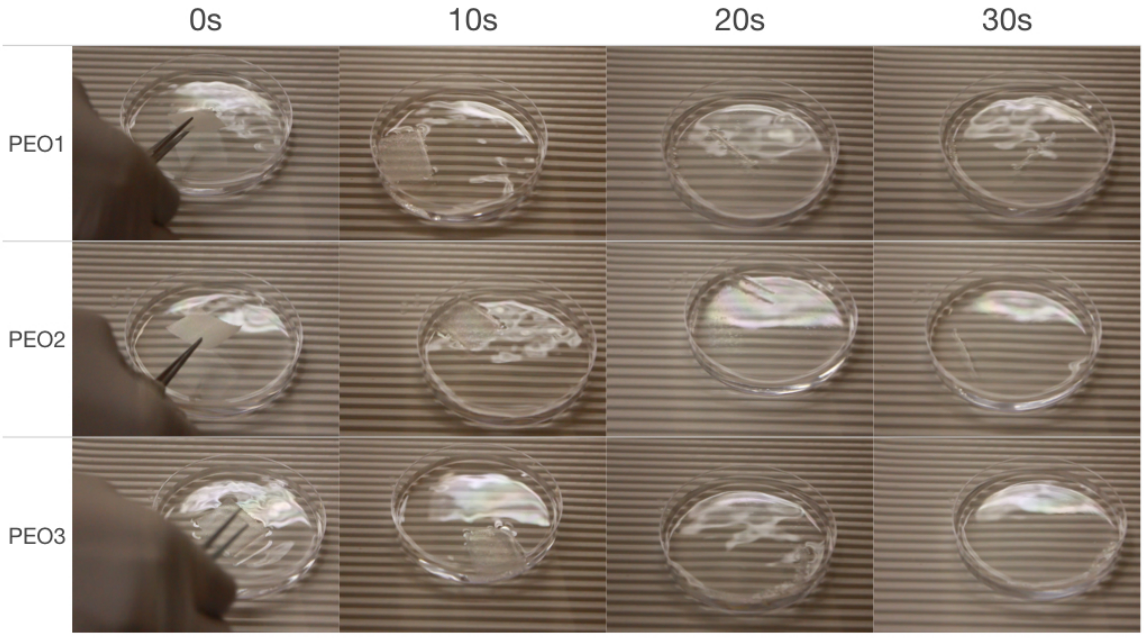

Figure 3.7. Images from disintegration testing of PEO N10 films (n=3) prepared at 80°C, 60 minute cure condition.

3.4.3 Impact of substrate properties on adhesion of the film to the substrate

Images of the surface topographies of the substrates of varying surface finish are shown in Figure 3.8 and the surface roughness values calculated for each of the as-received samples, as well as the sandblasted substrate, are summarized in Table 3.1. The mirror #8 and brush #4 topography revealed the striations from the polishing process used to obtain each finish. The topography of the unpolished sample revealed an irregular surface, typically seen with unpolished steel (Marshall, 1984). The sandblasted sample showed very distinct indentations from the abrasive treatment with relatively large beads (150-212 μm) producing a very coarse surface with high roughness value, R_a= 1080 nm.

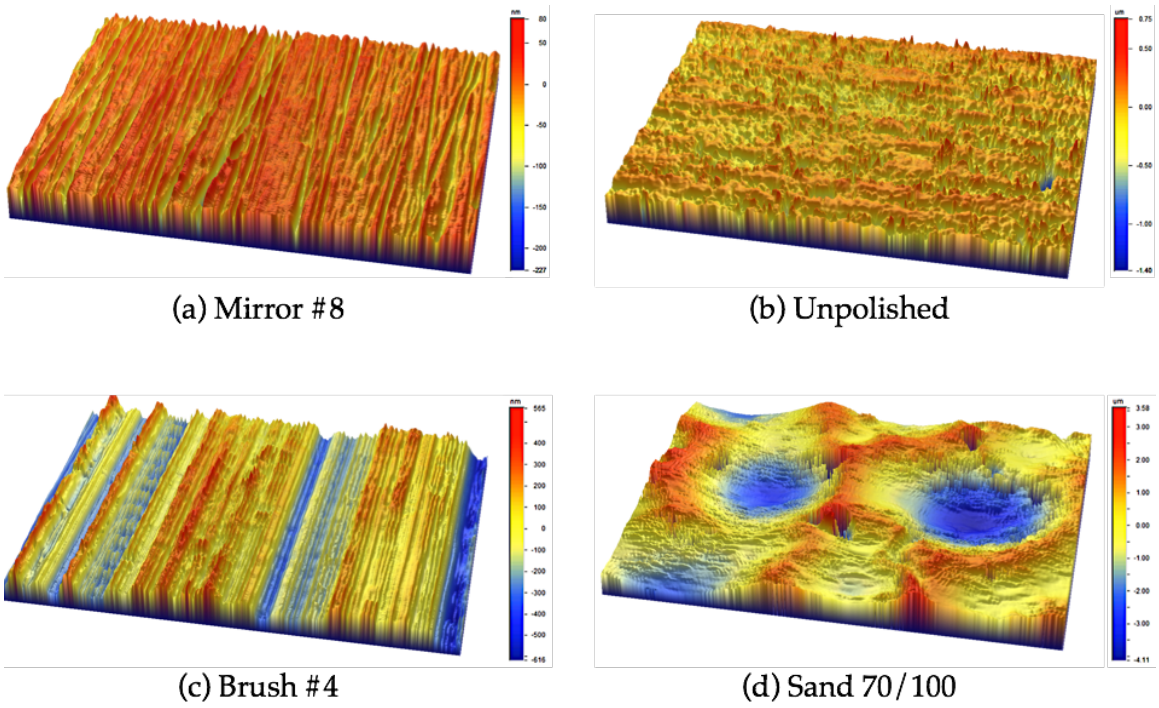

Figure 3.8. Images of surface topographies of (a) mirror #8, (b) unpolished, and (c) brush #4 finish as received, as well as (d) the sandblasted substrate prepared from abrasive treatment.

Table 3.1. Calculated substrate surface roughness values of as-received mirror, unpolished, and brush finish samples, as well as sandblasted substrate prepared from abrasive treatment. Values for average roughness, R_a, root mean squared roughness, R_q, and maximum height of roughness profile, R_t, reported, per equations 1, 2, and 3, respectively.

Substrate	Ra (nm)	Rq (nm)	Rt (um)
Mirror #8	20.04	26.99	0.31
Unpolished	111.87	150.79	2.15
Brush #4	154.45	185.71	1.18
Sand 70/100	1080	1370	7.69

Figure 3.9 summarizes the XPS data reported as atomic percentages for the surface of each of the substrates. All samples consisted of a carbon (54-58%) and oxygen (32-37%) rich surface layer. The sandblasted sample exhibited slightly elevated levels of Ni (0.79%) and Cr (6.62%) and slightly reduced Fe (1.75%) when compared to the as-received samples.

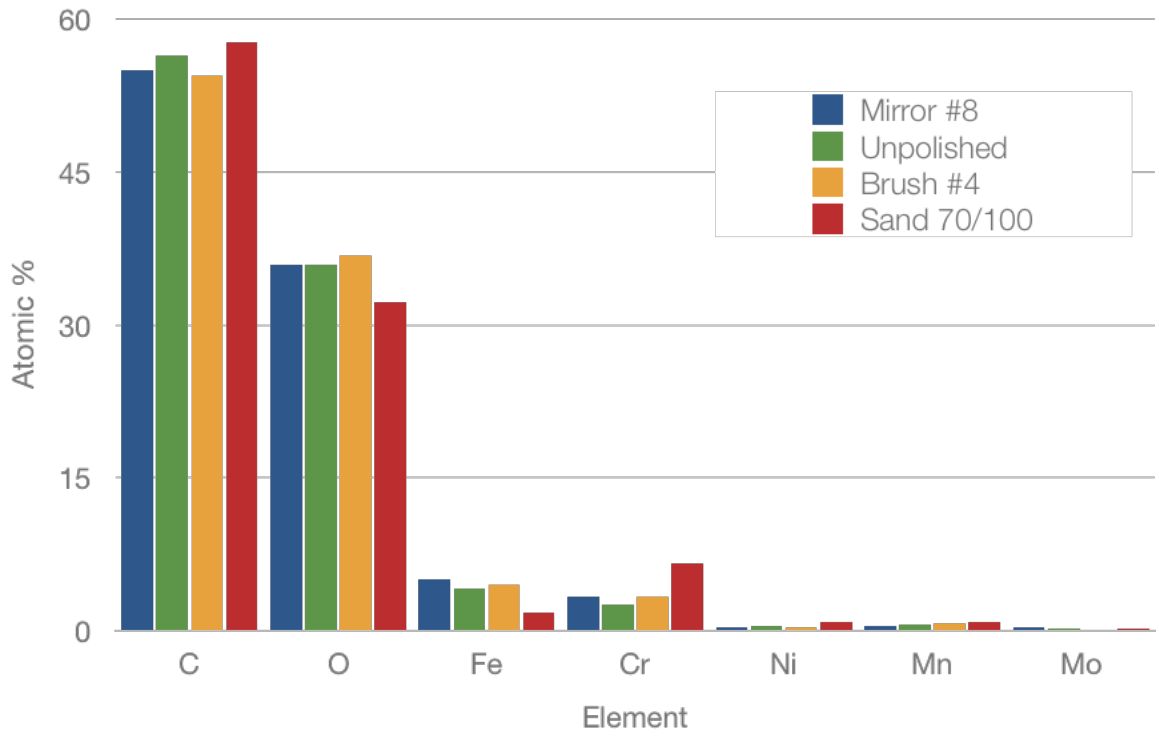

Figure 3.9. XPS data showing chemical composition in atomic % of substrate surfaces showing rich carbon (54-58%) and oxygen (32-37%) levels.

The measured contact angle and calculated surface energy of each substrate are reported in Table 3.2. The contact angles of water on these substrates were relatively high, indicative of a hydrophobic surface. These subsequently correlated with relatively low surface energies for all substrate surfaces, ranging from 31 to 36 mJ/m2.

Table 3.1. Average contact angles measured using water (n=3) and calculated solid surface energies of substrates of varying roughness according to Equation 3.4.

Substrate	Contact angle (°)	γs (mJ/m2)
Mirror #8	79.9	35.39
Unpolished	88.9	31.05
Brush #4	77.3	36.26
Sand 70/100	91.8	31.78

The peel energies to remove the cured films and scotch tape controls from the various substrates are shown in Figure 3.10. All samples exhibited an increasing peel force required to remove films from substrates with increasing surface roughness, with the exception of the removal of scotch tape from the sandblasted substrate. The mean peel energies of the scotch tape were 112, 235 and 547 J/m^2 to remove the film from the mirror #8, unpolished, and brush #4 finish, respectively. The removal of the scotch tape from the sandblasted sample showed lower peel energy of 209 J/m^2, slightly lower than that required for the removal from the unpolished substrate. The peel energies required to remove the PEO N10 film from all substrates were substantially lower than those needed to remove the scotch tape, requiring means values of 7, 20, 21 and 31 J/m^2 to remove the film from the mirror #8, unpolished, brush #4 and sandblasted finish, respectively, corresponding to mean peel forces in the range of 0.1 - 0.5 N.

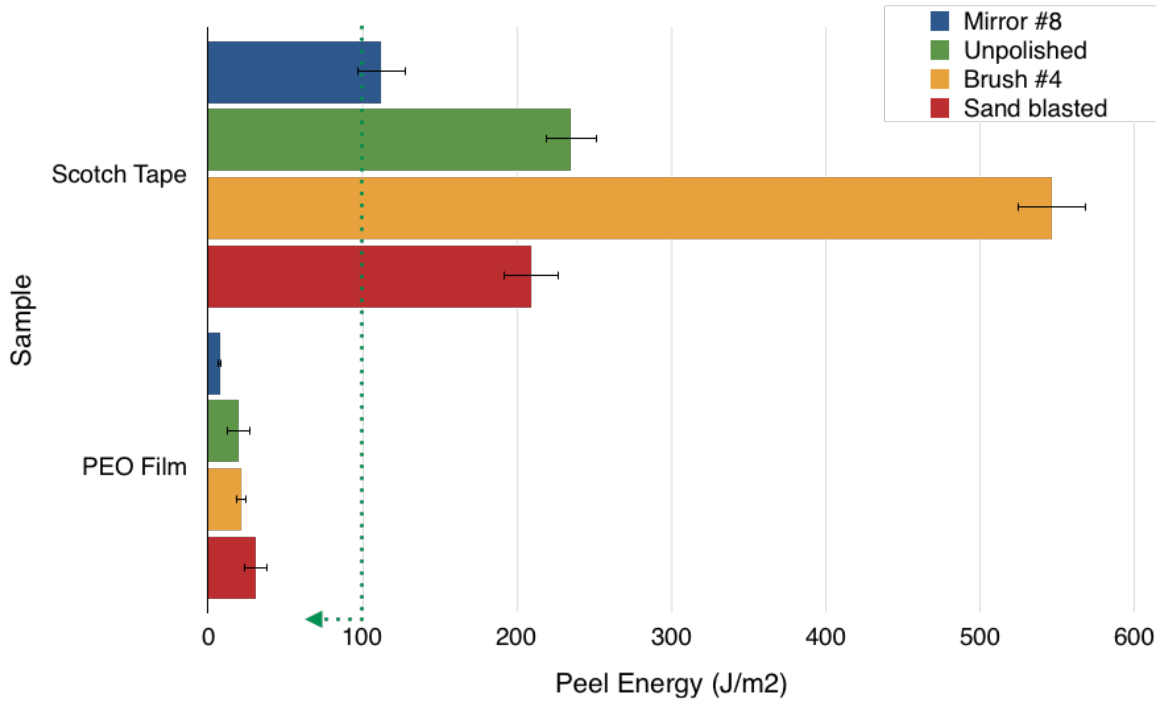

Figure 3.10. Peel energies measured to remove scotch tape (positive control, n=3) and PEO N10 films (n=3) from substrates of varying surface roughness.

3.5 DISCUSSION

3.5.1 Impact of applied voltage, distance from substrate, and environmental humidity on the deposition efficiency during ESPD

The resistivity of powders used for ESPD is critical to their performance. Insulating powders, classified as volume resistivity > 10^{10} Ωm, readily accumulate charge and exhibit slow charge dissipation or decay, allowing for strong adhesion to the grounded, conductive substrate (Bailey, 1998; Cazaux, 2007). However, excessive charge accumulation on the deposited powder particles can induce back ionization. Back ionization, or back corona, is a phenomenon where oppositely charged ions are produced which can neutralize incoming particles, thus preventing further deposition of powder

onto the substrate. In addition to limiting the powder layer thickness on the substrate, back ionization can also lead to surface defects, such as pitting, on the final film (Bailey, 1998; Cazaux, 2007; Prasad et al., 2016). Back ionization can be mitigated by methods such as incorporating free ion traps when using corona charging to reduce excess ion deposition on the substrate or reducing the resistivity and thus enabling faster charge dissipation of the coating material by formulating with conductive or antistatic additives; however, process parameters including lower charging voltage or higher environmental humidity can also significantly aid in reducing charge accumulation on the powder layer (Mazumder et al., 1997).

Given the dielectric properties of PEO, volume resistivity of 10^{10} - 10^{11} Ωm, it is a suitable powder for ESPD and has been previously utilized in this process to prepare drug-loaded films (Prasad et al., 2015). ESPD with PEO at 25 %RH appears to induce a self-limiting layer thickness, resulting in films of similar weights across all processing conditions, shown in Figure 3.2. Without sufficient environmental humidity to facilitate charge dissipation, the particle resistivity becomes the driving factor influencing deposition behavior. At this low humidity condition, the charged particles exhibit slow charge decay, leading to a high charge accumulation on the deposited powder layer. This charged powder layer then induces back ionization and prevents further powder deposition (Cazaux, 2007; Mazumder et al., 1997; Sims et al., 2000).

Increasing the environmental humidity can reduce particle resistivity. This effect is generally attributed to adsorbed moisture, which can reduce the particle surface resistivity and improve charge dissipation (Grosvenor and Staniforth, 1996; Karner and Urbanetz, 2011; Sharma et al., 2003). Increases in humidity can decrease resistivity by orders of magnitude; for example, Grosvenor et al. reported the resistivity of lactose and microcrystalline cellulose could be decreased from 10^{12} Ωm at 22 %RH to 10^{10} Ωm at 44

%RH (Grosvenor and Staniforth, 1996). With environmental humidity enabling reduced resistivity and faster charge dissipation, ESPD films produced at 40 %RH were not limited by the particle resistivity and were more influenced by other process parameters.

At each charging voltage, there was a decrease in the average film weight representing decreased deposition efficiency with increasing gun tip to substrate distance, shown in Figure 3.2. As the particles enter what is referred to as the transport region between the gun and the substrate, they are subject to several forces: aerodynamic forces from the compressed air used to spray the powder, the force on charged particles to follow the electric field produced by the electrode and grounded substrate, as well as the gravitational force of the particle itself. The smaller the distance between the gun tip and substrate, the more likely the particle will follow the electric field directed to the substrate and less material will be lost to overspray from the compressed air or to gravity. However, the gun tip to substrate distance affects the current flowing between the gun and the substrate; the closer the gun to the grounded substrate, the higher the current flow between the two, which corresponds to a higher number of free ions directed to the substrate. Thus, although more powder particles are depositing on the substrate at the 10 cm gun tip to substrate distance, so are more free ions. This increased deposition of free ions increases the probability of inducing back ionization (Guskov, 2002). For the low humidity condition, this was the likely cause of the drop in deposition weight seen with the 10 cm samples prepared with 60 and 80kV charging voltage when compared to those prepared at 20 and 30 cm at the same charging voltage.

At 40 %RH, an increasing deposition efficiency was seen when charging voltage was increased from 40 to 60kV. Increasing charging voltage can produce particles with a higher charge to mass ratios that exhibit stronger adhesion to the substrate to be coated. This can in turn increase deposition efficiency (Meng et al., 2009). However, if the

charging voltage is too high, back ionization can occur, leading to decreased deposition, as seen with the 80kV samples. This finding correlates well with other studies showing a loss of coating efficiency with higher charging voltage. Qiao et al. showed an increasing coating level achieved when electrostatically coating tablets with increasing charging voltage from 0 to 60kV; however, a decrease in levels were seen when using 80 to 100 kV (Qiao et al., 2010).

3.5.2 Impact of cure temperature and time on film formation, peel strength and mechanical properties

The mechanism of dry powder film formation, specifically with thermoplastic polymers, can be described by (1) deformation and coalescence of discrete powder particles, (2) spreading or leveling of the coalesced particles, and (3) the subsequent hardening of the film when removed from heat (Prasad et al., 2016; Sauer et al., 2013). The coalescence of discrete powder particles is a function of the viscosity and surface tension of the coating material at the cure temperature used, as well as the radius of the particles (Dillon et al., 1951). Curing temperatures are typically selected near or above the glass transition temperature for amorphous polymer systems and near or above the melting point for crystalline or semi-crystalline polymers to promote viscous flow. The minimum film formation temperature (MFFT) is another value utilized in the coating industry. MFFT is defined as the minimum temperature at which a continuous film will form for a given material, typically this value is near the T_g for many polymer systems (Jensen and Morgan, 1991; Keddie and Routh, 2010).

PEO N10 is a semi-crystalline polymer that exhibits a broad melt endotherm spanning 61-75°C (Prasad et al., 2015). When cured at 70°C, Figure 3.4 shows that after 15 minutes particles were still undergoing deformation and after 60 minutes the film

exhibits incomplete coalescence with visible voids. Visual observations made of the films correlate with these findings, as films were still opaque upon removing at 15 minutes, whereas films cured for 30 and 60 minutes were translucent. Films prepared at 80 and 90°C were transparent by 15 minutes, suggesting a transparent film could be indicative of achieving sufficient melt and/or film formation. Thus, at 70°C there was sufficient melt flow to initiate particle deformation and coalescence, but not to facilitate complete coalescence and film formation by 60 minutes due to high melt viscosity (Uhlmann and Grundke). Higher temperatures, at both 80 and 90°C, enabled a further decrease in melt viscosity to decrease the time needed for deformation and coalescence, with minimal voids observed after 15 minutes and complete film formation after 30 minutes.

The peel energies for removing cured films from the unpolished SS316 substrate were all relatively low, with mean values less than 21 J/m^2. Note that a good adhesive (i.e. tape) typically requires peel energies > 100 J/m^2 for removal (Gay, 2002). However, there was a slight increase in mean peel energies with values greater than 15 J/m^2 obtained for samples cured at 80°C for 60 minutes are those cured at 90°C. This can be attributed to increased spreading of the molten polymer across the substrate at these conditions due to the reduced melt viscosities at these temperatures and contact time. Increased spreading or wetting of coating material onto the substrate has been directly linked to increased coating efficiency (Sauer and McGinity, 2009; Smikalla et al., 2011). The corresponding increase in interfacial contact area between the coating and the substrate enhanced the adhesion between the two materials, leading to an increase, albeit a small increase, in adhesive strength (Kinloch, 1980).

The tensile strength of films cured at the varying conditions did not vary significantly, ranging from 0.6 to 0.9 MPa, with the exception of that of the 70°C, 15 minute condition. The 70°C, 15 minute film exhibited a significantly higher tensile

strength with a mean tensile strength around 1.6 MPa. In Figure 3.4, the 70°C, 15 minute sample showed a lesser degree of particle coalescence than the other time and temperature cure conditions and visual observations reported an opaque final film, indicating insufficient melt for film formation. Semi-crystalline polymers consist of both crystalline and amorphous regions. The crystalline regions are dense, typically described as lamellar regions of folded chains, and are mechanically stronger than the amorphous regions. This strength is attributed to the density and the increased degree of bonding between the polymer chains (i.e. hydrogen, van der Waals, etc.) (Peterlin, 1975; Ward and Sweeney, 2012). With a reduced degree of melt and coalescence seen with the films cured at 70°C for 15 minutes, the polymer retained a higher degree of crystallinity and thus exhibited a higher mechanical strength.

A disintegration test was conducted using films from the 80°C, 60 minute cure condition as this condition showed complete film formation and comparable mechanical properties as films from 80°C and 90°C samples at 30 and 60 minutes. Rapid disintegration was observed by 10-12 s with complete disintegration in less than one minute, confirming satisfactory performance of PEO-based orodispersible films. The authors previously confirmed rapid drug release of acetaminophen (APAP) from APAP: PEO orodispersible films prepared by ESPD, showing greater than 85% drug release by 2 minutes (Prasad et al., 2015).

3.5.3 Impact of substrate properties on adhesion of the film to the substrate

Stainless steel 316 was chosen as a substrate for this study as it the primary material of choice for the construction of pharmaceutical equipment due to its resistance to corrosion (Cramer and Covino, 2006; Marshall, 1984). This characteristic is attributed

to the formation of a dense, protective chromium oxide (Cr_2O_3) layer on the surface of the metal, preventing oxidation of the bulk composition, specifically preventing rust formation (Fe_2O_3) (Adams, 1983; Detry et al., 2010). Paired with its electrical conductivity (Ho and Chu, 1977), SS 316 is a suitable substrate for the preparation of free films by ESPD. As shown in Figure 3.8, there were clear contrasts between the surface topographies of each finish. The mirror and brush finish exhibited unidirectional striations from the grit polishing process, while the unpolished surface showed an irregular microstructure of a rolled or laminated stainless steel surface (Marshall, 1984). The sandblasted sample topography included circular depressions from the abrasive treatment beads. The roughness values reported in Table 2 quantify the increasing surface roughness with average roughness values, R_a, ranging from 20 to 154 nm for the as-received mirror #8 and the brush #4 finish, respectively, and jumping to 1080 nm with the sandblasted surface. Notably, the maximum height profile of the unpolished sample was greater than that of the brush #4 sample; this was due to the grit polishing process used to prepare the brush #4 finish.

While the bulk composition of SS316 chiefly consists of an iron alloy with Cr (16-18), Ni (10-14) Mo (2-3) and small amounts of other effective elements, the surface is comprised of a dense chromium oxide (Cr_2O_3) layer that prevents iron oxidation or rusting (Adams, 1983). When exposed to ambient air, the surface is further covered by carbon and oxygen. The heavy carbon and oxygen content is due to physical adsorption of hydrocarbon contamination, such as alcohols or esters, onto the surface of the metal (Adams, 1983; Mazumder et al., 2006). Carbon was measured at 54-58% and oxygen at 32-37% of the surface composition, shown in Figure 9, confirming the presence of an adsorbed hydrocarbon layer. This hydrocarbon layer contributed to the hydrophobic nature of the surface, with contact angles ranging from 77-92° (Faille et al., 2002; Flint et

al., 2000). The calculated surface energies for these surfaces were relatively low, ranging 31-36 mJ/m^2. These low surface energy, hydrophobic substrates facilitated a low degree of adhesion with the hydrophilic PEO N10 film. The Ni and Cr enrichment and corresponding decrease in Fe seen with the sandblasted sample is characteristic of the sample undergoing mechanical abrasive treatments and the reformation of the chromium oxide layer during acid treatment (Adams, 1983; Haidopoulos et al., 2006; Rohly et al., 2003). Overall, the XPS analyses confirm that these substrates did not differ significantly in their chemical composition. Thus, the substrates only differ in their surface roughness and topography.

The scotch tape, used as a reference for the peel test, showed a significant influence of substrate roughness on the mean peel energy, with > 100 J/m^2 of peel force required for the mirror finish and around 550 J/m^2 required for removal from the brush finish. Notably, the force required for the removal of the scotch tape from the sandblasted substrate was slightly lower than that for the unpolished substrate. This was attributed to the thin adhesive layer of the tape and the deep indentations of the sandblasted sample. The thin adhesive layer was unable to make contact with the surfaces along the inside of the deep indents. Thus, the tape was only adhered to the top surface of the substrate with gaps in the interfacial contact area corresponding to the indents. This resulted in a significantly lower interfacial contact area and reduced adhesion.

The PEO films were not as significantly impacted by the surface roughness of the substrate. Although a general trend was seen in that the peel energy increased with increasing surface roughness, the average peel force from all substrates was less than 31 J/m2. This signifies that the removal of the PEO film was robust and requires very little force, confirming that there was no significant adhesion or bonding between the polymer and metal substrate. This finding was consistent with the characterization of the SS316

substrate as a low-energy, hydrophobic surface. Thus, with the absence of chemical bonding or mechanical interlocking, the mechanism of adhesion between the PEO film and metal substrate is primarily due to weak Van der Waals and/or electrostatic forces (Kinloch, 2012; Ramarathnam et al., 1992). The incremental increases in adhesive peel energy with increasing roughness attributed to an increase in surface area of the roughened metal, leading to increased interfacial contact area between the film and substrate (Kinloch, 1980; Packham, 2003).

3.6 CONCLUSION

Electrostatic powder coating has been used extensively in the finishing industry as a solvent-free and energy efficient coating operation. Here, we have demonstrated that this process can be adapted and optimized to produce non-adhering, free films by utilizing a substrate that does not readily bond, mechanically or chemically, with the powder coating material. The effect of various processing parameters was evaluated on (1) the deposition efficiency, (2) film formation, and (3) removal of PEO N10 free films prepared using ESPD. At low humidity (25 %RH), the processing parameters studied showed little effect on overall deposition efficiency due to the onset of back ionization, whereas at increased humidity levels (40 %RH) trends of increasing deposition efficiency with decreasing gun tip to substrate distance and increasing voltage (up to 60kV) was observed. Back ionization was attributed to the self-limiting deposition efficiency at 25 %RH, as well as to the drop in deposition efficiency at 80 kV at 40 %RH. The PEO N10 films exhibited complete film formation by 30 minutes at 80 and 90°C. Peel testing of the films exhibited slightly increased adhesive strength (> 15 J/m2) for films cured at 80°C for 60 minutes or those cured at 90°C due to increased spreading and thus increased

interfacial contact area for adhesion. Adhesive strength was also tested with substrates of varying finishes and exhibited a trend of increasing adhesive strength with increasing roughness. This finding was again attributed to greater interfacial contact with the substrate. All PEO films were readily removed from the SS316 substrates due to the hydrophobic nature and low surface energy of the surface. The ESPD process was able to produce films with good mechanical properties, demonstrating its application as an alternative to the traditional solvent-casting manufacturing process. This study also serves as guidance for the evaluation of additional pharmaceutical compositions and substrates.

3.7 ACKNOWLEDGEMENTS

We gratefully acknowledge support from an American Foundation for Pharmaceutical Education Grant Fellowship to Leena Kumari Prasad. Additionally, we thank the National Science Foundation (Grant No. 0618242) for funding the Kratos Axis Ultra XPS used in this work.

3.8 REFERENCES

2015. The United States Pharmacopeial Convention. General Chapter: 1151 Pharmaceutical Dosage Forms. USP 38–NF 33 Rockville, MD: The United States Pharmacopeial Convention, The United States Pharmacopeia and The National Formulary.

Adams, R., 1983. A review of the stainless steel surface. Journal of Vacuum Science & Technology A 1, 12-18.

ASTM, 2013. A380/A380M Practice for Cleaning, Descaling, and Passivation of Stainless Steel Parts, Equipment, and Systems. Equipment and Systems.

Bailey, A.G., 1998. The science and technology of electrostatic powder spraying, transport and coating1. Journal of Electrostatics 45, 85-120.

Borges, A.F., Silva, C., Coelho, J.F.J., Simões, S., 2015. Oral films: Current status and future perspectives: I — Galenical development and quality attributes. Journal of Controlled Release 206, 1-19.

Cazaux, J., 2007. Critical thicknesses of electrostatic powder coatings from inside. Journal of Electrostatics 65, 764-774.

Constable, D.J.C., Jimenez-Gonzalez, C., Henderson, R.K., 2007. Perspective on Solvent Use in the Pharmaceutical Industry. Organic Process Research & Development 11, 133-137.

Cramer, S.D., Covino, B.S., 2006. Corrosion: Environments and industries. ASM International.

Detry, J.G., Sindic, M., Deroanne, C., 2010. Hygiene and cleanability: a focus on surfaces. Critical reviews in food science and nutrition 50, 583-604.

Dillon, R., Matheson, L., Bradford, E., 1951. Sintering of synthetic latex particles. Journal of Colloid Science 6, 108-117.

Dixit, R.P., Puthli, S.P., 2009. Oral strip technology: Overview and future potential. Journal of Controlled Release 139, 94-107.

Faille, C., Jullien, C., Fontaine, F., Bellon-Fontaine, M.-N., Slomianny, C., Benezech, T., 2002. Adhesion of Bacillus spores and Escherichia coli cells to inert surfaces: role of surface hydrophobicity. Canadian Journal of Microbiology 48, 728-738.

Flint, S.H., Brooks, J.D., Bremer, P.J., 2000. Properties of the stainless steel substrate, influencing the adhesion of thermo-resistant streptococci. Journal of Food Engineering 43, 235-242.

Gay, C., 2002. Stickiness—Some Fundamentals of Adhesion. Integrative and Comparative Biology 42, 1123-1126.

Good, R.J., 1992. Contact angle, wetting, and adhesion: a critical review. Journal of adhesion science and technology 6, 1269-1302.

Grodowska, K., Parczewski, A., 2010. Organic solvents in the pharmaceutical industry. Acta poloniae pharmaceutica 67, 3-12.

Grosvenor, M.P., Staniforth, J.N., 1996. The Influence of Water on Electrostatic Charge Retention and Dissipation in Pharmaceutical Compacts for Powder Coating. Pharmaceutical research 13, 1725-1729.

Guskov, S., 2002. Electrostatic phenomena in powder coating. Powder System Group Nordson Corporation.

Gutierrez-Rocca, J.C., Mcginity, J.W., 1993. Influence of aging on the physical-mechanical properties of acrylic resin films cast from aqueous dispersions and organic solutions. Drug Development and Industrial Pharmacy 19, 315-332.

Haidopoulos, M., Turgeon, S., Sarra-Bournet, C., Laroche, G., Mantovani, D., 2006. Development of an optimized electrochemical process for subsequent coating of 316 stainless steel for stent applications. J Mater Sci: Mater Med 17, 647-657.

Harmuth, C.M., 1982. Melt-blending method of forming pigmented powder coatings. Google Patents.

Ho, C.Y., Chu, T., 1977. Electrical resistivity and thermal conductivity of nine selected AISI stainless steels. DTIC Document.

Hogan, J.E., Page, T., Reeves, L., Staniforth, J.N., 2002. Powder coating composition for electrostatic coating of pharmaceutical substrates. Phoqus Limited.

Jensen, D., Morgan, L., 1991. Particle size as it relates to the minimum film formation temperature of latices. Journal of applied polymer science 42, 2845-2849.

Karner, S., Urbanetz, N.A., 2011. The impact of electrostatic charge in pharmaceutical powders with specific focus on inhalation-powders. Journal of Aerosol Science 42, 428-445.

Keddie, J.L., Routh, A.F., 2010. Particle Deformation, Fundamentals of Latex Film Formation: Processes and Properties. Springer Netherlands, Dordrecht, pp. 121-150.

Kianfar, F., Chowdhry, B.Z., Antonijevic, M.D., Boateng, J.S., 2012. Novel films for drug delivery via the buccal mucosa using model soluble and insoluble drugs. Drug Dev Ind Pharm 38, 1207-1220.

Kinloch, A., 2012. Adhesion and adhesives: science and technology. Springer Science & Business Media.

Kinloch, A.J., 1980. The science of adhesion. J Mater Sci 15, 2141-2166.

Marshall, P., 1984. Austenitic stainless steels: microstructure and mechanical properties. Springer Science & Business Media.

Mazumder, M.K., Sims, R.A., Biris, A.S., Srirama, P.K., Saini, D., Yurteri, C.U., Trigwell, S., De, S., Sharma, R., 2006. Twenty-first century research needs in electrostatic processes applied to industry and medicine. Chemical Engineering Science 61, 2192-2211.

Mazumder, M.K., Wankum, D.L., Sims, R.A., Mountain, J.R., Chen, H., Pettit, P., Chaser, T., 1997. Influence of powder properties on the performance of electrostatic coating process. Journal of Electrostatics 40–41, 369-374.

Meng, X., Zhu, J.J., Zhang, H., 2009. The characteristics of particle charging and deposition during powder coating processes with ultrafine powder. Journal of Physics D: Applied Physics 42, 065201.

Morales, J.O., McConville, J.T., 2011. Manufacture and characterization of mucoadhesive buccal films. European Journal of Pharmaceutics and Biopharmaceutics 77, 187-199.

Noonan, C.M., 1977. Thin film electrostatic epoxy coating powder. Google Patents.

Owens, D.K., Wendt, R., 1969. Estimation of the surface free energy of polymers. Journal of applied polymer science 13, 1741-1747.

Packham, D.E., 2003. Surface energy, surface topography and adhesion. International Journal of Adhesion and Adhesives 23, 437-448.

Patel, V.F., Liu, F., Brown, M.B., 2011. Advances in oral transmucosal drug delivery. Journal of Controlled Release 153, 106-116.

Peterlin, A., 1975. Structural model of mechanical properties and failure of crystalline polymer solids with fibrous structure. International Journal of Fracture 11, 761-780.

Prasad, L.K., Keen, J.M., LaFountaine, J.S., Maincent, J., Williams Iii, R.O., McGinity, J.W., 2015. Electrostatic powder deposition to prepare films for drug delivery. Journal of Drug Delivery Science and Technology 30, Part B, 501-510.

Prasad, L.K., McGinity, J.W., Williams Iii, R.O., 2016. Electrostatic powder coating: Principles and pharmaceutical applications. International Journal of Pharmaceutics 505, 289-302.

Preis, M., Woertz, C., Schneider, K., Kukawka, J., Broscheit, J., Roewer, N., Breitkreutz, J., 2014. Design and evaluation of bilayered buccal film preparations for local administration of lidocaine hydrochloride. European Journal of Pharmaceutics and Biopharmaceutics 86, 552-561.

Qiao, M., Zhang, L., Ma, Y., Zhu, J., Chow, K., 2010. A novel electrostatic dry powder coating process for pharmaceutical dosage forms: Immediate release coatings for tablets. European Journal of Pharmaceutics and Biopharmaceutics 76, 304-310.

Radebaugh, G.W., Murtha, J.L., Julian, T.N., Bondi, J.N., 1988. Methods for evaluating the puncture and shear properties of pharmaceutical polymeric films. International Journal of Pharmaceutics 45, 39-46.

Ramarathnam, G., Libertucci, M., Sadowski, M., North, T., 1992. Joining of polymers to metal. WELDING JOURNAL-NEW YORK- 71, 483-s.

Rohly, K., Istephanous, N., Belu, A., Untereker, D., Coscio, M., Heffelfinger, J., Thomas, R., Allen, J., Francis, R., Robinson, A., 2003. Effect of time, temperature, and solution composition on the passivation of 316L stainless steel for biomedical applications, Materials Science Forum. Trans Tech Publ, pp. 3017-3022.

Sastry, S.V., Nyshadham, J.R., Fix, J.A., 2000. Recent technological advances in oral drug delivery – a review. Pharmaceutical Science & Technology Today 3, 138-145.

Sauer, D., Cerea, M., DiNunzio, J., McGinity, J., 2013. Dry powder coating of pharmaceuticals: A review. International Journal of Pharmaceutics 457, 488-502.

Sauer, D., McGinity, J.W., 2009. Influence of additives on melt viscosity, surface tension, and film formation of dry powder coatings. Drug development and industrial pharmacy 35, 646-654.

Sauer, D., Zheng, W., Coots, L.B., McGinity, J.W., 2007. Influence of processing parameters and formulation factors on the drug release from tablets powder-coated with Eudragit® L 100-55. European Journal of Pharmaceutics and Biopharmaceutics 67, 464-475.

Shakya, P., Madhav, N.V.S., Shakya, A.K., Singh, K., 2011. Palatal mucosa as a route for systemic drug delivery: A review. Journal of Controlled Release 151, 2-9.

Sharma, R., Trigwell, S., Biris, A.S., Sims, R.A., Mazumder, M.K., 2003. Effect of ambient relative humidity and surface modification on the charge decay properties of polymer powders in powder coating. Industry Applications, IEEE Transactions on 39, 87-95.

Shen, B.d., Shen, C.y., Yuan, X.d., Bai, J.x., Lv, Q.y., Xu, H., Dai, L., Yu, C., Han, J., Yuan, H.l., 2013. Development and characterization of an orodispersible film containing drug nanoparticles. European Journal of Pharmaceutics and Biopharmaceutics 85, 1348-1356.

Sievens-Figueroa, L., Bhakay, A., Jerez-Rozo, J.I., Pandya, N., Romañach, R.J., Michniak-Kohn, B., Iqbal, Z., Bilgili, E., Davé, R.N., 2012. Preparation and characterization of hydroxypropyl methyl cellulose films containing stable BCS

Class II drug nanoparticles for pharmaceutical applications. International Journal of Pharmaceutics 423, 496-508.

Sims, R., Mazumder, M., Biris, A., Sharma, R., Kumar, D., 2000. Effect of electrical resistivity on the adhesion and thickness of electrostatically deposited powder layers, Industry Applications Conference, 2000. Conference Record of the 2000 IEEE. IEEE, pp. 820-823.

Smikalla, M., Mescher, A., Walzel, P., Urbanetz, N.A., 2011. Impact of excipients on coating efficiency in dry powder coating. International Journal of Pharmaceutics 405, 122-131.

Stegemann, S., Ecker, F., Maio, M., Kraahs, P., Wohlfart, R., Breitkreutz, J., Zimmer, A., Bar-Shalom, D., Hettrich, P., Broegmann, B., 2010. Geriatric drug therapy: Neglecting the inevitable majority. Ageing Research Reviews 9, 384-398.

Stegemann, S., Gosch, M., Breitkreutz, J., 2012. Swallowing dysfunction and dysphagia is an unrecognized challenge for oral drug therapy. International Journal of Pharmaceutics 430, 197-206.

Sudhakar, Y., Kuotsu, K., Bandyopadhyay, A.K., 2006. Buccal bioadhesive drug delivery — A promising option for orally less efficient drugs. Journal of Controlled Release 114, 15-40.

Uhlmann, P., Grundke, K., Influence of additives on interfacial phenomena during film formation of powder coatings. Journal of Coatings Technology 73, 59-65.

Visser, J.C., Dohmen, W.M.C., Hinrichs, W.L.J., Breitkreutz, J., Frijlink, H.W., Woerdenbag, H.J., 2015. Quality by design approach for optimizing the formulation and physical properties of extemporaneously prepared orodispersible films. International Journal of Pharmaceutics 485, 70-76.

Ward, I.M., Sweeney, J., 2012. Mechanical properties of solid polymers. John Wiley & Sons.

Wicks, Z.W., Jones, F.N., Pappas, S.P., Wicks, D.A., 2007. Organic coatings: science and technology, 3rd ed. Wiley-Interscience, Hoboken, N.J.

Young, T., 1805. An Essay on the Cohesion of Fluids. Philosophical Transactions of the Royal Society of London 95, 65-87.

Zhang, H., Zhang, J., Streisand, J., 2002. Oral Mucosal Drug Delivery. Clin Pharmacokinet 41, 661-680.

Chapter 4: Electrostatic Powder Deposition to Prepare Films for Drug Delivery[1]

4.1 ABSTRACT

An electrostatic powder deposition (ESPD) method was developed to prepare free films for drug delivery. Films were prepared using polyethylene oxide (PEO), a physical mixture of PEO and acetaminophen (APAP), and co-processed PEO and APAP particles. Compositions were charged by an electrostatic spray gun and deposited onto a grounded stainless steel coupon. The deposited powders were cured and free films were peeled from the substrate. Average drug content of the active films was 97% of theoretical. Films prepared using the physical mixture of the powders showed greater variability with an RSD of 11.9% compared to 1.8% from films prepared using co-processed particles. Mechanical testing of the prepared films showed lower puncture strength than commercially available Listerine® strips, but exhibited greater elongation prior to break. Active films showed up to 15% elongation compared to 1.6% from Listerine® strips and 3.8% from PEO films, due primarily to the plasticizing effect of APAP on PEO in the drug containing films. Both active films exhibited greater than 85% drug release in 2 minutes. This study is the first to demonstrate the application of ESPD to prepare free films for drug delivery; however, future studies of this technology are needed to determine its full potential.

[1] This work has been published in Prasad, L.K., Keen, J.M., LaFountaine, J.S., Maincent, J., Williams Iii, R.O., McGinity, J.W., 2015. Electrostatic powder deposition to prepare films for drug delivery. Journal of Drug Delivery Science and Technology 30, Part B, 501-510.

4.2 INTRODUCTION

The development of oral films for drug delivery has been a growing area of research as a valuable dosage form to increase patient compliance, eliminate the need for dosing with water, and/or bypass first pass metabolism using buccal delivery (Borges et al., 2015; Dixit and Puthli, 2009; Obermeier et al., 2008). Many patients, particularly in the pediatric and geriatric patient population, have difficulty swallowing tablets and capsules, making an oral film a desirable dosage form (Lam et al., 2014; Stegemann et al., 2010; Stegemann et al., 2012). Oral films are typically manufactured using solvent casting or hot melt extrusion (HME) (2015; Borges et al., 2015; Dixit and Puthli, 2009; Morales and McConville, 2011), each of which exhibits certain limitations. The limitations with solvent casting are largely based on the need for a solvent, aqueous or organic. Aqueous solutions have a slow rate of drying, with many aqueous solvent casting processes requiring up to 24 hours of drying time (Kianfar et al., 2012; Shen et al., 2013; Sievens-Figueroa et al., 2012; Visser et al., 2015). The use of organic solvents is particularly undesirable from an environmental standpoint and requires the manufacturing process train to include solvent handling and collection capabilities (Constable et al., 2007; Grodowska and Parczewski, 2010); residual solvent testing is required on the final drug product for any solvents considered toxic . Additionally, solvent casting can lead to sedimentation and/or phase separation during drying, resulting in nonhomogeneous films (Hopkinson and Myatt, 2002). Formulation development activities for solvent cast films include appropriate solvent selection and ensuring solution rheology is amenable to the casting process (Preis et al., 2014b). Similarly, the use of HME for film manufacture can be limited, as it requires that the active pharmaceutical ingredient (API) and polymer are stable under thermal and shear stress.

Additionally, the formulation must be developed such that the rheological properties of the molten material are amenable to extrusion, shaping and cutting (Lang et al., 2014).

We hypothesize that a modified dry powder coating process can be used as an alternative technique for the preparation of free films. The dry powder coating process has been adapted from the metal coating and finishing industry for use in pharmaceutical coating (Bailey, 1998; Sauer et al., 2013). The benefits with eliminating the use of organic or aqueous solvents include reduced energy consumption and drying times attributed with conventional solvent-based coating processes. Dry powder coating processes have been developed for tablets (Cerea et al., 2004; Huatan and Ross, 2011; Qiao et al., 2010a; Qiao et al., 2010b; Sauer et al., 2007), granules/pellets (Pearnchob and Bodmeier, 2003; Terebesi and Bodmeier, 2010), and other dosage forms (Nukala et al., 2010). Sauer et al. in a recent review article, reported on the various dry powder coating technologies being evaluated within the pharmaceutical industry, which include liquid assisted, thermal adhesion, and electrostatic coating (Sauer et al., 2013). Coating adhesion and coalescence of the film onto the surface of tablets or pellets are critical, particularly in the instances where the coating is providing a protective barrier or controlled release. Lack of adherence to the tablet is considered a defect or failure in coating process.

Adhesion of the coating polymer onto a tablet is primarily driven by interfacial interactions between the polymer and tablet excipients (McGinity and Felton, 2008; Podczeck, 1998). These interactions can include molecular interactions, primarily via hydrogen bonding. The degree of adhesion is influenced by the properties of the coating and substrate materials. Coating formulations usually incorporate a polymer as the film former, a plasticizer to reduce the polymer glass transition temperature, add flexibility to the formed film, and/or increase adhesive properties (Felton and McGinity, 1997;

Gutiérrez-Rocca and McGinity, 1994), an anti-tacking agent in small amounts to decrease tackiness of the applied coat, and pigments (Felton and McGinity, 2002). The coating formulation is dissolved and/or suspended in a solvent, which provides the capillary forces to form liquid bridges between the coating and substrate to aid in film formation and adhesion (McGinity and Felton, 2008). The tablet excipients also influence adhesion, strengthening it by molecular bonding with the coating excipients or hindering it, if for example the excipients are hydrophobic (Lehtola et al., 1995). Increased surface roughness of the tablet can provide greater interfacial area, leading to a greater degree of adhesion (Khan et al., 2001; Nadkarni et al., 1975).

Given a non-adhering substrate, such as a polished metal, dry powder coating processes could be adapted for the preparation of free films. Adhesion of a coating polymer to a metal substrate is primarily due to chemical bonding and mechanical interlocking; however, both are not readily formed and require pretreatment of the metal (Kozma and Olefjord, 1987; Lee, 1991; Ramarathnam et al., 1992). Chemical pretreatments often utilize phosphates, chromium, silanes or titanium zirconium to increase the surface energy by creating new chemical/function groups on the metal surface to promote chemical bonding with the coating material (Awaja et al., 2009; Butt and Kappl, 2009; Gettings and Kinloch, 1977; Lee, 1991; Moore and Dunham, 2008). Mechanical treatments are used increase surface roughness and allow polymers to penetrate into small interstitial spaces to increase adhesive strength by mechanically interlocking the coating onto the surface of the metal; these methods often include abrasive blasting or other mechanical etching techniques (Kinloch, 1980; Ramarathnam et al., 1992). Without pretreatment of the metal, the adhesive forces between the polymer and metal substrate are relatively weak and more a function of electrostatic and weak boundary layer forces (Lee, 1991). In this study, this weak interaction can be exploited in

order to use a metal surface as a temporary substrate for the preparation of free films using electrostatic powder deposition.

The aims of the present study were to develop free films utilizing an electrostatic powder deposition (ESPD) technique and investigate the properties of the prepared films including morphology, mechanical properties, drug content, content uniformity, and *in-vitro* drug release. Polyethylene oxide (PEO) and acetaminophen (APAP) were chosen as the hydrophilic polymer and model API, respectively.

4.3 MATERIALS AND METHODS

4.3.1 Materials

POLYOX™ WSR N10 NF produced by The Dow Chemical Company (Midland, MI, USA) was kindly donated by the distributor, Colorcon Inc. (Harleysville, PA, USA). Acetaminophen (APAP) was purchased from Spectrum Chemicals (New Brunswick, NJ, USA). Aerosil® R 972 was purchased from Evonik Industries (Essen, North Rhine-Westphalia, Germany). Listerine Pocketpaks® breath strips were purchased from a local pharmacy to be used as a reference for mechanical properties; the strips were cut to produce square samples for analysis. High performance liquid chromatography grade methanol and water were purchased from Fisher Scientific (Pittsburgh, PA, USA).

4.3.2 Particle Size Fractions

The majority of powders used for electrostatic coating processes utilize a mean particle size of around 30 μm with a d90 around or below 90 μm (Bailey, 1998; Mazumder et al., 1997; Staniforth and Grosvenor, 1995). Particles under 30 μm are classified as ultrafine and can exhibit poor flow properties (Meng et al., 2009a). Larger

particles, usually greater than 80-90 μm, tend to accumulate a lower charge-to-mass ratio upon charging and are more sensitive to charge loss, leading to poor adherence to the substrate (Barmuta and Cywiński, 2001; Meng et al., 2009a; Wang, 2005). Based on this information, PEO, APAP, and co-processed materials were sieved for 20 min using a sieve shaker to obtain 25-90 μm size fractions (500 – 170 mesh).

4.3.3 Blending

Appropriate amounts of sieved API, polymer and glidant were weighed into bottles and blended for 15 min using the Turbula® T2F blender (Glen Mills Inc., Clifton, NJ, USA) to prepare the physical mixture. API and polymer were weighed and blended for 15 min prior to co-processing by HME. Glidant was added to the milled co-processed material and blended for 15 min prior to prepare the final co-processed particles for use with the ESPD process. Both the physical mixture and co-processed particles consisted of 10% w/w APAP, 89.7% PEO, and 0.3% Aerosil® R 972.

4.3.4 Hot Melt Extrusion (HME)

A co-rotating twin-screw extruder, Leistritz Nano 16 (Leistritz, Sommerville, NJ, USA) was used to prepare co-processed APAP:PEO material. The feed rate was approximately 3 g/min using a volumetric feeder, Schenk AccuRate (Schenck AccuRate, Whitewater, WI, USA). The screw configuration only consisted of conveying elements (no mixing elements) and the screw speed was maintained at 100 rpm. The extrusion temperature profile of 65°C-75°C-80°C-85°C for zone 1-zone 2- zone 3-die was used. The extrudate was cut into smaller pieces as it exited the die.

4.3.5 Milling

Cryogenic milling was conducted using a Spex SamplePrep 6870 Freezer/Mill (Metuchen, NJ, USA). Samples were placed into polycarbonate vials with a magnetically driven impactor. Samples were immersed in liquid nitrogen, pre-cooled for 5 min, milled for 5 min at a frequency of 10 cycles per second (cps), with a pause of 2 min between cycles to prevent the magnetic coil and sample overheating. The co-processed material was milled for a total of 30 min.

4.3.6 Electrostatic Powder Deposition (ESPD)

The ESPD process consists of the following steps: powder charging, spraying and deposition, followed by curing and removal of the non-adhered film from the temporary metallic substrate. Powder is fed to a Nordson Vantage® Manual corona gun (Nordson Corporation, Westlake, OH, USA), charged with 80 kV voltage, and sprayed using 1.5 bar of atomizing pressure and 1.5 bar fluidizing pressure through a conical deflector. The negatively charged particles follow the trajectory of the electrostatic field between the tip of the gun and the grounded metallic substrate and deposit onto the surface of the grounded substrate, shown in Figure 4.1. For this study, a stainless steel substrate was covered with a non-conductive poly(ethylene terephthalate) (PET) (Melinex® 329) stencil, 175 μm thickness (shown in white). Resistivity of PET has been reported as greater than 10^{16} Ω (Han and Tay, 2008), making it an insulating material, thus preventing the charged powder from adhering to the stencil material. Charged particles deposit on the exposed surfaces (shown as grey) of the grounded substrate, shown in Figure 4.1. The use of this stencil eliminated the need to cut discrete films for characterization. After powder deposition, the substrate was placed in an infrared oven to allow the powder to coalesce into a film. The substrate was then removed from heat and

allowed to equilibrate to room temperature, whereupon the discrete films were removed from the temporary substrate. Films were prepared using PEO alone and the physical mixture, and co-processed particles.

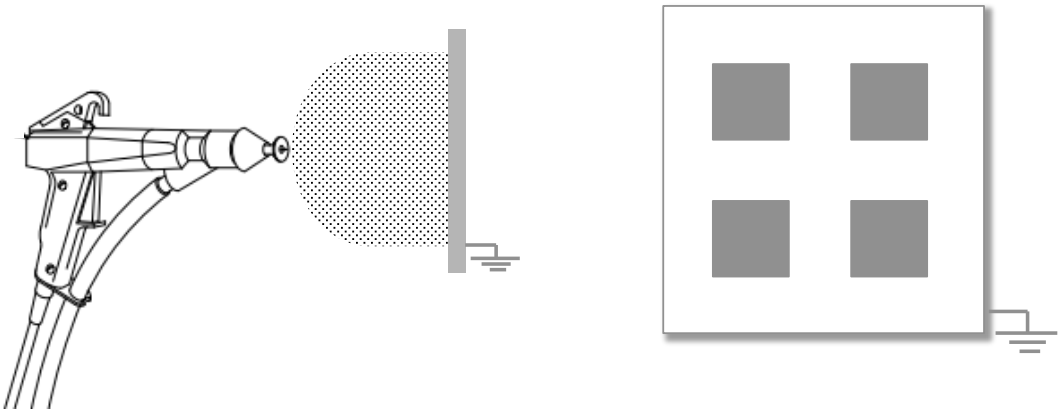

Figure 4.1 Schematic of ESPD process (left) and stencil over substrate (right).

4.3.7 Differential Scanning Calorimetry (DSC)

A TA Instruments Model Auto Q20 DSC (TA Instruments, New Castle, DE, USA) was used to characterize raw materials and processed samples. Raw materials were evaluated using a heat-cool-heat method, by first equilibrating samples at 25°C followed by heating to 225°C at a ramp rate of 10°C/min and then cooled at 5°C/min to -40°C, before repeating the heat cycle. The physical mixture, co-processed particles, and film samples were equilibrated at -20°C and then heated to 225°C at a ramp rate of 10°C/min During analyses, high purity nitrogen flowed through the sample chamber at a rate of 50 mL/min Data was analyzed using TA Universal Analysis 2000 software.

4.3.8 Powder X-ray Diffraction (PXRD)

PXRD analyses were conducted using MiniFlex 600 (Rigaku, Tokyo, Japan) operated at 40 kV and 15 mA using a variable + fixed slit condition. Data was collected in a continuous scan mode with a step size of 0.02° and step speed of 4°/min over a of 2θ range of 10° to 60°.

4.3.9 Scanning Electron Microscopy (SEM)

The surface morphology of the films was imaged by scanning electron microscopy (SEM). Samples were mounted onto pin stubs using conductive carbon adhesive tape and sputter coated with a 15 nm thickness of palladium/platinum under argon using a Cressington 208HR sputter coater (Cressington, Watford, UK). The Zeiss Supra field emission SEM (Zeiss, Oberkochen, Germany) was operated at an accelerating voltage of 5 kV to obtain images.

4.3.10 Mechanical Strength Testing

Samples were measured for weight and thickness. Thickness was measured using a Mitutoyo digital micrometer (Mitutoyo, Kawasaki, Japan). Samples were then tested on a Texture Analyzer TA-XTplus (Stable Microsystems, Godalming, Surrey, UK) using 5 kg load cell. Samples were mounted on a TA-108s-5 fixture (Texture Technologies, Hamilton, MA, USA) and punctured using a ¼" spherical probe moving at 1 mm/s. Measurement started when the probe had contact with the sample using a trigger force of 0.049 N. Exponent software (Stable Microsystems, Godalming, Surrey, UK) was used to process data.

Calculations for tensile strength and percent elongation are shown in equations 4.1 and 4.2, respectively as defined by Radebaugh et. al (Radebaugh et al., 1988).

$$\sigma_{TS} = \frac{F}{A_{cs}} \tag{4.1}$$

where F is the force at rupture (N) and A_{cs} is the cross sectional area of the film in the film holder (mm^2).

$$\%\, elongation = \left(\frac{\sqrt{r^2+D^2}-r}{r}\right) \times 100\% \tag{4.2}$$

where r is the radius of the film exposed to the probe in the same holder and D is the displacement of the probe from the point of contact with the film until rupture.

4.3.11 Assay and Content Uniformity Testing

Aliquots of blend were weighed and accurately transferred into volumetric flasks and dissolved in mobile phase (see HPLC section). Film assay samples were prepared using 10 films that were weighed and transferred into a volumetric flask and dissolved in mobile phase. The resulting solutions were then filtered through 0.2 μm PVDF filters and immediately transferred to 2-mL HPLC vials for analysis. Physical mixture, co-processed particles, and film assay were analyzed in triplicate. Content uniformity was determined by assaying 10 individual films and relative standard deviation (RSD) was determined per USP <905> Uniformity of Dosages Units (USP38-NF33, 2015).

4.3.12 High Performance Liquid Chromatography (HPLC)

APAP content was analyzed with a Thermo Scientific Dionex UltiMate 3000 HPLC system (Thermo Scientific, Sunnyvale, CA, USA). An Ultimate 3000 Autosampler was utilized to inject 10 μL samples. The HPLC system also included dual UltiMate 3000 Pumps and an UltiMate RS Variable Wavelength Detector. The system was operated under isocratic conditions with a methanol: water (1:3) mobile phase, using a flow rate of 1.5 ml/min. Injections were passed through a Phenomenex Luna® 5 μm C18(2) reverse phase column, 250 x 4.6mm (Phenomenex, Torrence, CA, USA) and absorbance at a wavelength of 243 nm was measured. Chromeleon Version 6.80 software (Thermo Scientific, Sunnyvale, CA, USA) was used to process all chromatography data.

4.3.13 Dissolution Testing

In vitro drug release testing was conducted using a USP dissolution apparatus 1 (basket method). Testing was conducted using a rotation speed of 50 rpm with 500 ml of deionized water held at 37°C. Samples were taken at 2, 5, 10, 15, 20, and 30 min and the dissolution medium was replenished to maintain constant volume. Samples were analyzed for drug content using the HPLC method described above.

4.4 RESULTS

A square stencil, 26.9 mm x 26.9 mm, was used to make the films for characterization in this study (Figure 4.2, top). Additional stencils were used to show the versatility of the ESPD process. Some of these shapes and sizes are shown in Fiugre 4.2 to illustrate the ability to form discrete shapes and sizes using the ESPD process.

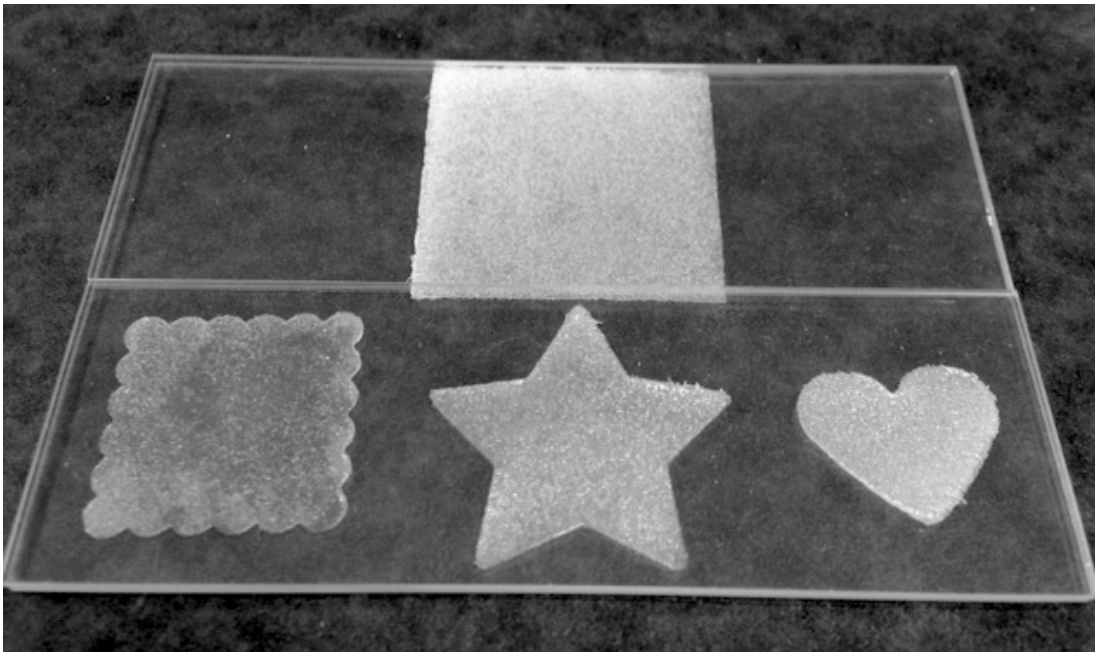

Figure 4.2 Films prepared by the ESPD process using various stencil shapes and sizes.

The APAP, PEO, physical mixture, co-processed particles, and films were evaluated by DSC. The resulting thermograms are shown in Figure 4.3. The APAP thermogram shows a melt endotherm around 169°C, while PEO exhibits a melt endotherm around 61.4°C. Upon cooling, a recrystallization peak was seen at 44.58°C for PEO during the cooling cycle. The second heating cycle for the APAP showed a glass transition temperature (T_g) of 25.7°C (data not shown), while the T_g of the PEO could not be detected due to the limitations of cooling capabilities of the chiller (maximum cooling to -40°C). The T_g of PEO is reported by the vendor to be around -50°C to -57°C. There is no APAP melt endotherm present in the physical mixture thermogram, indicating the API dissolves in molten PEO upon heating with complete dissolution prior to its melting point. This phenomenon correlates with previous findings of APAP:PEO mixtures, which show an increased solubility of APAP in PEO with increasing temperature (Yang et al.,

2010; Yang et al., 2011). The co-processed particles and films prepared using both the physical mixture and co-processed particles also show no APAP melt endotherm. Each drug-containing sample shows a depression of the PEO melt endotherm, characterizing of the plasticizing effect of dissolved APAP. This also correlates with the findings of Suwardie et al. that showed a decrease in viscosity of APAP:PEO mixtures with increasing APAP content up to 30-40% w/w (Suwardie et al., 2011; Yang et al., 2010).

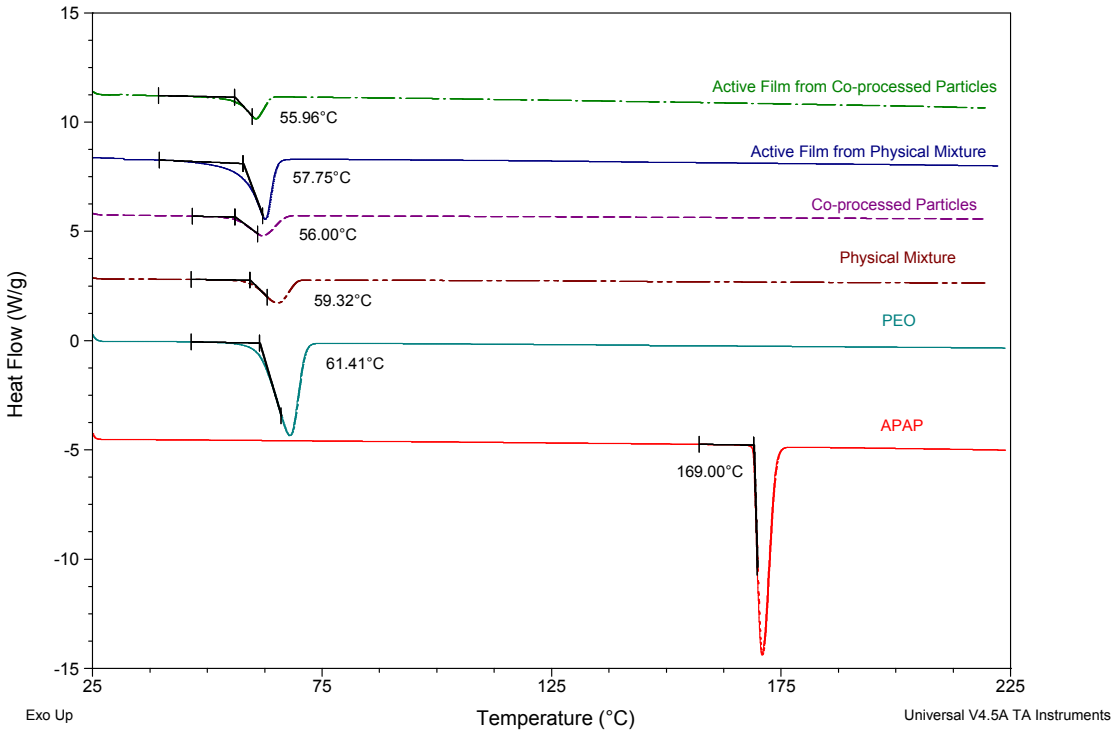

Figure 4.3 DSC thermograms of crystalline APAP, semi-crystalline PEO, physical mixture, co-processed particles, and active films prepared using physical mixture and co-processed particles.

The crystalline nature APAP, PEO, the physical mixture, co-processed particles, and active films were evaluated by PXRD. The diffraction patterns are shown in Figure

4.4. The diffraction peaks of the crystalline APAP can be seen in the physical mixture and films prepared using physical mixture. This confirms the presence of crystalline API in the PM, which could not be detected using DSC. The crystallinity in the film sample shows that the film curing process was not too aggressive as to dissolve the APAP into the PEO. Crystalline APAP is not detectable in the co-processed particles or the films prepared using these particles, confirming the APAP has converted to its amorphous form during processing and may be partially dissolved in the polymer. The crystalline peaks of the PEO are still seen in the processed samples; however, the intensity decreases upon processing with HME and decreases further upon film curing.

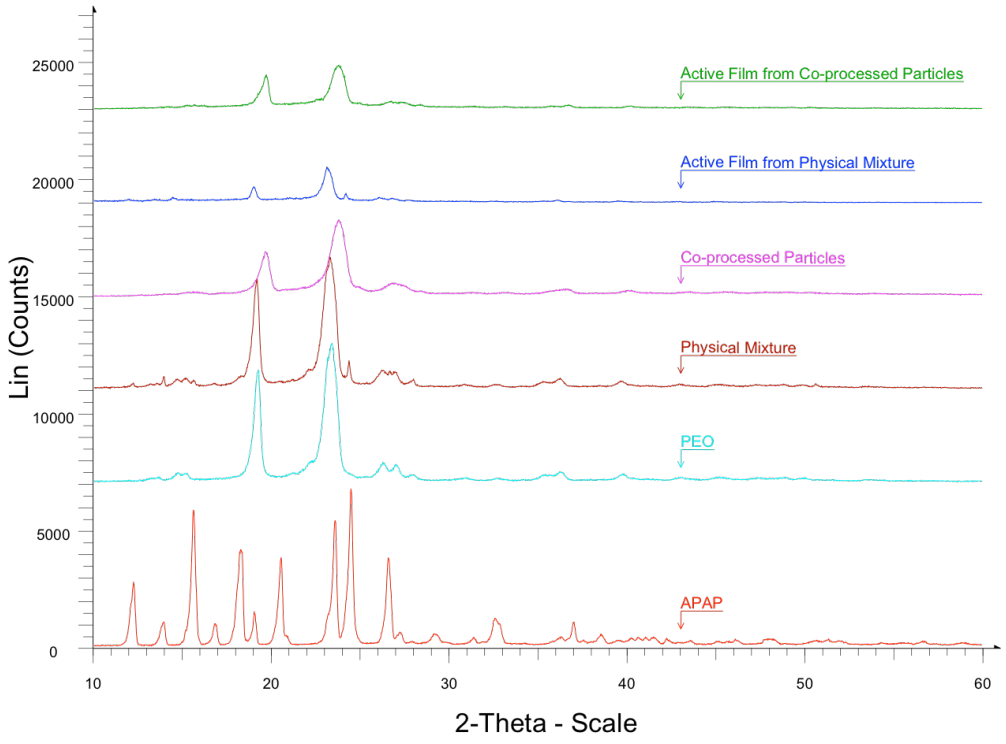

Figure 4.4 PXRD patterns of crystalline APAP, semi-crystalline PEO, physical mixture, co-processed particles, and active films prepared using physical mixture and co-processed particles.

Figure 4.5 shows the SEM micrographs for the PEO film and films prepared using the physical mixture and co-processed particles. The PEO film shows a smooth surface, indicative of complete coalescence of particles during curing. The film prepared using the physical mixture is also smooth, with the presence of imbedded APAP crystals. The film prepared using co-processed particles is mostly smooth, however the edges of particles and some small voids can be seen indicating incomplete coalescence.

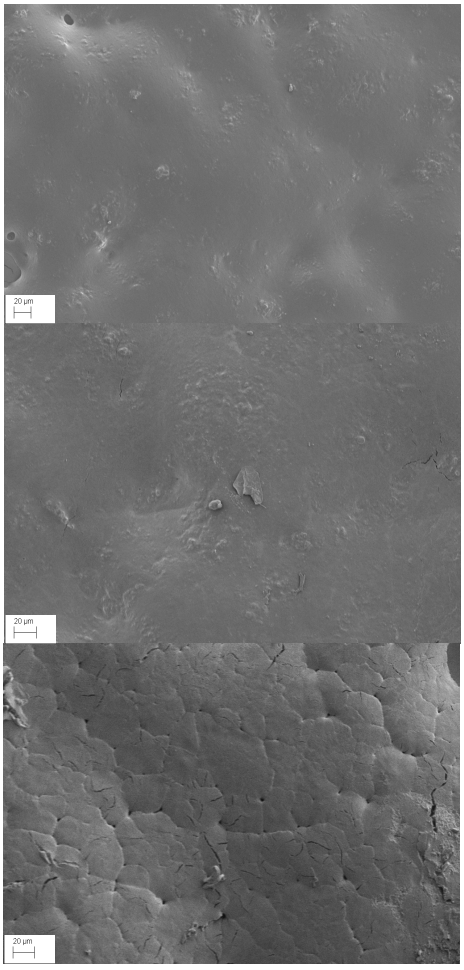

Figure 4.5 SEM micrographs of PEO film (top), active film from physical mixture (middle), active film from co-processed particles (bottom). White bar represents 20 µm.

The PEO and active films were characterized for mechanical strength. Representative force-displacement curves for each are shown in Figure 4.6. As a reference, a commercially available Listerine® breath strips were also tested. The Listerine® strip shows a steep curve before rupture around 3 N of force with little elongation, indicative of a brittle break. The PEO film shows a lower average break force around 1.8 N but a greater displacement prior to break compared to the Listerine strip. Both active films showed significantly greater average displacement at 2.8 and 2.9 mm, for the films prepared using physical mixture and co-processed particles, respectively. The average puncture force for the active film prepared using physical mixture was slightly lower than that of the film prepared using co-processed particles, shown in Table 4.1. Tensile strength and percent elongation were calculated for all films and are reported in Table 4.1. The active films showed similar puncture strength and tensile strength when compared to the PEO film; however, the percent elongation is nearly 4-fold greater.

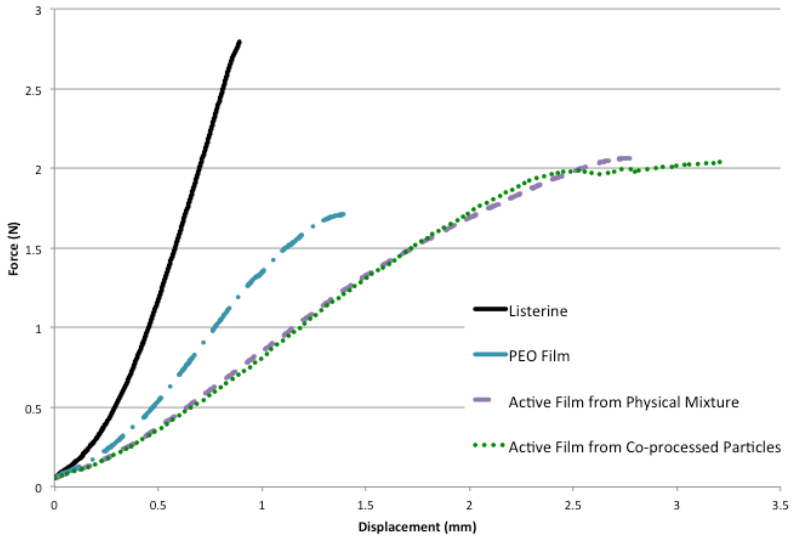

Figure 4.6 Representative force-displacement curves of Listerine® breath strip (reference), PEO film, and active films prepared using physical mixture and co-processed.

Table 4.1 Mechanical properties of Listerine strip (reference) and films prepared using ESPD, average (std. dev.), n=5.

Sample	Weight (mg)	Thickness (mm)	Average Burst Strength (N)	Tensile Strength (MPa)	Percent Elongation (%)
Listerine (reference)	21.3 (0.1)	0.046 (0.001)	3.01 (0.49)	2.07 (0.30)	1.6 (0.4)
PEO	53.4 (3.4)	0.066 (0.002)	1.79 (0.20)	0.86 (0.10)	3.8 (0.9)
Active film from physical mixture	52.6 (4.2)	0.069 (0.007)	1.72 (0.58)	0.80 (0.25)	14.5 (2.9)
Active film from co-processed particles	58.4 (5.0)	0.081 (0.007)	2.09 (0.89)	0.82 (0.31)	15.4 (3.7)

The physical mixture, co-processed particles and films prepared from each were assayed for drug content and individual films were tested for CU. The physical mixture drug content was determined to be 96.3% of theoretical, while the co-processed particles was 98.5% of theoretical. The average drug content of the films prepared using physical mixture and co-processed particles were comparable at 97% of theoretical, shown inTable 4.2. However, the variability with the films from the physical mixture was much greater, with CU testing indicating a RSD of 11.9% compared to 1.8% seen with the films prepared using co-processed particles.

The active films were tested for drug release. Sampling for these films were taken out to 30 min; however, greater than 85% release was seen by 2 min for both

films, indicating rapid dissolution of the dosage form. 100% release was reached by 10 min for both films and no change was seen after reaching 100% release (Figure 4.7).

Table 4.2 Physical mixture, co-processed particles, and active film drug content (n=3) and content uniformity of active films (n=10).

Sample	Drug Content, % theoretical (std. dev.)	Content Uniformity, %RSD
Physical mixture	96.3 (1.5)	n/a
Co-processed particles	98.5 (0.18)	n/a
Active film from physical mixture	97.1 (7.7)	11.9
Active film from co-processed particles	97.2 (0.93)	1.8

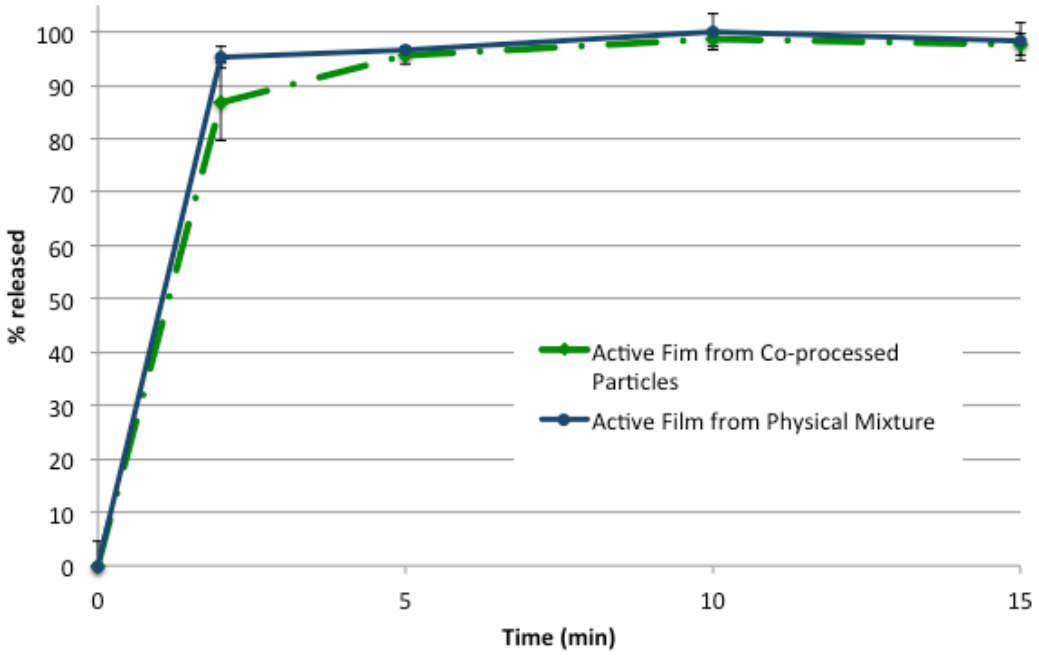

Figure 4.7 Drug release from films prepared using physical mixture and co-processed particles (n=6).

4.5 DISCUSSION

The charged powders were sprayed until the deposited powder was approximately flush with the stencil. The coupon was then placed in an infrared oven for curing. Pharmaceutical powders, in general, are considered insulating materials; therefore, they do not readily lose charge and are able to adhere to the substrate even after removal from the ground, allowing for transport the oven without loss of powder (Coelho, 1985; Grosvenor and Staniforth, 1996). Both the PEO and active films were cured at 80°C for 15 min; it was observed that the films were transparent after less than 5 min in the oven. Notably, given the time required for film formation using casting processes to allow for solvent evaporation, ESPD offers an advantage of significantly faster cure times, on the order of minutes versus hours (Abdelbary et al., 2014; Boateng et al., 2009; Koland et al., 2010). Upon removal of the films from the oven and equilibrating to room temperature, the films became opaque due to recrystallization of the PEO. The stencil was then removed, and the discrete films were removed from the substrate for characterization. The ability to produce discrete films using stencils allows for flexibility in the shape and size of the film, as shown in Figure 4.2, allowing for dose flexibility; the ability to make various shapes can also be an attractive feature for pediatric dosage forms. Specifically, this can be done without the need for cutting discrete films, as is often the case with solvent casting and HME processing of films (Low et al., 2013; Preis et al., 2014b), which can lead to drug product waste. As the charged powder only adheres to the exposed areas on the substrate, there is minimal waste. Additionally, the use of powder recirculation systems have been used with electrostatic processes (Barmuta and Cywiński, 2001), which could potentially be adapted for use in pharmaceutical manufacturing, further improving yield.

Co-processing by HME was conducted at relatively low temperatures to avoid thermal oxidation of PEO (Crowley et al., 2002; Scheirs et al., 1991); these temperatures were well below the degradation temperature of APAP (Gilpin and Zhou, 2004). The process produced a transparent extrudate, which became opaque upon cooling to room temperature due to recrystallization of PEO. Co-processing was incorporated to prepare homogenous particles of APAP:PEO for use with the ESPD process; however, as can be seen by the PXRD profile in Figure 4.4, APAP was rendered amorphous by the HME process. This was expected, as various studies have shown APAP to produce an amorphous solid dispersion with hot-melt mixing or HME at a 10% drug load; however, this drug load is not considered thermodynamically stable (Suwardie et al., 2011; Yang et al., 2013; Yang et al., 2010; Yang et al., 2011). Yang et al. showed a 10% drug load of APAP in PEO would recrystallize in weeks (Yang et al., 2010), which was in agreement with a Flory-Huggins predicted solubility of APAP in PEO of approximately 2.3% (Yang et al., 2013). For the purpose of this study, long-term physical stability was not required to evaluate the viability of the ESPD process to make free films.

No crystalline APAP was detected by DSC in any of the API-containing compositions due to the ability of the APAP to readily dissolve in the presence of molten PEO upon heating (Yang et al., 2010; Yang et al., 2011). The physical mixture and co-processed particle samples did show a suppressed melt endotherm of PEO of 59.3°C and 56.0°C, respectively, exhibiting the ability of APAP to plasticize the polymer. This melt suppression decreased further upon curing with the active films prepared from physical mixture and co-processed particles with PEO melt onset at 57.8°C and 55.96°C, respectively. These results show the plasticization of PEO in the presence of APAP increases with increased thermal exposure, as the co-processed particle samples showed a

greater melt depression than the physical mixture and both active film samples showed further suppression after curing.

PXRD confirmed crystalline APAP in the physical mixture, as well as in the film prepared using the physical mixture showing that the curing process did not facilitate API dissolution PEO upon heating. PXRD analysis also confirmed that no crystalline APAP was present in co-processed particles of the film prepared using the co-processed particles. PXRD did not show suppression of the PEO crystalline peaks in the physical mixture, as this blend was not exposed to heat during this analysis as it was during DSC analysis. Consistent with the data from DSC, the PXRD profiles showed a suppression of the PEO crystalline peak intensities in the co-processed particle samples and further suppression in the film samples prepared using both the physical mixture and co-processed particles.

Dry powder curing and film formation is driven by the reduction in polymer melt viscosity leading to particle deformation and coalescence (Dillon et al., 1951; Grosvenor, 1991; Kablitz and Urbanetz, 2007). Curing temperatures at or above the glass transition temperature (T_g) of the polymer allows for the viscous flow needed for film formation. As PEO is a semi-crystalline polymer, melt flow can be achieved when cured above its melting point. Curing was conducted at 80°C, above PEO's melting point of 61°C and well above the APAP T_g of around 25°C. Lower molecular weights of PEO, including the N10 grade used in this study, are considered self-plasticizing due to their excellent thermoplastic properties and low viscosity (Crowley et al., 2002; Prodduturi et al., 2007). Additionally, APAP has been shown to act as a plasticizer, further reducing the viscosity of PEO (Yang et al., 2010). From the SEM images shown in Figure 4.5, the PEO and films from the physical mixture produced smooth films indicating thorough coalescence of the deposited particles. While the film prepared form the co-processed particles is

mostly smooth, the edges of particles and some small voids can be seen. Longer cure times and/or higher cure temperatures could be evaluated to produce a smoother final film using co-processed particles. The use of plasticizers has been widely studied to reduce the polymer T_g (Qiao et al., 2013; Smikalla et al., 2011), to produce capillary forces between polymer particles (Kablitz and Urbanetz, 2007; Klar and Urbanetz, 2009), as well as to alter the properties of the final film, i.e. flexibility. The addition of a plasticizer, either to the co-processed formulation or adsorbed on the particle surface, could be another alternative to increase film formation efficiency without increasing curing time or temperature.

At this time, there are no standard test methods or acceptance criteria for mechanical properties of films for drug delivery. Initial test methods were adapted from the plastics industry, such as ASTM D882 – Tensile Properties of Thin Plastic Sheeting; however, more recently, puncture tests have become more widely utilized as they are less prone to set-up error, do not require specified shape for the test specimen, and allow for better handling of brittle or otherwise fragile samples (2013; Khuathan and Pongjanyakul, 2014; Nesseem et al., 2011; Preis et al., 2014a; Sriamornsak and Kennedy, 2006). The force-displacement curves from puncture testing, Figure 4.6, show that the commercially available Listerine® strip exhibits a brittle break with a steep slope and sharp break, whereas the films prepared using ESPD showed more elongation and plastic deformation prior to puncture and a more curved profile. The APAP-containing films, both from physical mixture and co-processed particles, show significantly greater plasticity, with around 15% elongation compared to the 4% elongation seen with the PEO film. This data corroborates the DSC data showing the ability of APAP to plasticize PEO. As a reference, Preis et al. tested 8 commercially available oral films and reported relatively low percent elongations ranging from 1.0 to 4.4% for the majority of the films. The

corresponding force-displacement curves from these marketed oral films were similar to the Listerine® strips, showing steep curves and little elongation, indicative of a brittle break (Preis et al., 2014a). The films prepared by ESPD in this study, and specifically the active films, exhibited excellent plasticity prior to break, which can be advantageous from a handling perspective both for the patient and for packaging processes.

The average puncture force for the ESPD films were similar to or slightly lower than that of the Listerine® strip, as shown in Table 4.1. The calculated tensile strengths for the PEO film and active films from physical mixture and co-processed particles were 0.86, 0.80, and 0.82, respectively, whereas the tensile strength for the Listerine® strip was calculated as 2.07. Tensile strength normalizes for film thickness and as reported in Table 4.1, the Listerine® strip is about 30% thinner than the PEO film resulting in higher tensile strength values. The average thickness of the PEO and films prepared using the physical mixture is comparable at 66 and 69 μm, respectively. The average thickness of the films using co-processed particles is slightly higher at 81 μm; this thicker value can be attributed to the slightly higher weights for this sample set, and possibly due to the incomplete coalescence and leveling of the film during curing. Overall, the ESPD films were easier to handle during test set-up, as they were not brittle in nature.

In this study, two active film formulations were prepared using ESPD: one using a physical mixture of APAP and PEO and the other using co-processed, homogenous particles of APAP and PEO. Most materials for dry powder coating are co-processed to form homogenous composite particles (Craven, 1982; Hogan et al., 1996; Theodore and Labana, 1973) which can include the film forming polymer, plasticizer, crosslinking agents, and/or other processing aids, as needed. Thus, the uniformity of physical mixtures after electrostatic powder deposition processing has not been thoroughly investigated and we are the first to present such information, as it is an appropriate

consideration for pharmaceutical applications. The physical mixture and co-processed particle assay were measured at 96.3 and 98.5%, respectively. The standard deviation for the co-processed particles assay was very low at 0.18, confirming the HME process produced homogenous particles. The assay values for the active films from the physical mixture and co-processed particles were comparable at around 97%; however, the content uniformity testing showed that the films from the physical mixture were highly variable with a RSD of 11.9% compared a RSD of 1.8% seen with the films prepared using co-processed particles.

Bailey highlighted some of the powder properties that could affect the ESPD process, which include particle size, shape, fluidity, and resistivity (Bailey, 1998). The effect of particle size and distribution has been widely studied (Barmuta and Cywiński, 2001; Meng et al., 2009a). Corona charging and spraying of particles can lead to electroseparation of particles of a wide particle size distribution. Studies by Barmuta et al. and Meng et al. showed the preferential deposition of the smaller particles during electrostatic coating. Because of this, narrow particle size distributions are recommended for electrostatic coating processes. Additionally, mean particle sizes of 30-40 μm are recommended for coating processes. Below this size, particles are classified as fine or ultra-fine and have a tendency for poor fluidization, increased cohesion, and high mass-to-charge ratios that can lead to back-ionization and decreased deposition efficiency. Alternatively, larger particles sizes of 80-90 μm exhibit lower mass-to-charge ratios and are more sensitive to charge loss, leading to poor adhesion (Bailey, 1998; Meng et al., 2009b; Meng et al., 2009c). In this study, size fractions of 25-90 μm were collected of the APAP and PEO to prepare the physical mixture. The observed variability around an acceptable average drug content as opposed to producing only superpotent or subpotent films indicate that one of the components of the physical mixture was not substantially

smaller or larger than the other within the 25-90 μm size fraction. Therefore, electroseparation as a function of particle size may not the primary cause of the variability in this system. The disparate particle shapes of the APAP and PEO may contribute to the variability in ESPD; the APAP crystals have a more needle-like shape while the PEO particles are more spherical (Yang et al., 2010). The larger aspect ratio of the APAP can lead to a variable charge accumulation and fluidization behavior (Hassan and Lau, 2009; Karner et al., 2014) and therefore, lead to variable deposition. Lastly, the resistivity of the individual components must be considered. Bailey classified powders with resistivity greater than 10^{13} Ωm as most suitable for use with electrostatic coating processes as they do not readily dissipate accumulated charge. This leads to good adhesion properties. Powders with resistivity less than 10^{10} Ωm are generally classified as low resistance materials; they can deposit to grounded substrates, but adhesion is poor as they quickly loose their charge. The behavior of powders within the range between 10^{10} - 10^{13} Ωm is difficult to predict (Bailey, 1998). The vendor reported values of volume resistivity values for APAP and PEO are $>10^{14}$ Ωm and 10^{10}-10^{11} Ωm, respectively. Although, PEO falls within the unpredictable behavior range of per Bailey's classification, PEO used in this study has been shown to deposit and adhere well, as exhibited by the successful preparation of films by ESPD. However, the difference in the resistivity values may lead to some variability in deposition behavior. Again, as this was the first proof-of-concept study evaluating the uniformity of ESDP using a physical mixture containing an active component, additional studies are needed to verify the sources of this variability.

Dissolution testing was conducted to investigate drug release from the active films prepared using ESPD. Although there is no standardized acceptance criteria for immediate release oral films, immediate release solid oral dosage forms target 80-85%

release by 15 min for BCS I drug substances or rapidly dissolving drug products (1997; 2000). Both active films showed greater than 85% release after 2 min. Although the films prepared using the physical mixture were characterized has containing crystalline APAP, while the films prepared using co-processed particles consisted of amorphous APAP from the HME process, this did not affect the immediate release properties of the dosage form. This will not always be the case and the solid-state properties and physical stability of the API must be considered when formulating and processing films using ESPD. In this study APAP was used only as a model drug to show the ability to prepare oral films for drug delivery using the ESPD process. The results of this study confirm that ESPD process was able to prepare rapidly dissolving films of APAP and PEO for oral drug delivery.

4.6 CONCLUSION

There is a growing interest in the use of oral films as a dosage form, particularly in pediatric and geriatric populations. While solvent casting and HME have been traditionally used for the manufacture of oral films, these methods also have disadvantages or challenges to their application. Based on the results presented, it can be concluded that ESPD is a viable manufacturing method for preparing free films for drug delivery. This process allows for a high degree of flexibility in preparation of films with discrete shapes and sizes, without the need for cutting. Additionally, the curing times for the ESPD are significantly reduced when compared to solvent casting processes, which can require hours for solvent evaporation. As ESPD is already utilized in other industries, many formulation attributes and processing parameters have already been investigated and much of this knowledge can be translated or expanded for use of this

technique for pharmaceutical manufacturing. Continued development of this technology is needed to firmly establish this technique for pharmaceutical manufacturing portfolio and determine its range of capabilities.

4.7 REFERENCES

ICH topic Q3C(R5) Impurities: Guidelines for Residual Solvents. International Conference on Harmonization.

1997. Guidance for Industry: Dissolution Testing of Immediate Release Solid Oral Dosage Forms. US Department of Health and Human Services FDA,Center for Drug Evaluation and Research (CDER). in: US Department of Health and Human Services FDA, C.f.D.E.a.R.C. (Ed.). US Department of Health and Human Services FDA,Center for Drug Evaluation and Research (CDER), US Department of Health and Human Services FDA,Center for Drug Evaluation and Research (CDER).

2000. ICH Topic Q6A: Specifications: Test Procedures and Acceptance Criteria for New Drug Substances and New Drug Products: Chemical Substances. (CPMP/ICH/367/96) European Medicines Agency.

2013. TA.XTPlus Application Study: Film Testing ASTM D882 vs TA-108S-5i, in: Corp., T.T. (Ed.), http://www.texturetechnologies.com.

2015. The United States Pharmacopeial Convention. General Chapter: 1151 Pharmaceutical Dosage Forms. USP 38–NF 33 Rockville, MD: The United States Pharmacopeial Convention, The United States Pharmacopeia and The National Formulary.

Abdelbary, A., Bendas, E., Ramadan, A., Mostafa, D., 2014. Pharmaceutical and Pharmacokinetic Evaluation of a Novel Fast Dissolving Film Formulation of Flupentixol Dihydrochloride. AAPS PharmSciTech 15, 1603-1610.

Awaja, F., Gilbert, M., Kelly, G., Fox, B., Pigram, P.J., 2009. Adhesion of polymers. Progress in Polymer Science 34, 948-968.

Bailey, A.G., 1998. The science and technology of electrostatic powder spraying, transport and coating1. Journal of Electrostatics 45, 85-120.

Barmuta, P., Cywiński, K., 2001. Electroseparation and efficiency of deposition during electrostatic powder coating. Journal of Electrostatics 51–52, 239-244.

Boateng, J.S., Stevens, H.N.E., Eccleston, G.M., Auffret, A.D., Humphrey, M.J., Matthews, K.H., 2009. Development and mechanical characterization of solvent-cast polymeric films as potential drug delivery systems to mucosal surfaces. Drug Development and Industrial Pharmacy 35, 986-996.

Borges, A.F., Silva, C., Coelho, J.F.J., Simões, S., 2015. Oral films: Current status and future perspectives: I — Galenical development and quality attributes. Journal of Controlled Release 206, 1-19.

Butt, H.-J., Kappl, M., 2009. Surface and Interfacial Forces, 1 ed. Wiley, Hoboken.

Cerea, M., Zheng, W., Young, C.R., McGinity, J.W., 2004. A novel powder coating process for attaining taste masking and moisture protective films applied to tablets. International Journal of Pharmaceutics 279, 127-139.

Coelho, R., 1985. The electrostatic characterization of insulating materials. Journal of Electrostatics 17, 13-27.

Constable, D.J.C., Jimenez-Gonzalez, C., Henderson, R.K., 2007. Perspective on Solvent Use in the Pharmaceutical Industry. Organic Process Research & Development 11, 133-137.

Craven, J.M., 1982. Powder coating composition for automotive topcoat. Google Patents.

Crowley, M.M., Zhang, F., Koleng, J.J., McGinity, J.W., 2002. Stability of polyethylene oxide in matrix tablets prepared by hot-melt extrusion. Biomaterials 23, 4241-4248.

Dillon, R.E., Matheson, L.A., Bradford, E.B., 1951. Sintering of synthetic latex particles. Journal of Colloid Science 6, 108-117.

Dixit, R.P., Puthli, S.P., 2009. Oral strip technology: Overview and future potential. Journal of Controlled Release 139, 94-107.

Felton, L., McGinity, J., 2002. Influence of Insoluble Excipients on Film Coating Systems. Drug Development & Industrial Pharmacy 28, 225.

Felton, L.A., McGinity, J.W., 1997. Influence of plasticizers on the adhesive properties of an acrylic resin copolymer to hydrophilic and hydrophobic tablet compacts. International Journal of Pharmaceutics 154, 167-178.

Gettings, M., Kinloch, A.J., 1977. Surface analysis of polysiloxane/metal oxide interfaces. J Mater Sci 12, 2511-2518.

Gilpin, R., Zhou, W., 2004. Studies of the Thermal Degradation of Acetaminophen Using a Conventional HPLC Approach and Electrospray Ionization-Mass Spectrometry. Journal of chromatographic science 42, 15-20.

Grodowska, K., Parczewski, A., 2010. Organic solvents in the pharmaceutical industry. Acta poloniae pharmaceutica 67, 3-12.

Grosvenor, M.P., 1991. The physico-mechanical properties of electrostatically deposited polymers for use in pharmaceutical powder coating. University of Bath.

Grosvenor, M.P., Staniforth, J.N., 1996. The Influence of Water on Electrostatic Charge Retention and Dissipation in Pharmaceutical Compacts for Powder Coating. Pharmaceutical research 13, 1725-1729.

Gutiérrez-Rocca, J., McGinity, J.W., 1994. Influence of water soluble and insoluble plasticizers on the physical and mechanical properties of acrylic resin copolymers. International Journal of Pharmaceutics 103, 293-301.

Han, Z., Tay, B., 2008. Electrical conductivity of poly (ethylene terephthalate) modified by titanium plasma. Journal of applied polymer science 107, 3332-3336.

Hassan, M., Lau, R., 2009. Effect of Particle Shape on Dry Particle Inhalation: Study of Flowability, Aerosolization, and Deposition Properties. AAPS PharmSciTech 10, 1252-1262.

Hogan, J.E., Page, T., Reeves, L., Staniforth, J.N., 1996. Powder coating composition for electrostatic coating of pharmaceutical substrates. Google Patents.

Hopkinson, I., Myatt, M., 2002. Phase Separation in Ternary Polymer Solutions Induced by Solvent Loss. Macromolecules 35, 5153-5160.

Huatan, H., Ross, R., 2011. Treatment of adrenal insufficiency.

Kablitz, C.D., Urbanetz, N.A., 2007. Characterization of the film formation of the dry coating process. European Journal of Pharmaceutics and Biopharmaceutics 67, 449-457.

Karner, S., Littringer, E.M., Urbanetz, N.A., 2014. Triboelectrics: The influence of particle surface roughness and shape on charge acquisition during aerosolization and the DPI performance. Powder Technology 262, 22-29.

Khan, H., Fell, J.T., Macleod, G.S., 2001. The influence of additives on the spreading coefficient and adhesion of a film coating formulation to a model tablet surface. International Journal of Pharmaceutics 227, 113-119.

Khuathan, N., Pongjanyakul, T., 2014. Modification of quaternary polymethacrylate films using sodium alginate: Film characterization and drug permeability. International Journal of Pharmaceutics 460, 63-72.

Kianfar, F., Chowdhry, B.Z., Antonijevic, M.D., Boateng, J.S., 2012. Novel films for drug delivery via the buccal mucosa using model soluble and insoluble drugs. Drug Dev Ind Pharm 38, 1207-1220.

Kinloch, A.J., 1980. The science of adhesion. J Mater Sci 15, 2141-2166.

Klar, F., Urbanetz, N.A., 2009. The role of capillary force promoters in dry coating procedures – Evaluation of acetylated monoglyceride, isopropyl myristate and palmitate. European Journal of Pharmaceutics and Biopharmaceutics 71, 124-129.

Koland, M., Sandeep, V.P., Charyulu, N.R., 2010. Fast Dissolving Sublingual Films of Ondansetron Hydrochloride: Effect of Additives on in vitro Drug Release and Mucosal Permeation. Journal of Young Pharmacists : JYP 2, 216-222.

Kozma, L., Olefjord, I., 1987. Surface treatment of steel for structural adhesive bonding. Materials Science and Technology 3, 954-962.

Lam, J.K.W., Xu, Y., Worsley, A., Wong, I.C.K., 2014. Oral transmucosal drug delivery for pediatric use. Advanced Drug Delivery Reviews 73, 50-62.

Lang, B., McGinity, J.W., Williams, R.O., 2014. Hot-melt extrusion – basic principles and pharmaceutical applications. Drug Development and Industrial Pharmacy 40, 1133-1155.

Lee, L.-H., 1991. Fundamentals of adhesion. Springer Science & Business Media.

Lehtola, V.M., Heinämäki, J.T., Nikupaavo, P., Yliruusi, J.K., 1995. Effect of Some Excipjents and Compression Pressure on the Adhesion of Aqueous-Based Hydroxypropyl Methylcellulose Film Coatings to Tablet Surface. Drug Development and Industrial Pharmacy 21, 1365-1375.

Low, A.Q.J., Parmentier, J., Khong, Y.M., Chai, C.C.E., Tun, T.Y., Berania, J.E., Liu, X., Gokhale, R., Chan, S.Y., 2013. Effect of type and ratio of solubilising polymer on characteristics of hot-melt extruded orodispersible films. International Journal of Pharmaceutics 455, 138-147.

Mazumder, M.K., Wankum, D.L., Sims, R.A., Mountain, J.R., Chen, H., Pettit, P., Chaser, T., 1997. Influence of powder properties on the performance of electrostatic coating process. Journal of Electrostatics 40–41, 369-374.

McGinity, J.W., Felton, L.A., 2008. Aqueous Polymeric Coatings for Pharmaceutical Dosage Forms, 3 ed. Informa Healthcare, New York.

Meng, X., Zhang, H., Zhu, J., 2009a. Characterization of particle size evolution of the deposited layer during electrostatic powder coating processes. Powder Technology 195, 264-270.

Meng, X., Zhu, J., Zhang, H., 2009b. Influences of different powders on the characteristics of particle charging and deposition in powder coating processes. Journal of Electrostatics 67, 663-671.

Meng, X., Zhu, J.J., Zhang, H., 2009c. The characteristics of particle charging and deposition during powder coating processes with ultrafine powder. Journal of Physics D: Applied Physics 42, 065201.

Moore, R., Dunham, B., 2008. Zirconization™: The future of coating pretreatment processes: Alternative, phosphate-free, eco-friendly pretreatment procedure addresses energy and chemical consumption while improving product quality. Metal Finishing 106, 46-55.

Morales, J.O., McConville, J.T., 2011. Manufacture and characterization of mucoadhesive buccal films. European Journal of Pharmaceutics and Biopharmaceutics 77, 187-199.

Nadkarni, P.D., Kildsig, D.O., Kramer, P.A., Banker, G.S., 1975. Effect of surface roughness and coating solvent on film adhesion to tablets. Journal of Pharmaceutical Sciences 64, 1554-1557.

Nesseem, D.I., Eid, S.F., El-Houseny, S.S., 2011. Development of novel transdermal self-adhesive films for tenoxicam, an anti-inflammatory drug. Life Sciences 89, 430-438.

Nukala, R., Boyapally, H., Slipper, I., Mendham, A., Douroumis, D., 2010. The Application of Electrostatic Dry Powder Deposition Technology to Coat Drug-Eluting Stents. Pharmaceutical research 27, 72-81.

Obermeier, P., Kohr, T., Kramer, K.T., Klokkers, K., 2008. Oral, Quickly Disintegrating Film, which Cannot be Spit Out, for an Antiemetic or Antimigraine Agent.

Pearnchob, N., Bodmeier, R., 2003. Coating of pellets with micronized ethylcellulose particles by a dry powder coating technique. International Journal of Pharmaceutics 268, 1-11.

Podczeck, F., 1998. Particle-particle adhesion in pharmaceutical powder handling. World Scientific.

Preis, M., Knop, K., Breitkreutz, J., 2014a. Mechanical strength test for orodispersible and buccal films. International Journal of Pharmaceutics 461, 22-29.

Preis, M., Woertz, C., Schneider, K., Kukawka, J., Broscheit, J., Roewer, N., Breitkreutz, J., 2014b. Design and evaluation of bilayered buccal film preparations for local administration of lidocaine hydrochloride. European Journal of Pharmaceutics and Biopharmaceutics 86, 552-561.

Prodduturi, S., Urman, K., Otaigbe, J., Repka, M., 2007. Stabilization of hot-melt extrusion formulations containing solid solutions using polymer blends. AAPS PharmSciTech 8, E152-E161.

Qiao, M., Luo, Y., Zhang, L., Ma, Y., Stephenson, T.S., Zhu, J., 2010a. Sustained release coating of tablets with Eudragit® RS/RL using a novel electrostatic dry powder coating process. International Journal of Pharmaceutics 399, 37-43.

Qiao, M., Zhang, L., Ma, Y., Zhu, J., Chow, K., 2010b. A novel electrostatic dry powder coating process for pharmaceutical dosage forms: Immediate release coatings for tablets. European Journal of Pharmaceutics and Biopharmaceutics 76, 304-310.

Qiao, M., Zhang, L., Ma, Y., Zhu, J., Xiao, W., 2013. A novel electrostatic dry coating process for enteric coating of tablets with Eudragit® L100-55. European Journal of Pharmaceutics and Biopharmaceutics 83, 293-300.

Radebaugh, G.W., Murtha, J.L., Julian, T.N., Bondi, J.N., 1988. Methods for evaluating the puncture and shear properties of pharmaceutical polymeric films. International Journal of Pharmaceutics 45, 39-46.

Ramarathnam, G., Libertucci, M., Sadowski, M., North, T., 1992. Joining of polymers to metal. WELDING JOURNAL-NEW YORK- 71, 483-s.

Sauer, D., Cerea, M., DiNunzio, J., McGinity, J., 2013. Dry powder coating of pharmaceuticals: A review. International Journal of Pharmaceutics 457, 488-502.

Sauer, D., Zheng, W., Coots, L.B., McGinity, J.W., 2007. Influence of processing parameters and formulation factors on the drug release from tablets powder-coated with Eudragit® L 100-55. European Journal of Pharmaceutics and Biopharmaceutics 67, 464-475.

Scheirs, J., Bigger, S.W., Delatycki, O., 1991. Characterizing the solid-state thermal oxidation of poly (ethylene oxide) powder. Polymer 32, 2014-2019.

Shen, B.d., Shen, C.y., Yuan, X.d., Bai, J.x., Lv, Q.y., Xu, H., Dai, L., Yu, C., Han, J., Yuan, H.l., 2013. Development and characterization of an orodispersible film containing drug nanoparticles. European Journal of Pharmaceutics and Biopharmaceutics 85, 1348-1356.

Sievens-Figueroa, L., Bhakay, A., Jerez-Rozo, J.I., Pandya, N., Romañach, R.J., Michniak-Kohn, B., Iqbal, Z., Bilgili, E., Davé, R.N., 2012. Preparation and characterization of hydroxypropyl methyl cellulose films containing stable BCS Class II drug nanoparticles for pharmaceutical applications. International Journal of Pharmaceutics 423, 496-508.

Smikalla, M., Mescher, A., Walzel, P., Urbanetz, N.A., 2011. Impact of excipients on coating efficiency in dry powder coating. International Journal of Pharmaceutics 405, 122-131.

Sriamornsak, P., Kennedy, R.A., 2006. A novel gel formation method, microstructure and mechanical properties of calcium polysaccharide gel films. International Journal of Pharmaceutics 323, 72-80.

Staniforth, J.N., Grosvenor, M.P., 1995. Electrostatic coating of substrates of medicinal products. Google Patents.

Stegemann, S., Ecker, F., Maio, M., Kraahs, P., Wohlfart, R., Breitkreutz, J., Zimmer, A., Bar-Shalom, D., Hettrich, P., Broegmann, B., 2010. Geriatric drug therapy: Neglecting the inevitable majority. Ageing Research Reviews 9, 384-398.

Stegemann, S., Gosch, M., Breitkreutz, J., 2012. Swallowing dysfunction and dysphagia is an unrecognized challenge for oral drug therapy. International Journal of Pharmaceutics 430, 197-206.

Suwardie, H., Wang, P., Todd, D.B., Panchal, V., Yang, M., Gogos, C.G., 2011. Rheological study of the mixture of acetaminophen and polyethylene oxide for hot-melt extrusion application. European Journal of Pharmaceutics and Biopharmaceutics 78, 506-512.

Terebesi, I., Bodmeier, R., 2010. Optimised process and formulation conditions for extended release dry polymer powder-coated pellets. European Journal of Pharmaceutics and Biopharmaceutics 75, 63-70.

Theodore, A., Labana, S., 1973. Powdered coating compositions containing glycidyl methacrylate copolymers with anhydride crosslinking agents and flow control agent. Google Patents.

Visser, J.C., Dohmen, W.M.C., Hinrichs, W.L.J., Breitkreutz, J., Frijlink, H.W., Woerdenbag, H.J., 2015. Quality by design approach for optimizing the formulation and physical properties of extemporaneously prepared orodispersible films. International Journal of Pharmaceutics 485, 70-76.

Wang, F., 2005. title. Ph.D., The University of Western Ontario (Canada), Ann Arbor.

Yang, M., Wang, P., Gogos, C., 2013. Prediction of acetaminophen's solubility in poly(ethylene oxide) at room temperature using the Flory–Huggins theory. Drug Development and Industrial Pharmacy 39, 102-108.

Yang, M., Wang, P., Huang, C.-Y., Ku, M.S., Liu, H., Gogos, C., 2010. Solid dispersion of acetaminophen and poly(ethylene oxide) prepared by hot-melt mixing. International Journal of Pharmaceutics 395, 53-61.

Yang, M., Wang, P., Suwardie, H., Gogos, C., 2011. Determination of acetaminophen's solubility in poly(ethylene oxide) by rheological, thermal and microscopic methods. International Journal of Pharmaceutics 403, 83-89.

Chapter 5: Influence of benzocaine loading on the properties and performance of polyethylene oxide films prepared by electrostatic powder deposition[1]

5.1 ABSTRACT

In this study, we report the use of an electrostatic dry powder process commonly used in the finishing industry to prepare pharmaceutical orodispersible films with increasing drug loadings. Due to the inherent small size of orodispersible films for ease of administration and rapid dissolution, higher drug loadings are at times necessary to support the dose requirements of the active ingredient. Here, we report for the first time that orodispersible films with drug: polymer ratios from 1:9 (10% drug loading) to 2:3 (40% drug loading) were prepared by electrostatic powder deposition (ESPD). This novel ESPD technique was utilized to prepare orodispersible films of benzocaine (BNZ) for the treatment of oral and throat pain. Physical mixtures or composite particles of BNZ and polyethylene oxide (PEO) were utilized to prepare films at varying drug loads to investigate deposition uniformity. The electrical, solid state, and thermal properties of composite particles were investigated using a high resistance meter, powder x-ray diffraction (PXRD), differential scanning calorimetry (DSC), and rheology. The peel energy and mechanical properties, including percent elongation and tensile strength of the films, were determined using a texture analyzer. It was confirmed that composite particles were necessary to prepare films at all drug loadings to achieve acceptable potency and uniformity, as films produced with physical mixtures were superpotent due to segregation attributed to the particle size and electrical resistivity differences between

[1] This work has been submitted for publication.

BNZ and PEO. The composite particles additionally showed lower viscosity profiles with increasing drug loading, enabling reduced cure temperatures. Films produced using composite particles exhibited low adhesion to the substrate and rapid *in vitro* drug release. The BNZ: PEO (2:3) composite particles showed a higher degree of crystalline BNZ content than the lower drug loads, resulting in reduced tensile strength and percent elongation, as well as a slightly reduced dissolution rate.

5.2 INTRODUCTION

Oral films, or orodispersible films (ODFs), have emerged as a promising dosage form due to their ease of administration (Hoffmann et al., 2011). These thin films disperse rapidly when placed in the oral cavity, negating the need for water or swallowing. The incidence of dysphagia or difficulty in swallowing can impact up to one third of the general population in their lifetime (Stegemann et al., 2012), with higher prevalence in geriatric populations and those affected by esophageal conditions (i.e. GERD) or central nervous system disorders (i.e. stoke, Parkinson's disease, Alzheimer's disease, etc.) (Bhattacharyya, 2014; Cho et al., 2015; Stegemann et al., 2010; Takizawa et al., 2016). The rapid disintegration of oral films, and thus reduced choking risk, also provides an effective dosage form for pediatric populations (Ali et al., 2014; Preis, 2015; Slavkova and Breitkreutz, 2015).

ODFs are predominantly manufactured by solvent casting whereby a solution or suspension containing the active pharmaceutical ingredient (API), polymer, plasticizer, and optionally other excipients (i.e. taste masking agents, etc.) is cast or spread on a substrate. The cast material is then passed through an oven or other drying element to evaporate the solvent and produce the final dried film (Borges et al., 2015a, b; Dixit and

Puthli, 2009; Morales and McConville, 2011). The major limitation surrounding this process is the use of aqueous or organic solvent. Aqueous systems may require long drying times given the high heat of vaporization of water (Kianfar et al., 2012; Shen et al., 2013; Sievens-Figueroa et al., 2012; Visser et al., 2015). Organic solvents can significantly reduce drying times; however, testing is required on the final drug product to confirm residual solvent levels below ICH guidelines. Additionally, as most organic solvents are classified as flammable, processing with these solvents requires manufacturing facilities to be equipped with solvent handling and collection capabilities (Constable et al., 2007; Grodowska and Parczewski, 2010). Lastly, the use of aqueous and organic solvents may be detrimental to the physical or chemical stability of the API (Bose and Bogner, 2007).

The desire to eliminate solvent from drug product manufacturing processes has yielded increased developmental efforts in dry powder coating processes, including electrostatic dry powder coating (Bose and Bogner, 2007; Luo et al., 2008; Qiao et al., 2010a; Qiao et al., 2010b; Qiao et al., 2013; Sauer et al., 2013; Yang et al., 2015). Recently, the electrostatic dry powder coating process was modified to utilize a temporary, non-adhering substrate to prepare ODFs (Prasad et al., 2015). This process of electrostatic powder deposition (ESPD) involves (1) the charging and spraying of powder onto a grounded, conductive substrate; (2) the curing of the deposited powder; and (3) the removal of the cured film from the substrate.

Although the small size of ODFs promotes to its ease of administration and rapid disintegration, it can also limit the incorporated dose (Boateng et al., 2010; Borges et al., 2015b). Increasing drug loading in solvent cast films can lead to aggregation of API in solution or upon drying, resulting in non-uniform films (Morales and McConville, 2011; Perumal et al., 2008). To reduce this aggregation propensity, additional excipients are

typically added to the casting solution, such as stabilizing surfactants or viscosity increasing agents (Bhakay et al., 2016; Bodmeier and Paeratakul, 1989; Morales and McConville, 2011). These excipients can require processing changes, such as the need for longer drying times or higher drying temperatures, which can negatively impact the stability of the API (Myers, 2008). We hypothesize that uniform ODFs of increasing drug loading can be prepared using composite particles of API and polyethylene oxide (PEO) with the ESPD process.

The objective of the present study was to investigate the influence of drug loading on the preparation of benzocaine (BNZ) and PEO oral films, as well as on the film mechanical and drug release properties. BNZ was chosen as a model compound due to its indication as a local anesthetic of oral and pharyngeal mucous membranes, such as for sore throat pain, making it attractive for an ODF dosage form. Low molecular weight PEO (MW 100,000) was chosen as the carrier polymer due its hydrophilic properties and low glass transition temperature (-50 to -57 °C), which promotes a self-plasticizing behavior. The specific aims were to study the impact of drug load on: (i) film drug content uniformity using physical mixtures versus composite particles, (ii) electrical, solid state, and thermal properties of the composite particles, (iii) peel energy to remove the film from the substrate, (iv) mechanical properties of the film, and (v) the drug release from the films.

5.3 MATERIALS AND METHODS

5.3.1 Materials

POLYOX™ WSR N10 NF was generously donated by Colorcon® (West Point, PA, USA). Benzocaine USP was purchased from Spectrum Chemicals (New Brunswick,

NJ, USA). High-performance liquid chromatography-grade solvents were purchased from Fisher Scientific (Pittsburgh, PA, USA).

5.3.2 Blend Preparation

Appropriate amounts of API and polymer were weighed into bottles, manually mixed for 30 s, and passed through a 30 mesh (595 μm opening) sieve for deagglomeration. Screened materials were then blended for 15 min using a Turbula® T2F blender (Clifton, NJ, USA). Bulk API and polymer were sieved and material between 25 μm (500 mesh) and 90 μm (170 mesh) was collected prior to blend preparation for physical mixtures.

5.3.3 Hot Melt Extrusion (HME)

A co-rotating, twin-screw Leistritz Nano 16 extruder (Sommerville, NJ, USA) was used to prepare composite particles. The screw design consisted of a combination of conveying and kneading elements were used in order from feed zone to the die: 3 × GRA3-20-30, 4 × GFA3-15-30, 3 × GFA3-10-30, 2 × KB73-15-30°, 1 × GRA3-20-30, 1 × GFA3-15-30, 1 × GFA3-10-30. The screw speed was maintained at 100 rpm and a temperature profile of 70°C-90°C-95°C-100°C for zone 1-zone 2- zone 3-die was used. The feed rate was approximately 3 g/min using a volumetric feeder, Brabender MT-1 (Duisburg, Germany). The resulting extrudate was cut using a Randcastle Extrusion Systems pelletizer (Cedar Grove, NJ, USA).

The pellets were further milled using a cryogenic mill, Spex SamplePrep 6870 Freezer/Mill (Metuchen, NJ, USA). Pellets were placed into polycarbonate vials with a magnetically driven impactor. Samples were immersed in liquid nitrogen, pre-cooled for

5 min, milled for 5 min at a frequency of 10 cycles per second (cps), with a pause of 2 min between cycles to prevent the magnetic coil and sample overheating. The co-processed material was milled for a total of 30 min. Milled materials were sieved and material between 25 μm (500 mesh) and 90 μm (170 mesh) was collected for use with ESPD.

5.3.4 Particle Size Distribution

Sympatec HELOS (Pennington, NJ, USA) particle analysis was performed with an R3 lens (0.5/0.9–175 μm). The powders were dry dispersed at a pressure of 3.0 bar using a Rodos T4 disperser (Pennington, NJ, USA). Each measurement was performed in triplicate and the instrument's statistical software was used to calculate the average particle size distribution. The evaluation software was WINDOX 5.6.0.0 and the high-resolution laser diffractions (HRLD) method was selected as the evaluation method.

5.3.5 Electrical Resistance Measurement

Compacts for analysis were prepared by weighing approximately 500 mg of material and compressing into a compact using a 13mm flat faced die. Compacts were compressed using a hydraulic press with 3000 lbs of force. Resistance measurements were performed using a custom resistivity cell coupled with a Hewlett Packard HP 4329A High Resistance Meter (Palo Alto, CA, USA).

5.3.6 Differential Scanning Calorimetry (DSC)

A TA Instruments Model Auto Q20 DSC (New Castle, DE, USA) was used to characterize raw materials, blends and composite samples. Samples were evaluated by

first equilibrating samples at 20°C followed by heating to 100°C at a ramp rate of 10°C/min. During analyses, high purity nitrogen flowed through the sample chamber at a rate of 50 mL/min Data was analyzed using TA Universal Analysis 2000 software.

5.3.7 Powder X-ray Diffraction (PXRD)

PXRD analyses were conducted using a Rigaku MiniFlex 600 (Tokyo, Japan) operated at 40 kV and 15 mA using a variable + fixed slit condition. Data was collected in a continuous scan mode with a step size of 0.02° and step speed of 2°/min over a of 2θ range of 5° to 60°.

5.3.8 Rheology

Compacts for analysis were prepared by weighing approximately 1 g of material and compressing into a slug using a 25 mm flat faced die. As described previously (Gupta et al., 2014), slugs were compressed using a hydraulic press with 5000 lbs of force for 5 s. Rheology experiments were performed with a TA Discovery Hybrid Rheometer 3 (New Castle, DE). The sample was placed between two parallel 25 mm plates after zero gap calibration. Samples were conditioned for 60 s at 30 °C, followed by a temperature sweep from 30 °C to 100 °C at 5 °C increments. Complex viscosity measurements were made using an oscillation of 0.1 rad/s, while maintaining an axial force at 0.1- 0.3 N.

5.3.9 Electrostatic Powder Deposition (ESPD)

A schematic of the electrostatic powder deposition process is shown in Figure 5.1. Powder was fed to a Nordson Vantage® Manual corona gun (Westlake, OH, USA) and sprayed using compressed air using 0.5 bar fluidizing/atomizing pressure, with a charging

voltage of 60kV. Stainless steel 316 (SS 316), 0.060" (1.524 mm) thickness, was used as the grounded substrate. The bulk composition of the unpolished SS 316 was reported as follows: (wt. %): C (0.28) Cr (16.58), Ni (10.08), Mo (2.04), Mn (1.46), Si (0.29), P (0.03), S (≤ 0.01) and Fe (balance). The gun-to-substrate distance was ~20 cm (4 inches) and the relative humidity was 45 %RH (+/- 3 %RH). The gun-to-substrate distance was ~30 cm (8 inches) for the deposition uniformity sample preparation, as a larger substrate was used. After powder deposition, the substrate was placed in an infrared oven to cure. The resulting films were peeled from the substrate and film weight and thickness were measured. Thickness was measured using a Mitutoyo digital micrometer (Mitutoyo, Kawasaki, Japan).

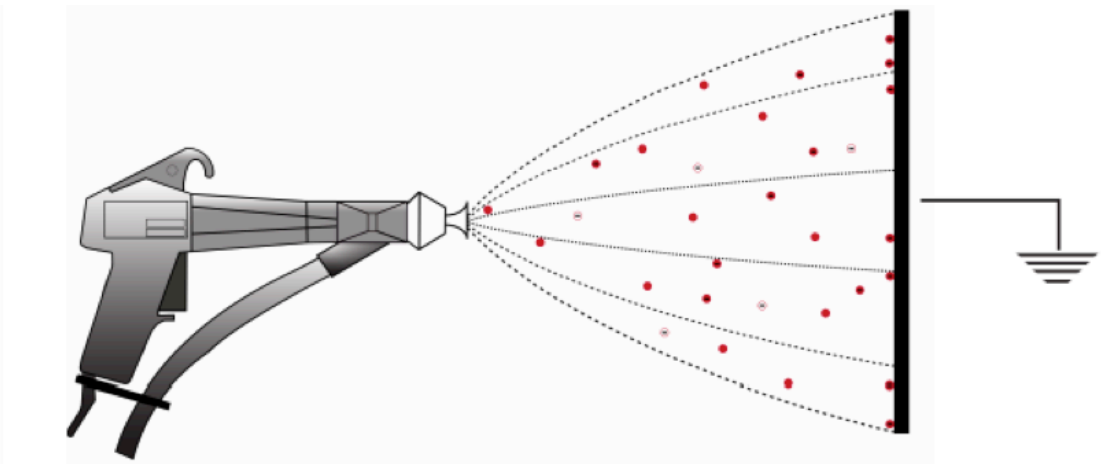

Figure 11. Schematic of electrostatic powder deposition using corona gun and grounded conductive substrate.

5.3.10 Adhesive Strength Testing

Samples for adhesion testing were equilibrated for at least 24 hours at room temperature. Adhesive testing was carried out using a 90° peel test fixture (TA-305A) on

a Stable Micro Systems TA-XT (Godalming, Surrey, UK) equipped with a 5 kg load cell. The test was conducted with a crosshead speed of 0.2 mm/s. Exponent software (Godalming, Surrey, UK) was used to process data. The peel energy was calculated by equation 5.1.

$$G_a = \frac{F_{avg}}{b}(1 - \cos\theta) \tag{5.1}$$

where F_{avg} is the average force of removal, b is the width of the sample, and θ is the angle of peel force. θ=90° for the test fixture used in this study.

5.3.11 Mechanical Strength Testing

Mechanical properties of films were tested on a Stable Micro Systems TA-XTplus (Godalming, Surrey, UK) using 5 kg load cell. Samples were mounted on a Texture Technologies TA-108s-5 fixture (Hamilton, MA, USA) and punctured using a ¼" spherical probe moving at 1 mm/s. Exponent software (Godalming, Surrey, UK) was used to process data. Tensile strength and percent elongation were calculated as shown in equations 5.2 and 5.3, respectively, as defined by Radebaugh et al. (Radebaugh et al., 1988).

$$\sigma_{TS} = \frac{F}{A_{cs}} \tag{5.2}$$

where F is the force at rupture (N) and A_{cs} is the cross sectional area of the film in the film holder (mm^2).

$$\% \, elongation = \left(\frac{\sqrt{r^2+D^2}-r}{r}\right) \times 100\% \quad (5.3)$$

where r is the radius of the film exposed to the probe in the same holder and D is the displacement of the probe from the point of contact with the film until rupture.

5.3.12 Assay and Content Uniformity Testing

Aliquots of blends, physical mixture, and composite particles were weighed and accurately transferred into volumetric flasks and dissolved in mobile phase (see HPLC section). Film assay samples were prepared by accurately weighing and transferring the film into a volumetric flask and dissolved in mobile phase. The resulting solutions were then filtered through 0.2 μm PVDF filters and immediately transferred to 2-mL HPLC vials for analysis. Blend, physical mixture, and co-processed particles were analyzed in triplicate; films were analyzed using n=10 samples.

5.3.13 High Performance Liquid Chromatography (HPLC)

Benzocaine content was analyzed with a Thermo Scientific Dionex UltiMate 3000 HPLC system (Sunnyvale, CA, USA). An Ultimate 3000 Autosampler was utilized to inject 10 μL samples. The HPLC system also included dual UltiMate 3000 Pumps and an UltiMate RS Variable Wavelength Detector. The system was operated under isocratic conditions with 0.05% phosphoric acid: acetonitrile (1:1) mobile phase, using a flow rate of 1.0 mL/min. Injections were passed through a Phenomenex Luna® 5 μm C18(2) reverse phase column, 250 x 4.6mm (Torrence, CA, USA) and absorbance at a

wavelength of 285 nm was measured. Chromeleon Version 6.80 software (Sunnyvale, CA, USA) was used to process all chromatography data.

5.3.14 Dissolution Testing

In vitro drug release testing was conducted using a USP dissolution apparatus 5 (paddle over disk method). Testing was conducted using a rotation speed of 100 rpm with 500 ml of Sørensen's buffer, pH 6.8 held at 37°C. Films were cut such that each sample contained an equivalent 12mg dose of BNZ. Films were placed in mesh sample holders (16 mesh) before being immersed in the dissolution vessel. Samples were taken at 1, 3, 5, 10, 15, and 30 min and the dissolution medium was replenished to maintain constant volume. Samples were analyzed for drug content using the HPLC method described above.

5.4 RESULTS

The physical mixture and sieve cut of composite particles were assayed for drug content and used to normalize the film assay values. The physical mixture potency ranged from 101.8-111.1%, while the composite particles ranged from 99.8-105.5%. The normalized drug content of the films prepared using physical mixtures and composite particles are shown in Figure 5.2. The films prepared using composite particles showed acceptable potency values ranging from 95.3-106.0%, while the films prepared using physical mixtures were all significantly super potent with values ranging from 127.3-169.2%. The films prepared from physical mixtures also showed significantly higher variability with standard deviations up to 27%.

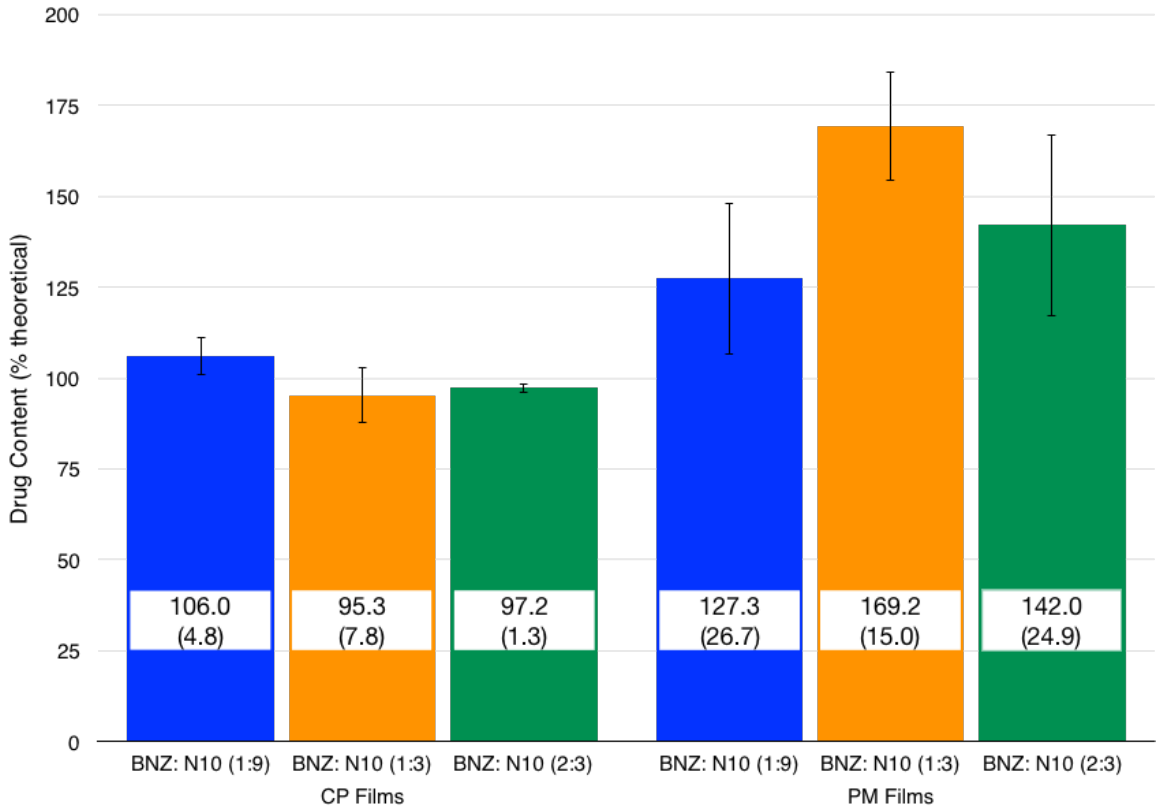

Figure 5.12. Normalized drug content of films (n=10) prepared using composite particles (CP) and physical mixture (PM) of BNZ: PEO at 1:9, 1:3, and 2:3 ratios. Values indicate average drug content (standard deviation).

The particle size distributions of the PEO and BNZ sieve cuts are shown in Figure 5.3. The BNZ showed a smaller and broader particle size distribution than the PEO. The particle size distribution of the BNZ was d_{10} = 6.49, d_{50} = 24.09, d_{90} = 69.04 with a span of 2.6. The particle size distribution of the PEO was d_{10} = 12.07, d_{50} = 46.90, d_{90} = 90.94 with a span of 1.7.

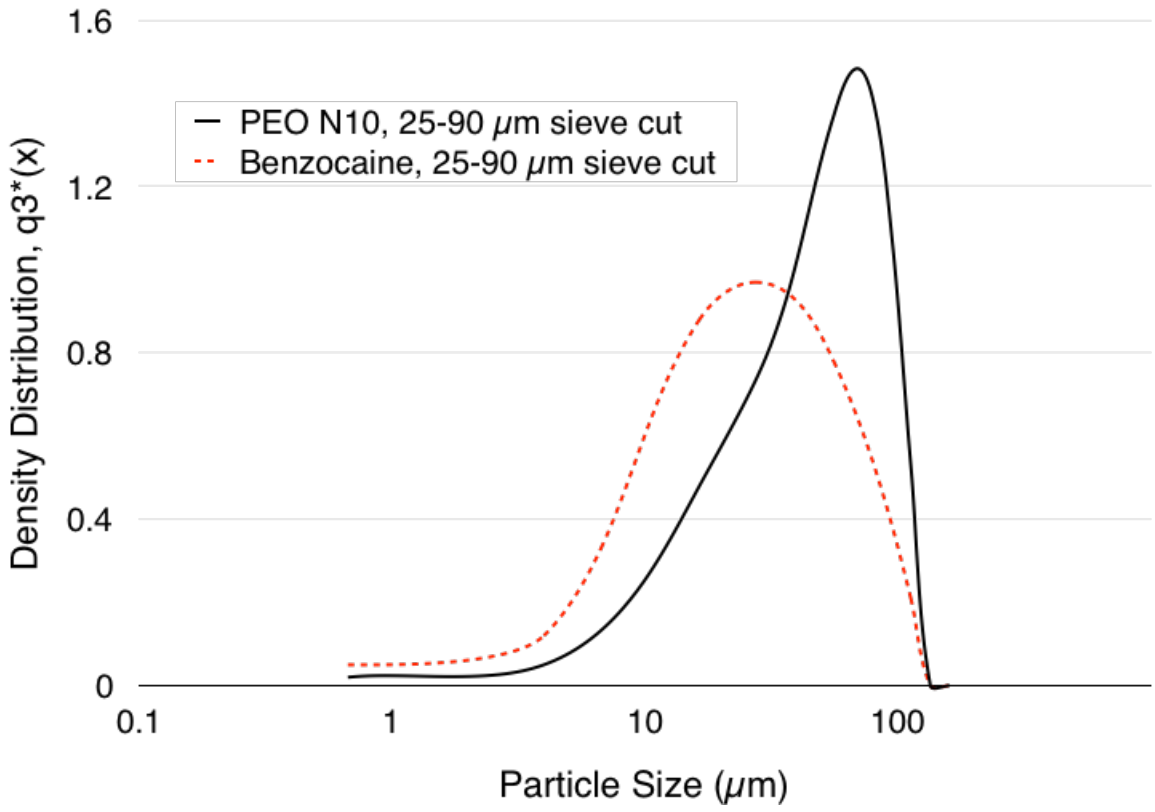

Figure 5.3. Particle size distributions of PEO and BNZ collected from sieve cut between 25 μm (500 mesh) and 90 μm (170 mesh).

The measured resistance of the BNZ, PEO, and composite particles are shown in Figure 5.4. The electrical resistance of BNZ was measured at 0.8 x 10^{14} Ω while that of PEO was significantly lower at 1.8 x 10^{8} Ω. The electrical resistance of the composite particles did not vary significantly with measured values at 0.4 x 10^{8}, 0.2 x 10^{8}, and 0.6 x 10^{8} Ω, for the 1:9, 1:3, and 2:3 ratios, respectively.

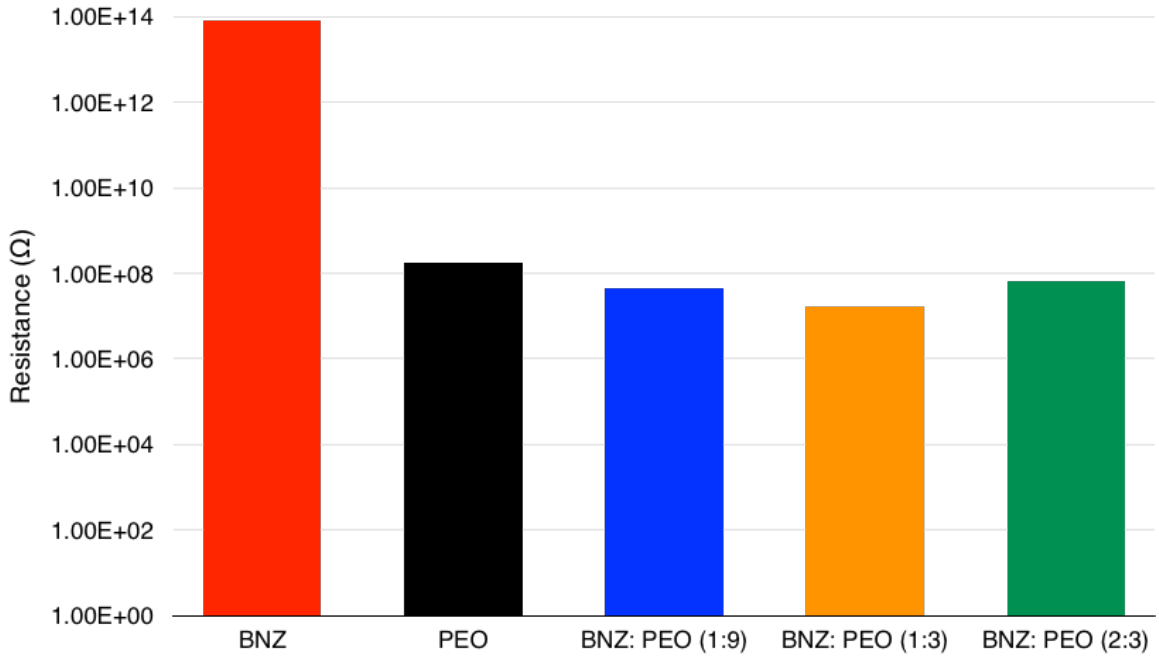

Figure 5.4. Average electrical resistance (n=3) for BNZ, PEO and composite particles of BNZ: PEO at 1:9, 1:3, and 2:3 ratios. Error bars are non-distinguishable.

The PXRD diffractograms are shown in Figure 5.5. PEO is a semi-crystalline polymer showing distinct diffraction peaks at 2θ angles around 19° and 23°. BNZ is a crystalline API exhibiting high intensity diffraction peaks at 2θ angles around 17° and 20°, as well a series of smaller peaks. The BNZ: PEO (1:9) blend diffraction profile shows that crystalline BNZ is detectable at the lower drug loading, showing BNZ peaks around 17° and 20°. The composite particles of BNZ:PEO (1:9) do not exhibit crystalline drug peaks, indicating the BNZ is in its amorphous state at this drug loading. Broad and low intensity BNZ peaks can be seen in the (1:3) particles and with increased intensity in the (2:3) particles, indicating the presence of crystalline BNZ in these higher drug load

composite particles. PEO diffraction peaks were seen in all the processed particles, but they exhibited less intensity than the bulk material.

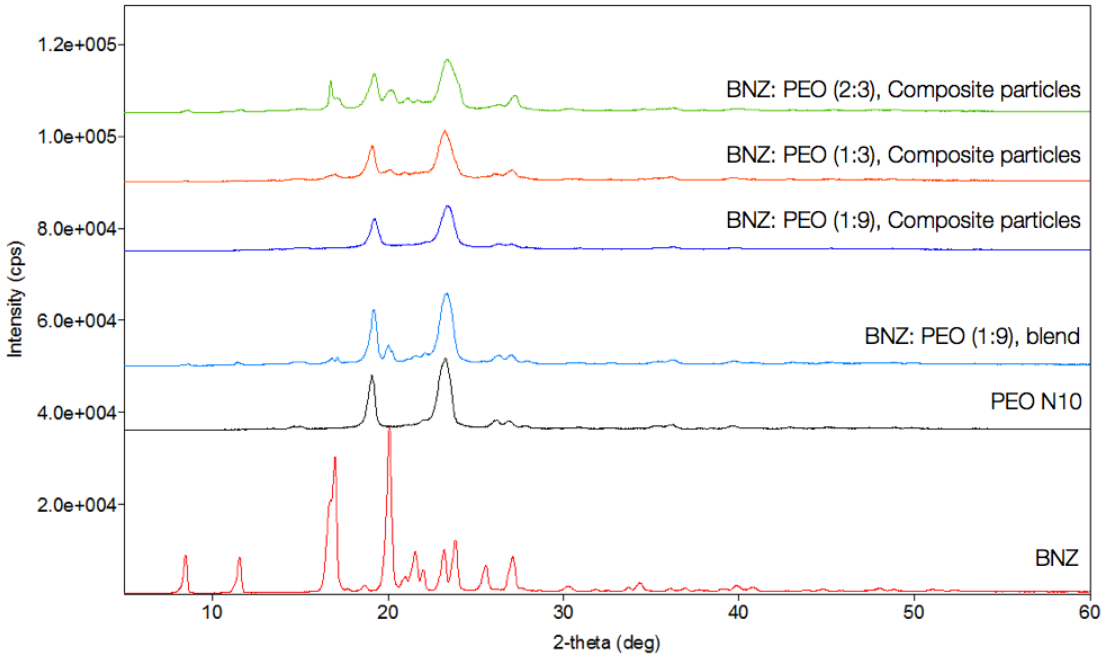

Figure 5.5. PXRD diffractograms of BNZ, PEO, BNZ: PEO (1:9) blend, and composite particles of BNZ: PEO at 1:9, 1:3, and 2:3 ratios.

The DSC profiles of the raw materials and composite particles of BNZ and PEO are shown in Figure 5.6. The melting point of BNZ and PEO N10 were measured at 89.65 °C and 61.20 °C, respectively, consistent with values reported in the literature (Fulias et al., 2013; Gobble et al., 2013; Prasad et al., 2015). The melting point of PEO was suppressed upon processing with BNZ, with melting points of 54.12 °C, 38.16 °C, and 37.49 °C measured for BNZ: PEO (1:9), (1:3), and (2:3), respectively. No crystalline BNZ was detected in the thermograms of the composite particles.

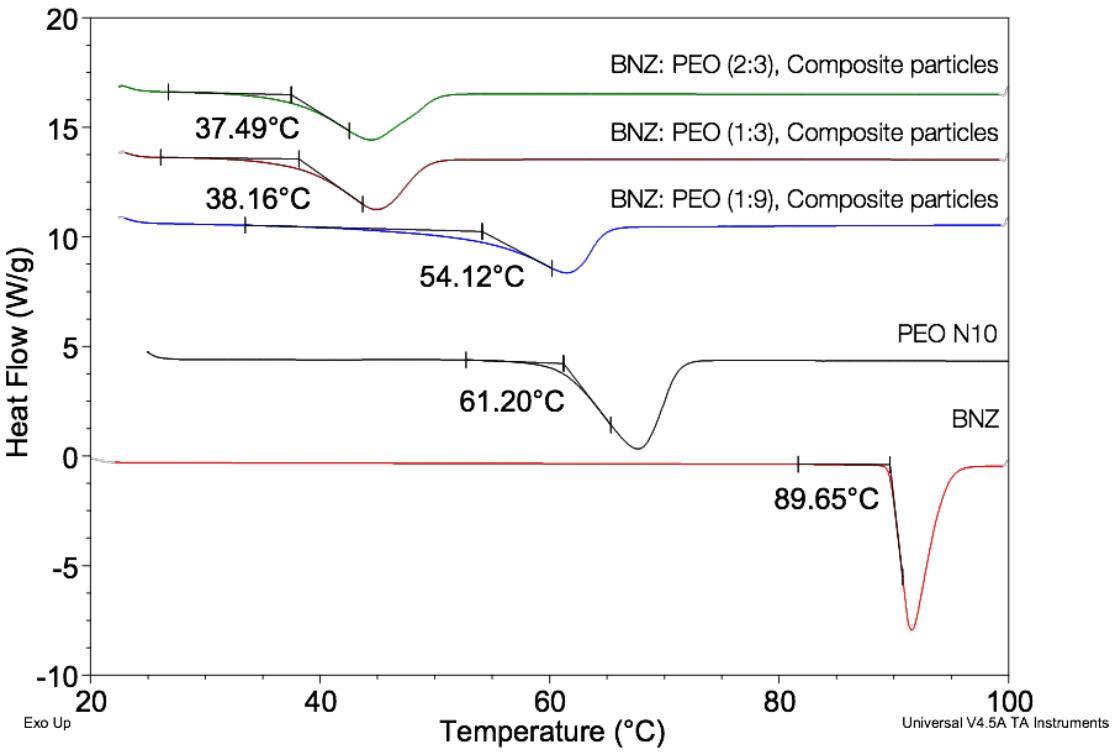

Figure 5.6. DSC thermograms of BNZ, PEO, and composite particles of BNZ: PEO at 1:9, 1:3, and 2:3 ratios.

The complex viscosity as a function of temperature for PEO and composite particles of BNZ: PEO at 1:9, 1:3, and 2:3 ratios are shown in Figure 5.7. The highlighted area indicate the complex viscosity range of temperatures shown to promote film formation in a previous study (Prasad et al., 2016a), specifically between 80 °C and 90 °C. The addition of BNZ resulted in a significant plasticization effect where lower complex viscosities were seen with higher drug loading. The temperatures needed to achieve complex viscosities comparable to those shown to promote film formation with

PEO are significantly lower with BNZ: PEO formulations. For example, PEO achieves a complex viscosity of approximately 45000 Pa s at 90 °C. The composite particles achieve comparable complex viscosities at approximately 60 °C, 55 °C, and 45 °C for the 1:9, 1:3, and 2:3 BNZ: PEO ratios, respectively.

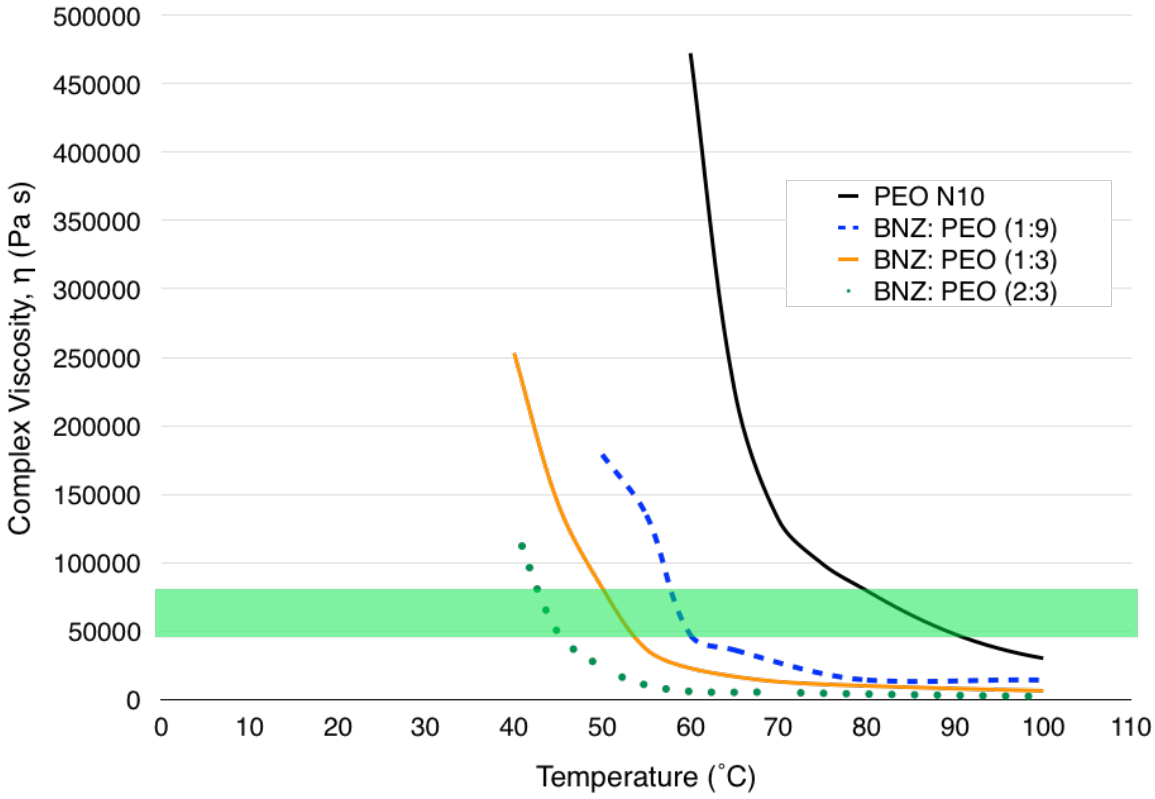

Figure 5.7. Average complex viscosity (n=3) as a function of temperature for PEO and composite particles of BNZ: PEO at 1:9, 1:3, and 2:3 ratios. Highlighted region indicates complex viscosity range of temperatures shown to promote film formation with PEO determined by Prasad et al. (Prasad et al., 2016a).

The peel energies to remove the cured films are shown in Figure 5.8. The samples exhibited an increase in the peel force required to remove films from substrates with

increasing drug loading. The average peel energies to remove the BNZ: PEO (1:9), (1:3), and (2:3) were 6.1, 21.9, and 46.1 J/m^2, respectively. The BNZ: PEO (2:3) also showed a propensity to tear towards the end of the peel test.

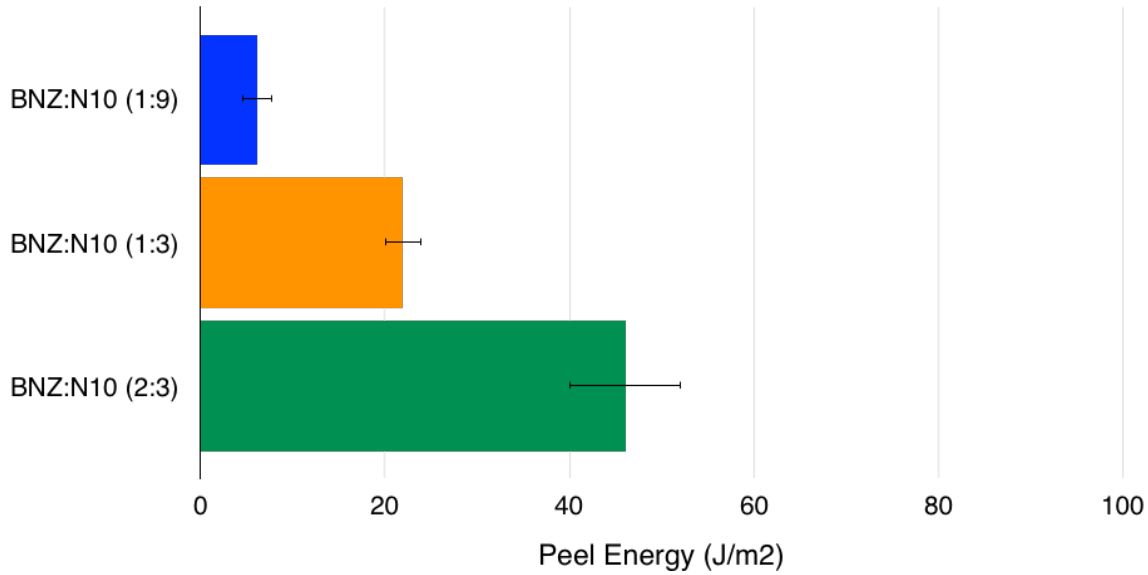

Figure 5.8. Average peel energies (n=3) to remove films from substrate for films prepared using composite particles of BNZ: PEO at 1:9, 1:3, and 2:3 ratios

The tensile strength and percent elongation for the films of each drug load are shown in Figure 5.9. The films show an increase in tensile strength from 0.89 to 1.6 MPa and an increase in percent elongation from 14.5 to 24.0% with an increase in drug loading from (1:9) to (1:3). However, both tensile strength and percent elongation significantly decrease for the BNZ: PEO (2:3) films, with mean values of 0.4 MPa and 5.1%, respectively.

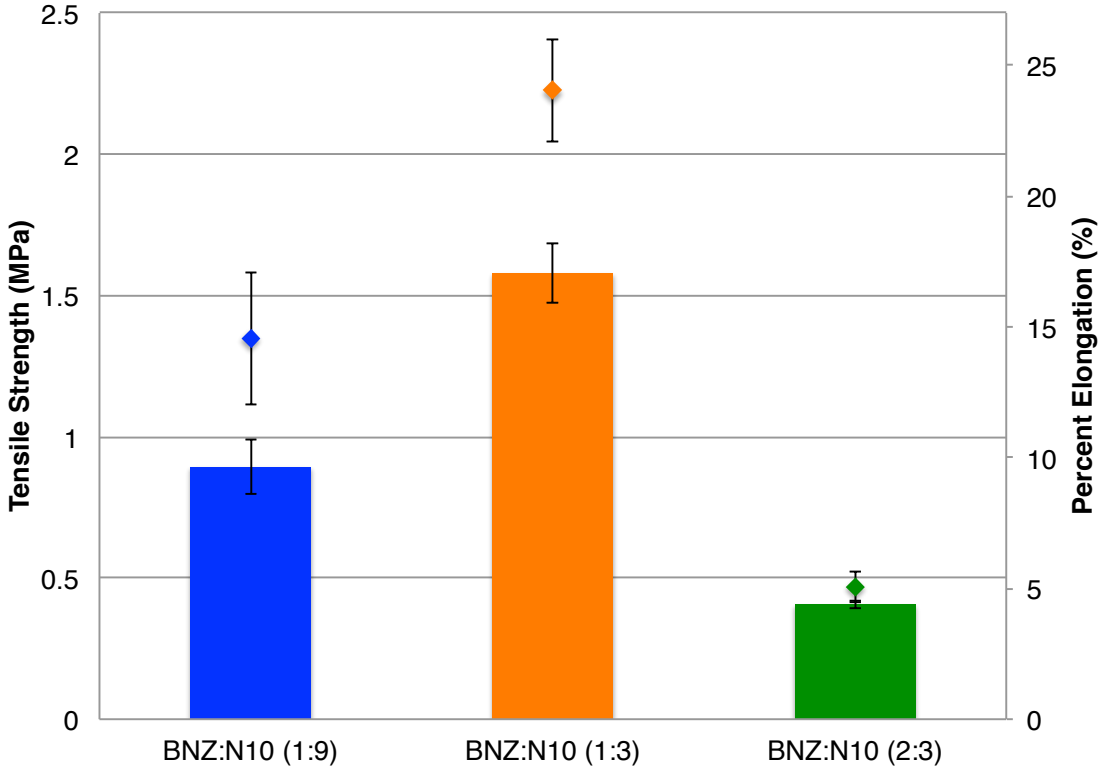

Figure 5.9. Average tensile strength (bars) and percent elongation (points) (n=3) of films prepared using composite particles of BNZ: PEO at 1:9, 1:3, and 2:3 ratios

In-vitro drug release testing was conducted using films prepared with composite particles and resulting drug release profiles are shown in Figure 5.10. Rapid drug release was seen with all the BNZ: PEO films with greater than 85% drug release by 10 minutes. The BNZ: PEO (1:9) films showed 87% release by 3 minutes and 100% by 5 minutes. The BNZ:PEO (1:3) films showed a faster release profile with 96% release by 1 minute and 100% by 3 minutes. The BNZ: PEO (2:3) films showed a slightly slower release with 97% release by 10 minutes and 100% by 15 minutes.

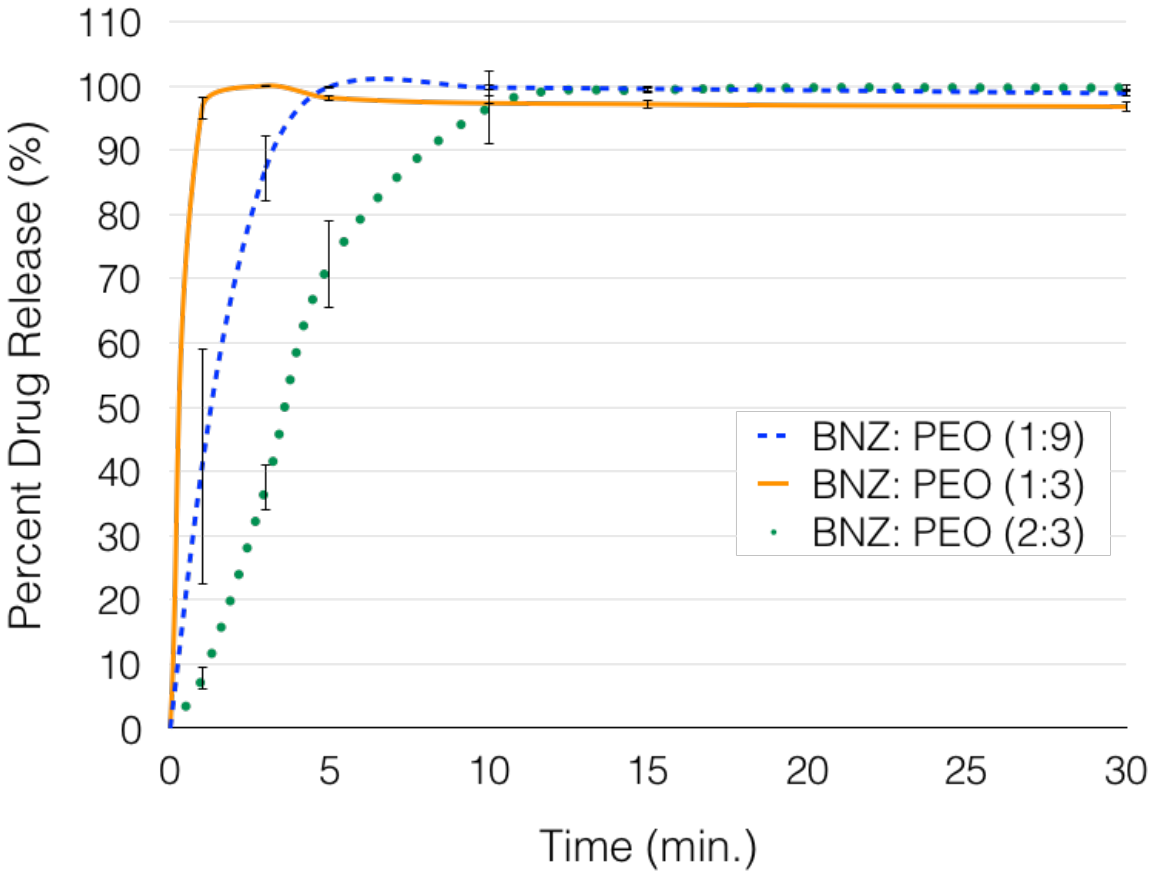

Figure 5.10. Drug release of films (n=3) prepared using composite particles of BNZ: PEO at 1:9, 1:3, and 2:3 ratios.

5.5 Discussion

5.5.1 Impact of drug load on film drug content uniformity using physical mixtures versus composite particles

The average drug content of films prepared using composite particles, reported in Figure 5.2, was between 95-106% whereas that measured for physical mixtures was superpotent with values of 127-169%. Additionally, no clear trend was seen with increasing drug load. The standard deviations are significantly higher when processing

with physical mixtures. The authors previously showed the ability to obtain comparable average drug content when preparing films using a physical mixture of acetaminophen (APAP) and PEO at a 1:9 ratio, but also reported a significantly higher variability when using the physical mixture with 11.9% RSD compared to 1.8% RSD with composite particles (Prasad et al., 2015).

Physical mixtures of BNZ and PEO were prepared with sieve cuts of each bulk material, as described in the methods section. However, Figure 5.3 shows that the BNZ sieve cut material showed a smaller and broader particle size distribution than that of the PEO sieve cut. Smaller particles are able to accumulate more charge during electrostatic charging due to their higher surface area (Bailey, 1998; Mazumder et al., 1997; Prasad et al., 2016b; Ratanatriwong and Barringer, 2007). These particles with greater charging efficiency can preferentially deposit on the grounded substrate (Amefia et al., 2006; Meng et al., 2009). Additionally, the electrical resistance of the BNZ, 10^{14} Ω, was significantly higher that that of the PEO, 10^{8} Ω. Particles with higher resistance values tend to accumulate and retain more charge than those with lower resistance (Bailey, 1998). The higher resistivity and smaller particle size distribution of the BNZ contributed to the preferential deposition of BNZ from the physical mixture, resulting in superpotent films.

These results are in line with electrostatic coating guidelines from the finishing industry, including the manufacture of composite coating materials and milling particles to a small and narrow particle size distribution (Harmuth, 1982; Hogan et al., 2002; Noonan, 1977; Wicks et al., 2007). Composite particles enable uniform deposition of components that may not exhibit ideal resistivity for processing, as well as ensure uniform distribution of API or functional additives such as liquid plasticizers and antistatic agents. The manufacture of films by ESPD using composite particles of API

and polymer enable the preparation of films with increasing drug load with a higher degree of control for maintaining dose uniformity. The remainder of this work is focused only on films prepared using composite particles.

5.5.2 Impact of drug loading on electrical, solid state, and thermal properties of the composite particles

The BNZ: PEO composite particles exhibited electrical resistance close to that of the PEO, as shown in Figure 5.4. Mixtures of materials with varying resistance (or conversely of varying conductivity) usually exhibit negligible changes in electrical properties until a critical concentration is reached. Above this critical concentration, sometimes referred to as a percolation threshold, there is a steep change, usually orders of magnitude, in electrical resistance (Arenhart et al., 2016; Landauer, 1978; Sun et al., 2009). In the BNZ: PEO composite particles, the BNZ content is the minor and more resistant species; thus the electrical conductivity and overall resistance of the composite system is driven by the bulk PEO. The comparable electrical properties of the BNZ: PEO composite particles suggest that the particle charging and deposition behavior should not vary with drug loading within the ranges used in this study. This is additionally advantageous as the high resistivity of the BNZ particles is undesirable for processing. High resistivity particles promote higher charge accumulation and thus a higher incidence of back-ionization (Prasad et al., 2016b).

The PXRD diffractograms show that the BNZ in the BNZ: PEO (1:9) and (1:3) composite particles are mostly amorphous. The low intensity BNZ peaks in the 1:3 particles and the increased intensity seen in the 2:3 particles indicate a limit to the miscibility of BNZ in PEO, resulting in particles containing both amorphous and crystalline BNZ. The DSC thermograms of the composite particles indicate a significant

depression and broadening of the PEO melt endotherm with increasing drug load. The depression of the PEO melting point indicates that the BNZ is either partially miscible or intimately mixed with the amorphous regions of the PEO. No BNZ melt endotherm is seen any of the composite particle thermograms, indicating the crystalline BNZ detected via PXRD at the higher drug loadings is either not detectable at the levels present via DSC and/or is miscible with PEO in the molten state at elevated temperatures.

The rheological properties of PEO and the BNZ: PEO composite particles were assessed to provide guidance on the curing temperature. PEO is an advantageous polymer for thermal processing due to its low melting point, enabling melt flow at relatively low temperatures. The DSC summarized above shows that BNZ acts as a plasticizer, further reducing the melting point of the BNZ: PEO system. This suggests that lower temperatures may be able to achieve viscosities necessary for film formation. Film formation of powder particles is driven by the deformation and coalescence of neighboring particles, followed by the reduction of void space and leveling of the final film (Andrei et al., 2000; Sauer et al., 2013). Following the Frenkel theory of viscous spheres under surface tension, the time for film formation is driven directly by polymer viscosity and particle size and indirectly by surface tension (Keddie and Routh, 2010).

The authors previously showed that film formation with PEO alone was achieved at 80 °C and 90 °C by 30 minutes (Prasad et al., 2016a). The complex viscosities associated with PEO at this temperature range are highlighted in Figure 5.7, encompassing 45,000 to 80,000 Pa s. The composite particles show significantly lower complex viscosity curves than the neat PEO, with viscosities within the highlighted range at lower temperatures with increasing drug load. Based on the rheology data, the following temperatures (and corresponding average complex viscosity) were selected for each formulation: 60 °C (47000 Pa s), 55 °C (37000 Pa s), and 45 °C (48000 Pa s) for the

1:9, 1:3, and 2:3 ratios of BNZ: PEO. Although the 2:3 ratio showed a similar onset of melt as the 1:3 ratio using DSC analysis, the viscosity profile indicated a further plasticization effect. This effect can be attributed to the crystalline BNZ acting as an impurity or dispersed additive in the polymer affecting its melt behavior and facilitating a further decrease in the required cure temperature. This phenomenon is analogous to the addition of dispersed additives in the plastics industry to improve processability, among other attributes. Owusu-Nkwantabisah et al. showed the addition of 5% dispersed calcium stearate to polyethersulfone resulted in a 40% reduction in viscosity, enabling lower melt extrusion processing temperatures (Owusu-Nkwantabisah et al., 2016). Note that if there are strong interactions between the dispersed particles and the polymer, the additive could produce an increase in viscosity. For example, a study conducted with PEO and doped with carbon black showed strong interactions lead to increased melt viscosity and subsequent onset of polymer degradation (Malik et al., 2006).

5.5.3 Impact of drug loading on peel energy required to remove film from the substrate

As shown in Figure 5.8, the average peel energy to remove the BNZ: PEO film increased with increasing drug load. This increase of 6.1, 21.9, to 46.1 J/m^2 for BNZ: PEO (1:9), (1:3), and (2:3), respectively, were all still relatively low. Adhesives, such as tape, typically require peel energies of 100-1000 J/m^2 to remove (Gay, 2002); thus, energies below 100 J/m^2 are considered to exhibit a low degree of adhesion.

This trend of increased adhesion is analogous to the phenomenon of "sticking" during tablet compression. Sticking occurs when powder adhesion to tablet tooling (punches or die) becomes greater than the compact cohesion leading to powder transfer or sticking to the tooling surface (Mollereau et al., 2013). The sticking phenomenon is

mainly attributed to the adhesion of API to steel surfaces, such as SS316 commonly used in pharmaceutical processing, particularly in high drug load formulations. The mechanism of this adhesion tends to be attributed to weak van der Waals forces between the API and the tablet punch steel surface and can be greater when the metal is oxidized (i.e. rust) (Waknis et al., 2014). Waknis et al. also showed an increase in adhesion or tendency to stick to steel when using API polymorphs with higher surface energy and surface polarity. This was attributed to interactions between polar functional groups of the API and the Lewis-base character of the stainless steel (Podczeck, 1999). However, the sticking behavior in tablet compression is much more complex, with factors including API morphology, moisture content, lubricant distribution, compression dwell time, tooling geometry, as well as other formulation aspects and processing parameters (Sakata and Yamaguchi, 2011; Tousey, 2003).

BNZ is slightly hydrophobic with a $P_{oct/water}$ coefficient of 37.8 (de Matos Alves Pinto et al., 2000), lipophilic with a log P of 1.9 (Clarke et al., 2004), exhibits a relatively high surface energy of 67.1 mJ/m^2 (Zografi and Tam, 1976), and has low polar surface area (Peña et al., 2006). However, as shown in Figure 5.5, the bulk of the BNZ in the films is present in the amorphous form with partial crystallinity seen in the BNZ: PEO (1:3) and (2:3) formulations. Notably, the amorphous form of a solid can exhibit higher surface energy and polarity than its crystalline counterpart (Newell et al., 2001; Puri et al., 2010; Zhang et al., 2006). The polarity and surface energy of the BNZ increase the interactions and overall work of adhesion between the film and the oxide layer of the passivated stainless steel substrate (Flint et al., 2000; Good, 1992; Podczeck, 1999; Waknis et al., 2014). Thus, the increased adhesion between the BNZ: PEO films with increased drug loading can be directly attributed to the increased interfacial contact

between the BNZ, especially the amorphous BNZ, and the passivated stainless steel surface.

5.5.4 Impact of drug loading on mechanical properties of the film

The tensile strength BNZ: PEO films increased from 0.89 to 1.58 MPa when the drug: polymer ratio was increased from 1:9 to 1:3, respectively, as shown in Figure 5.9. A corresponding increase in percent elongation was also seen from 14.5% to 24.0%. Prasad et al. reported tensile strength of 0.86 MPa and percent elongation of 3.8% for a PEO films prepared using ESPD containing no API (Prasad et al., 2015), confirming BNZ acts as a plasticizer to increase the overall strength and plasticity of the final PEO film. However, a significant drop in tensile strength and percent elongation was seen with the BNZ: PEO (2:3) film with average values of 0.41 MPa and 5.1%, respectively. This decrease in strength and plasticity can be attributed to the presence of crystalline BNZ dispersed throughout the film at this higher drug load. The reduction in film strength and elongation due to dispersed solid particles has been reported for various film coating systems using insoluble pigments and opacifiers such as titanium dioxide (Aulton et al., 1984; Okhamafe and York, 1984; Rowe, 1983). Crowley et al. also reported an inverse relationship between these mechanical properties and drug loading when preparing films containing guaifenesin and a higher molecular weight grade of PEO, with PXRD analysis and SEM images confirming that the guaifenesin was dispersed as crystalline particles throughout the film (Crowley et al., 2004). This mechanism around this reduction involves localized cracking and crack propagation around the solid inclusions leading to more brittle break behavior (Rowe and Roberts, 1992).

5.5.5 Impact of drug loading on drug release from the films

The BNZ: PEO films exhibited rapid drug release, as shown in Figure 5.10. The faster drug release profile of the BNZ: PEO (1:3) films versus the (1:9) films can be attributed to the smaller size of the BNZ: PEO (1:3) film due to the higher drug loading. The PXRD analysis showed that the BNZ: PEO (1:9) and (1:3) composite particles consisted of mostly amorphous BNZ, thus the rapid hydration of the PEO-based films lead to the rapid dissolution rate of the incorporated amorphous API (Abu-Diak et al., 2012). The PXRD analysis showed that the BNZ: PEO (2:3) composite particles consisted of a higher degree of crystalline BNZ. The presence of crystalline BNZ led to a slower dissolution rate from the BNZ: PEO (2:3) films, that from the films that contained mostly amorphous BNZ.

5.6 CONCLUSION

In this study, we investigated the influence of drug loading on (i) film drug content uniformity using physical mixtures versus composite particles, (ii) electrical, solid state, and thermal properties of composite particles, (iii) peel energy to remove the film from the substrate, (iv) mechanical properties of the film, and (v) the drug release from BNZ: PEO films. Physical mixtures produced superpotent films due greater charge accumulation and preferential deposition driven by the smaller particle size and higher resistivity of the BNZ particles. Uniform ODFs of increasing drug loading were prepared using composite particles of BNZ and PEO. This finding indicates that films prepared using composite particles by ESPD can enable greater control of film homogeneity than seen with conventional solvent casting methods. Additionally, the BNZ containing composite particles exhibited lower viscosities at lower temperatures, enabling reduced cure temperatures and reduced thermal exposure to the incorporated API. The electrical

resistance of the composite particles was dictated by that of bulk PEO; this property can promote robust charging and deposition behavior with varying drug load, as well as reduce the impact of the high resistivity and corresponding high charge accumulation of the BNZ. Films of all drug loadings exhibited low degree of adhesion to the substrate. The increase in BNZ content initially showed a positive impact on tensile strength and percent elongation; however, the presence of crystalline BNZ dispersed in the BNZ: PEO (2:3) composition promoted cracks and crack propagation leading to a drop in mechanical strength. This crystalline content also resulted in a slightly slowed drug release profile, when compared to the rapid drug release of greater than 85% drug release by 3 minutes for the BNZ: PEO (1:9) and (1:3) films.

5.7 REFERENCES

Abu-Diak, O.A., Jones, D.S., Andrews, G.P., 2012. Understanding the performance of melt-extruded poly (ethylene oxide)–bicalutamide solid dispersions: Characterisation of microstructural properties using thermal, spectroscopic and drug release methods. Journal of pharmaceutical sciences 101, 200-213.

Ali, A.A., Charoo, N.A., Abdallah, D.B., 2014. Pediatric drug development: formulation considerations. Drug development and industrial pharmacy 40, 1283-1299.

Amefia, A.E., Abu-Ali, J.M., Barringer, S.A., 2006. Improved functionality of food additives with electrostatic coating. Innovative Food Science & Emerging Technologies 7, 176-181.

Andrei, D.C., Hay, J.N., Keddie, J.L., Sear, R.P., Yeates, S.G., 2000. Surface levelling of thermosetting powder coatings: theory and experiment. Journal of Physics D: Applied Physics 33, 1975.

Arenhart, R.G., Barra, G.M.O., Fernandes, C.P., 2016. Simulation of percolation threshold and electrical conductivity in composites filled with conductive particles: Effect of polydisperse particle size distribution. Polymer Composites 37, 61-69.

Aulton, M., Abdul-Razzak, M., Hogan, J., 1984. PART 2: The Influence of Solid Inclusions. Drug Development and Industrial Pharmacy 10, 541-561.

Bailey, A.G., 1998. The science and technology of electrostatic powder spraying, transport and coating1. Journal of Electrostatics 45, 85-120.

Bhakay, A., Vizzotti, E., Li, M., Davé, R., Bilgili, E., 2016. Incorporation of Fenofibrate Nanoparticles Prepared by Melt Emulsification into Polymeric Films. Journal of Pharmaceutical Innovation 11, 53-63.

Bhattacharyya, N., 2014. The Prevalence of Dysphagia among Adults in the United States. Otolaryngology -- Head and Neck Surgery 151, 765-769.

Boateng, J.S., Auffret, A.D., Matthews, K.H., Humphrey, M.J., Stevens, H.N.E., Eccleston, G.M., 2010. Characterisation of freeze-dried wafers and solvent evaporated films as potential drug delivery systems to mucosal surfaces. International Journal of Pharmaceutics 389, 24-31.

Bodmeier, R., Paeratakul, O., 1989. Evaluation of Drug-Containing Polymer Films Prepared from Aqueous Latexes. Pharmaceutical research 6, 725-730.

Borges, A.F., Silva, C., Coelho, J.F.J., Simões, S., 2015a. Oral films: Current status and future perspectives II — Intellectual property, technologies and market needs. Journal of Controlled Release 206, 108-121.

Borges, A.F., Silva, C., Coelho, J.F.J., Simões, S., 2015b. Oral films: Current status and future perspectives: I — Galenical development and quality attributes. Journal of Controlled Release 206, 1-19.

Bose, S., Bogner, R.H., 2007. Solventless pharmaceutical coating processes: a review. Pharmaceutical development and technology 12, 115-131.

Cho, S.Y., Choung, R.S., Saito, Y.A., Schleck, C.D., Zinsmeister, A.R., Locke, G.R., Talley, N.J., 2015. Prevalence and risk factors for dysphagia: a USA community study. Neurogastroenterology & Motility 27, 212-219.

Clarke, E.G.C., Widdop, B., Osselton, M.D., Moffat, A.C., 2004. Clarke's analysis of drugs and poisons: in pharmaceuticals, body fluids and postmortem material. Pharmaceutical Press, London; Chicago.

Constable, D.J.C., Jimenez-Gonzalez, C., Henderson, R.K., 2007. Perspective on Solvent Use in the Pharmaceutical Industry. Organic Process Research & Development 11, 133-137.

Crowley, M.M., Fredersdorf, A., Schroeder, B., Kucera, S., Prodduturi, S., Repka, M.A., McGinity, J.W., 2004. The influence of guaifenesin and ketoprofen on the properties of hot-melt extruded polyethylene oxide films. European Journal of Pharmaceutical Sciences 22, 409-418.

de Matos Alves Pinto, L., Kiyoko Yokaichiya, D., Fernandes Fraceto, L., de Paula, E., 2000. Interaction of benzocaine with model membranes. Biophysical Chemistry 87, 213-223.

Dixit, R.P., Puthli, S.P., 2009. Oral strip technology: Overview and future potential. Journal of Controlled Release 139, 94-107.

Flint, S.H., Brooks, J.D., Bremer, P.J., 2000. Properties of the stainless steel substrate, influencing the adhesion of thermo-resistant streptococci. Journal of Food Engineering 43, 235-242.

Fulias, A., Vlase, G., Grigorie, C., Ledeţi, I., Albu, P., Bilanin, M., Vlase, T., 2013. Thermal behaviour studies of procaine and benzocaine. J Therm Anal Calorim 113, 265-271.

Gay, C., 2002. Stickiness—Some Fundamentals of Adhesion. Integrative and Comparative Biology 42, 1123-1126.

Gobble, C., Gutterman, A., Chickos, J.S., 2013. Some thermodynamic properties of benzocaine. Structural Chemistry 24, 1903-1907.

Good, R.J., 1992. Contact angle, wetting, and adhesion: a critical review. Journal of adhesion science and technology 6, 1269-1302.

Grodowska, K., Parczewski, A., 2010. Organic solvents in the pharmaceutical industry. Acta poloniae pharmaceutica 67, 3-12.

Gupta, S.S., Meena, A., Parikh, T., Serajuddin, A.T., 2014. Investigation of thermal and viscoelastic properties of polymers relevant to hot melt extrusion, I: Polyvinylpyrrolidone and related polymers. Journal of Excipients and Food Chemicals 5, 32-45.

Harmuth, C.M., 1982. Melt-blending method of forming pigmented powder coatings. Google Patents.

Hoffmann, E.M., Breitenbach, A., Breitkreutz, J., 2011. Advances in orodispersible films for drug delivery. Expert opinion on drug delivery 8, 299-316.

Hogan, J.E., Page, T., Reeves, L., Staniforth, J.N., 2002. Powder coating composition for electrostatic coating of pharmaceutical substrates. Phoqus Limited.

Keddie, J.L., Routh, A.F., 2010. Particle Deformation, Fundamentals of Latex Film Formation: Processes and Properties. Springer Netherlands, Dordrecht, pp. 121-150.

Kianfar, F., Chowdhry, B.Z., Antonijevic, M.D., Boateng, J.S., 2012. Novel films for drug delivery via the buccal mucosa using model soluble and insoluble drugs. Drug Dev Ind Pharm 38, 1207-1220.

Landauer, R., 1978. Electrical conductivity in inhomogeneous media, Electrical transport and optical properties of inhomogeneous media. AIP Publishing, pp. 2-45.

Luo, Y., Zhu, J., Ma, Y., Zhang, H., 2008. Dry coating, a novel coating technology for solid pharmaceutical dosage forms. International Journal of Pharmaceutics 358, 16-22.

Malik, P., Castro, M., Carrot, C., 2006. Thermal degradation during melt processing of poly(ethylene oxide), poly(vinylidenefluoride-co-hexafluoropropylene) and their blends in the presence of additives, for conducting applications. Polymer Degradation and Stability 91, 634-640.

Mazumder, M.K., Wankum, D.L., Sims, R.A., Mountain, J.R., Chen, H., Pettit, P., Chaser, T., 1997. Influence of powder properties on the performance of electrostatic coating process. Journal of Electrostatics 40–41, 369-374.

Meng, X., Zhang, H., Zhu, J., 2009. Characterization of particle size evolution of the deposited layer during electrostatic powder coating processes. Powder Technology 195, 264-270.

Mollereau, G., Mazel, V., Busignies, V., Tchoreloff, P., Mouveaux, F., Rivière, P., 2013. Image Analysis Quantification of Sticking and Picking Events of Pharmaceutical Powders Compressed on a Rotary Tablet Press Simulator. Pharmaceutical research 30, 2303-2314.

Morales, J.O., McConville, J.T., 2011. Manufacture and characterization of mucoadhesive buccal films. European Journal of Pharmaceutics and Biopharmaceutics 77, 187-199.

Myers, G.L., 2008. High dose film compositions and methods of preparation. Monosol Rx, Llc.

Newell, H.E., Buckton, G., Butler, D.A., Thielmann, F., Williams, D.R., 2001. The Use of Inverse Phase Gas Chromatography to Measure the Surface Energy of Crystalline, Amorphous, and Recently Milled Lactose. Pharmaceutical research 18, 662-666.

Noonan, C.M., 1977. Thin film electrostatic epoxy coating powder. Google Patents.

Okhamafe, A.O., York, P., 1984. Effect of solids-polymer interactions on the properties of some aqueous-based tablet film coating formulations. II. Mechanical characteristics. International journal of pharmaceutics 22, 273-281.

Owusu-Nkwantabisah, S., Staudt, C., Lesser, A.J., 2016. Improving flame retardancy and melt processability of polyethersulfone using low molecular weight additives. Journal of Applied Polymer Science 133.

Peña, M.A., Reíllo, A., Escalera, B., Bustamante, P., 2006. Solubility parameter of drugs for predicting the solubility profile type within a wide polarity range in solvent mixtures. International Journal of Pharmaceutics 321, 155-161.

Perumal, V., Govender, T., Lutchman, D., Mackraj, I., 2008. Investigating a new approach to film casting for enhanced drug content uniformity in polymeric films. Drug development and industrial pharmacy 34, 1036-1047.

Podczeck, F., 1999. Investigations into the reduction of powder adhesion to stainless steel surfaces by surface modification to aid capsule filling. International Journal of Pharmaceutics 178, 93-100.

Prasad, L.K., Keen, J.M., LaFountaine, J.S., Maincent, J., Williams Iii, R.O., McGinity, J.W., 2015. Electrostatic powder deposition to prepare films for drug delivery. Journal of Drug Delivery Science and Technology 30, Part B, 501-510.

Prasad, L.K., LaFountaine, J.S., Keen, J.M., McGinity, J.W., Williams III, R.O., 2016a. Influence of process parameters on the preparation of pharmaceutical films by electrostatic powder deposition. International Journal of Pharmaceutics (Revision Submitted).

Prasad, L.K., McGinity, J.W., Williams Iii, R.O., 2016b. Electrostatic powder coating: Principles and pharmaceutical applications. International Journal of Pharmaceutics 505, 289-302.

Preis, M., 2015. Orally Disintegrating Films and Mini-Tablets—Innovative Dosage Forms of Choice for Pediatric Use. AAPS PharmSciTech 16, 234-241.

Puri, V., Dantuluri, A.K., Kumar, M., Karar, N., Bansal, A.K., 2010. Wettability and surface chemistry of crystalline and amorphous forms of a poorly water soluble drug. European Journal of Pharmaceutical Sciences 40, 84-93.

Qiao, M., Luo, Y., Zhang, L., Ma, Y., Stephenson, T.S., Zhu, J., 2010a. Sustained release coating of tablets with Eudragit® RS/RL using a novel electrostatic dry powder coating process. International Journal of Pharmaceutics 399, 37-43.

Qiao, M., Zhang, L., Ma, Y., Zhu, J., Chow, K., 2010b. A novel electrostatic dry powder coating process for pharmaceutical dosage forms: Immediate release coatings for tablets. European Journal of Pharmaceutics and Biopharmaceutics 76, 304-310.

Qiao, M., Zhang, L., Ma, Y., Zhu, J., Xiao, W., 2013. A novel electrostatic dry coating process for enteric coating of tablets with Eudragit® L100-55. European Journal of Pharmaceutics and Biopharmaceutics 83, 293-300.

Radebaugh, G.W., Murtha, J.L., Julian, T.N., Bondi, J.N., 1988. Methods for evaluating the puncture and shear properties of pharmaceutical polymeric films. International Journal of Pharmaceutics 45, 39-46.

Ratanatriwong, P., Barringer, S., 2007. Particle size, cohesiveness and charging effects on electrostatic and nonelectrostatic powder coating. Journal of Electrostatics 65, 704-708.

Rowe, R., 1983. Modulus enhancement in pigmented tablet film coating formulations. International Journal of Pharmaceutics 14, 355-359.

Rowe, R., Roberts, R., 1992. Simulation of crack propagation in tablet film coatings containing pigments. International journal of pharmaceutics 78, 49-57.

Sakata, Y., Yamaguchi, H., 2011. Improvement of sticking in tablet compaction for tocopherol acetate. Drug development and industrial pharmacy 37, 1049-1059.

Sauer, D., Cerea, M., DiNunzio, J., McGinity, J., 2013. Dry powder coating of pharmaceuticals: A review. International Journal of Pharmaceutics 457, 488-502.

Shen, B.d., Shen, C.y., Yuan, X.d., Bai, J.x., Lv, Q.y., Xu, H., Dai, L., Yu, C., Han, J., Yuan, H.l., 2013. Development and characterization of an orodispersible film containing drug nanoparticles. European Journal of Pharmaceutics and Biopharmaceutics 85, 1348-1356.

Sievens-Figueroa, L., Bhakay, A., Jerez-Rozo, J.I., Pandya, N., Romañach, R.J., Michniak-Kohn, B., Iqbal, Z., Bilgili, E., Davé, R.N., 2012. Preparation and characterization of hydroxypropyl methyl cellulose films containing stable BCS Class II drug nanoparticles for pharmaceutical applications. International Journal of Pharmaceutics 423, 496-508.

Slavkova, M., Breitkreutz, J., 2015. Orodispersible drug formulations for children and elderly. European Journal of Pharmaceutical Sciences 75, 2-9.

Stegemann, S., Ecker, F., Maio, M., Kraahs, P., Wohlfart, R., Breitkreutz, J., Zimmer, A., Bar-Shalom, D., Hettrich, P., Broegmann, B., 2010. Geriatric drug therapy: Neglecting the inevitable majority. Ageing Research Reviews 9, 384-398.

Stegemann, S., Gosch, M., Breitkreutz, J., 2012. Swallowing dysfunction and dysphagia is an unrecognized challenge for oral drug therapy. International Journal of Pharmaceutics 430, 197-206.

Sun, Y., Bao, H.-D., Guo, Z.-X., Yu, J., 2009. Modeling of the Electrical Percolation of Mixed Carbon Fillers in Polymer-Based Composites. Macromolecules 42, 459-463.

Takizawa, C., Gemmell, E., Kenworthy, J., Speyer, R., 2016. A Systematic Review of the Prevalence of Oropharyngeal Dysphagia in Stroke, Parkinson's Disease, Alzheimer's Disease, Head Injury, and Pneumonia. Dysphagia 31, 434-441.

Tousey, M.D., 2003. Sticking and picking: some causes and remedies. Tablets and capsules.

Visser, J.C., Dohmen, W.M.C., Hinrichs, W.L.J., Breitkreutz, J., Frijlink, H.W., Woerdenbag, H.J., 2015. Quality by design approach for optimizing the formulation and physical properties of extemporaneously prepared orodispersible films. International Journal of Pharmaceutics 485, 70-76.

Waknis, V., Chu, E., Schlam, R., Sidorenko, A., Badawy, S., Yin, S., Narang, A.S., 2014. Molecular Basis of Crystal Morphology-Dependent Adhesion Behavior of Mefenamic Acid During Tableting. Pharmaceutical research 31, 160-172.

Wicks, Z.W., Jones, F.N., Pappas, S.P., Wicks, D.A., 2007. Organic coatings: science and technology, 3rd ed. Wiley-Interscience, Hoboken, N.J.

Yang, Q., Ma, Y., Zhu, J., 2015. Applying a novel electrostatic dry powder coating technology to pellets. European Journal of Pharmaceutics and Biopharmaceutics 97, Part A, 118-124.

Zhang, J., Ebbens, S., Chen, X., Jin, Z., Luk, S., Madden, C., Patel, N., Roberts, C.J., 2006. Determination of the Surface Free Energy of Crystalline and Amorphous Lactose by Atomic Force Microscopy Adhesion Measurement. Pharmaceutical research 23, 401-407.

Zografi, G., Tam, S.S., 1976. Wettability of Pharmaceutical Solids: Estimates of Solid Surface Polarity. Journal of Pharmaceutical Sciences 65, 1145-1149.

Chapter 6: Summary and Conclusions

6.1 Summary of Results

In this work, the application of electrostatic powder deposition to prepare orodispersible films was investigated as an alternative, solvent-free manufacturing method. The influence of process parameters, drug content, and drug loading on the performance and properties of polyethylene oxide based films were investigated. The results indicate that films prepared using this process exhibit favorable mechanical properties with rapid disintegration and drug release. Additionally, deposition of composite particles is advantageous as they exhibit desirable electrical properties, ensure film drug content uniformity, and enable reduced cure temperatures.

6.1.1 Influence of Process Parameters and Substrate Properties on the Properties of Films Prepared by Electrostatic Powder Deposition

The results of this study demonstrate that electrostatic powder deposition can be utilized to produce non-adhering, free films by utilizing a substrate that will not readily adhere with the powder. Low humidity conditions resulted in self-limiting deposition behavior due to the onset of back ionization, whereas increased humidity levels enabled increased deposition efficiency with decreasing gun tip to substrate distance and increasing voltage (up to 60kV). All cured films were readily removed from the SS316 substrates, even with increased surface roughness, due to the hydrophobic nature and low surface energy of the substrate. The ESPD process was able to produce films with favorable mechanical properties and rapid disintegration.

6.1.2 Impact of Acetaminophen on the Properties and Performance of Polyethylene Oxide Orodispersible Films Prepared by Electrostatic Powder Deposition

The results of this study show that uniform active films can be prepared using electrostatic powder deposition. However, films prepared using a physical mixture of the acetaminophen and polyethylene with electrostatic powder deposition showed greater drug content variability with a relative standard deviation of 11.9% compared to 1.8% from films prepared using composite particles. The active films exhibited favorable mechanical properties as the acetaminophen exhibited a plasticizing effect on the polyethylene oxide. The active films exhibited greater than 85% drug release in two minutes, demonstrating satisfactory performance as an orodispersible dosage form.

6.1.3 Influence of Benzocaine Loading on the Properties and Performance of Polyethylene Oxide Orodispersible Films Prepared by Electrostatic Powder Deposition

The results of this study further confirmed the advantage of preparing films using electrostatic powder deposition using composite particles versus physical mixtures. Physical mixtures of benzocaine and polyethylene oxide produced superpotent films attributed to greater charge accumulation and preferential deposition driven by the smaller particle size and higher resistivity of the benzocaine particles. Films prepared using composite particles of increasing drug load were confirmed to have uniform drug content, indicating films prepared using composite particles by electrostatic powder deposition can enable greater control of film homogeneity than seen with conventional solvent casting methods. Composite particles also exhibited lower viscosity temperature profiles, enabling reduced cure temperatures. The electrical resistance of the composite particles, for the drug loading range studied, was driven by that of polyethylene oxide.

The composite particles of the highest drug load showed greater crystalline benzocaine content than the lower drug loads, resulting in a decrease in mechanical properties and a slightly reduced dissolution rate.

Bibliography

ICH topic Q3C(R5) Impurities: Guidelines for Residual Solvents. International Conference on Harmonization.

1997. Guidance for Industry: Dissolution Testing of Immediate Release Solid Oral Dosage Forms. US Department of Health and Human Services FDA,Center for Drug Evaluation and Research (CDER). in: US Department of Health and Human Services FDA, C.f.D.E.a.R.C. (Ed.). US Department of Health and Human Services FDA,Center for Drug Evaluation and Research (CDER), US Department of Health and Human Services FDA,Center for Drug Evaluation and Research (CDER).

2000. ICH Topic Q6A: Specifications: Test Procedures and Acceptance Criteria for New Drug Substances and New Drug Products: Chemical Substances. (CPMP/ICH/367/96) European Medicines Agency.

2013. TA.XTPlus Application Study: Film Testing ASTM D882 vs TA-108S-5i, in: Corp., T.T. (Ed.), http://www.texturetechnologies.com.

2015. The United States Pharmacopeial Convention. General Chapter: 1151 Pharmaceutical Dosage Forms. USP 38–NF 33 Rockville, MD: The United States Pharmacopeial Convention, The United States Pharmacopeia and The National Formulary.

Abdelbary, A., Bendas, E., Ramadan, A., Mostafa, D., 2014. Pharmaceutical and Pharmacokinetic Evaluation of a Novel Fast Dissolving Film Formulation of Flupentixol Dihydrochloride. AAPS PharmSciTech 15, 1603-1610.

Abu-Diak, O.A., Jones, D.S., Andrews, G.P., 2012. Understanding the performance of melt-extruded poly (ethylene oxide)–bicalutamide solid dispersions: Characterisation of microstructural properties using thermal, spectroscopic and drug release methods. Journal of pharmaceutical sciences 101, 200-213.

Adamiak, K., 2003. Analysis of charge transport in high resistivity conductors under different conduction models. Journal of Electrostatics 57, 325-335.

Adams, R., 1983. A review of the stainless steel surface. Journal of Vacuum Science & Technology A 1, 12-18.

Ali, A.A., Charoo, N.A., Abdallah, D.B., 2014. Pediatric drug development: formulation considerations. Drug development and industrial pharmacy 40, 1283-1299.

Amefia, A.E., Abu-Ali, J.M., Barringer, S.A., 2006. Improved functionality of food additives with electrostatic coating. Innovative Food Science & Emerging Technologies 7, 176-181.

Andrei, D.C., Hay, J.N., Keddie, J.L., Sear, R.P., Yeates, S.G., 2000. Surface levelling of thermosetting powder coatings: theory and experiment. Journal of Physics D: Applied Physics 33, 1975.

Arenhart, R.G., Barra, G.M.O., Fernandes, C.P., 2016. Simulation of percolation threshold and electrical conductivity in composites filled with conductive particles: Effect of polydisperse particle size distribution. Polymer Composites 37, 61-69.

ASTM, 2013. A380/A380M Practice for Cleaning, Descaling, and Passivation of Stainless Steel Parts, Equipment, and Systems. Equipment and Systems.

Aulton, M., Abdul-Razzak, M., Hogan, J., 1984. PART 2: The Influence of Solid Inclusions. Drug Development and Industrial Pharmacy 10, 541-561.

Awaja, F., Gilbert, M., Kelly, G., Fox, B., Pigram, P.J., 2009. Adhesion of polymers. Progress in Polymer Science 34, 948-968.

Bailey, A.G., 1984. Electrostatic phenomena during powder handling. Powder Technology 37, 71-85.

Bailey, A.G., 1998. The science and technology of electrostatic powder spraying, transport and coating1. Journal of Electrostatics 45, 85-120.

Barletta, M., Gisario, A., 2009. Electrostatic spray painting of carbon fibre-reinforced epoxy composites. Progress in Organic Coatings 64, 339-349.

Barmuta, P., Cywiński, K., 2001. Electroseparation and efficiency of deposition during electrostatic powder coating. Journal of Electrostatics 51–52, 239-244.

Barringer, S.A., Sumonsiri, N., 2015. Electrostatic Coating Technologies for Food Processing. Annual Review of Food Science and Technology 6, 157-169.

Bhakay, A., Vizzotti, E., Li, M., Davé, R., Bilgili, E., 2016. Incorporation of Fenofibrate Nanoparticles Prepared by Melt Emulsification into Polymeric Films. Journal of Pharmaceutical Innovation 11, 53-63.

Bhattacharyya, N., 2014. The Prevalence of Dysphagia among Adults in the United States. Otolaryngology -- Head and Neck Surgery 151, 765-769.

Blythe, A., 1984. Electrical resistivity measurements of polymer materials. Polymer testing 4, 195-209.

Boateng, J.S., Auffret, A.D., Matthews, K.H., Humphrey, M.J., Stevens, H.N.E., Eccleston, G.M., 2010. Characterisation of freeze-dried wafers and solvent evaporated films as potential drug delivery systems to mucosal surfaces. International Journal of Pharmaceutics 389, 24-31.

Boateng, J.S., Stevens, H.N.E., Eccleston, G.M., Auffret, A.D., Humphrey, M.J., Matthews, K.H., 2009. Development and mechanical characterization of solvent-

cast polymeric films as potential drug delivery systems to mucosal surfaces. Drug Development and Industrial Pharmacy 35, 986-996.

Bodmeier, R., Paeratakul, O., 1989. Evaluation of Drug-Containing Polymer Films Prepared from Aqueous Latexes. Pharmaceutical research 6, 725-730.

Borges, A.F., Silva, C., Coelho, J.F.J., Simões, S., 2015a. Oral films: Current status and future perspectives II — Intellectual property, technologies and market needs. Journal of Controlled Release 206, 108-121.

Borges, A.F., Silva, C., Coelho, J.F.J., Simões, S., 2015b. Oral films: Current status and future perspectives: I — Galenical development and quality attributes. Journal of Controlled Release 206, 1-19.

Bose, S., Bogner, R.H., 2007. Solventless pharmaceutical coating processes: a review. Pharmaceutical development and technology 12, 115-131.

Butt, H.-J., Kappl, M., 2009. Surface and Interfacial Forces, 1 ed. Wiley, Hoboken.

Byron, P., Peart, J., Staniforth, J., 1997. Aerosol Electrostatics I: Properties of Fine Powders Before and After Aerosolization by Dry Powder Inhalers. Pharmaceutical research 14, 698-705.

Callol, J.R., Yan, J.Y., 2001. Protective coating for a stent with intermediate radiopaque coating. US6174329.

Carter, P.A., Rowley, G., Fletcher, E.J., Stylianopoulos, V., 1998. Measurement of Electrostatic Charge Decay in Pharmaceutical Powders and Polymer Materials Used in Dry Powder Inhaler Devices. Drug Development and Industrial Pharmacy 24, 1083-1088.

Castle, G.P., 2011. A century of development in applied electrostatics; nothing static here. Dielectrics and Electrical Insulation, IEEE Transactions on 18, 1361-1365.

Cazaux, J., 2007. Critical thicknesses of electrostatic powder coatings from inside. Journal of Electrostatics 65, 764-774.

Cerea, M., Zheng, W., Young, C.R., McGinity, J.W., 2004. A novel powder coating process for attaining taste masking and moisture protective films applied to tablets. International Journal of Pharmaceutics 279, 127-139.

Chang, K.-N., Chen, Y.-K., Huang, S.-H., Chen, C.-W., Lai, C.-Y., Chen, C.-C., 2012. Penetration of charged particles through metallic tubes. Journal of Aerosol Science 48, 10-17.

Cho, S.Y., Choung, R.S., Saito, Y.A., Schleck, C.D., Zinsmeister, A.R., Locke, G.R., Talley, N.J., 2015. Prevalence and risk factors for dysphagia: a USA community study. Neurogastroenterology & Motility 27, 212-219.

Chow, K., Zhu, K., Tan, R.H., Heng, P.S., 2008. Investigation of Electrostatic Behavior of a Lactose Carrier for Dry Powder Inhalers. Pharmaceutical research 25, 2822-2834.

Clarke, E.G.C., Widdop, B., Osselton, M.D., Moffat, A.C., 2004. Clarke's analysis of drugs and poisons: in pharmaceuticals, body fluids and postmortem material. Pharmaceutical Press, London; Chicago.

Coelho, R., 1985. The electrostatic characterization of insulating materials. Journal of Electrostatics 17, 13-27.

Constable, D.J.C., Jimenez-Gonzalez, C., Henderson, R.K., 2007. Perspective on Solvent Use in the Pharmaceutical Industry. Organic Process Research & Development 11, 133-137.

Cramer, S.D., Covino, B.S., 2006. Corrosion: Environments and industries. ASM International.

Craven, J.M., 1982. Powder coating composition for automotive topcoat. Google Patents.

Crowley, M.M., Fredersdorf, A., Schroeder, B., Kucera, S., Prodduturi, S., Repka, M.A., McGinity, J.W., 2004. The influence of guaifenesin and ketoprofen on the properties of hot-melt extruded polyethylene oxide films. European Journal of Pharmaceutical Sciences 22, 409-418.

Crowley, M.M., Zhang, F., Koleng, J.J., McGinity, J.W., 2002. Stability of polyethylene oxide in matrix tablets prepared by hot-melt extrusion. Biomaterials 23, 4241-4248.

de Matos Alves Pinto, L., Kiyoko Yokaichiya, D., Fernandes Fraceto, L., de Paula, E., 2000. Interaction of benzocaine with model membranes. Biophysical Chemistry 87, 213-223.

DesRosiers Lachiver, E., Abatzoglou, N., Cartilier, L., Simard, J.-S., 2006. Insights into the Role of Electrostatic Forces on the Behavior of Dry Pharmaceutical Particulate Systems. Pharmaceutical research 23, 997-1007.

Detry, J.G., Sindic, M., Deroanne, C., 2010. Hygiene and cleanability: a focus on surfaces. Critical reviews in food science and nutrition 50, 583-604.

Dillon, R., Matheson, L., Bradford, E., 1951a. Sintering of synthetic latex particles. Journal of Colloid Science 6, 108-117.

Dillon, R.E., Matheson, L.A., Bradford, E.B., 1951b. Sintering of synthetic latex particles. Journal of Colloid Science 6, 108-117.

Dixit, R.P., Puthli, S.P., 2009. Oral strip technology: Overview and future potential. Journal of Controlled Release 139, 94-107.

Faille, C., Jullien, C., Fontaine, F., Bellon-Fontaine, M.-N., Slomianny, C., Benezech, T., 2002. Adhesion of Bacillus spores and Escherichia coli cells to inert surfaces: role of surface hydrophobicity. Canadian Journal of Microbiology 48, 728-738.

Felton, L., McGinity, J., 2002. Influence of Insoluble Excipients on Film Coating Systems. Drug Development & Industrial Pharmacy 28, 225.

Felton, L.A., McGinity, J.W., 1996. Influence of tablet hardness and hydrophobicity on the adhesive properties of an acrylic resin copolymer. Pharmaceutical development and technology 1, 381-389.

Felton, L.A., McGinity, J.W., 1997. Influence of plasticizers on the adhesive properties of an acrylic resin copolymer to hydrophilic and hydrophobic tablet compacts. International Journal of Pharmaceutics 154, 167-178.

Flint, S.H., Brooks, J.D., Bremer, P.J., 2000. Properties of the stainless steel substrate, influencing the adhesion of thermo-resistant streptococci. Journal of Food Engineering 43, 235-242.

Fulias, A., Vlase, G., Grigorie, C., Ledeţi, I., Albu, P., Bilanin, M., Vlase, T., 2013. Thermal behaviour studies of procaine and benzocaine. J Therm Anal Calorim 113, 265-271.

Fulton, J.L., Deverman, G.S., Matson, D.W., Yonker, C.R., Taylor, C.D., McClain, J.B., Crowley, J.M., 2011. System and method for enhanced electrostatic deposition and surface coatings. US20110238161.

Gay, C., 2002. Stickiness—Some Fundamentals of Adhesion. Integrative and Comparative Biology 42, 1123-1126.

Gettings, M., Kinloch, A.J., 1977. Surface analysis of polysiloxane/metal oxide interfaces. J Mater Sci 12, 2511-2518.

Giacometti, J., Oliveira Jr, O.N., 1992. Corona charging of polymers. Electrical Insulation, IEEE Transactions on 27, 924-943.

Gibson, N., 1997. Static electricity — an industrial hazard under control? Journal of Electrostatics 40–41, 21-30.

Gilpin, R., Zhou, W., 2004. Studies of the Thermal Degradation of Acetaminophen Using a Conventional HPLC Approach and Electrospray Ionization-Mass Spectrometry. Journal of chromatographic science 42, 15-20.

Glor, M., 1985. Hazards due to electrostatic charging of powders. Journal of Electrostatics 16, 175-191.

Glor, M., 2003. Ignition hazard due to static electricity in particulate processes. Powder Technology 135–136, 223-233.

Glover, W., Chan, H.-K., 2004. Electrostatic charge characterization of pharmaceutical aerosols using electrical low-pressure impaction (ELPI). Journal of Aerosol Science 35, 755-764.

Gobble, C., Gutterman, A., Chickos, J.S., 2013. Some thermodynamic properties of benzocaine. Structural Chemistry 24, 1903-1907.

Good, R.J., 1992. Contact angle, wetting, and adhesion: a critical review. Journal of adhesion science and technology 6, 1269-1302.

Gray, J.E., Luan, B., 2002. Protective coatings on magnesium and its alloys — a critical review. Journal of Alloys and Compounds 336, 88-113.

Grodowska, K., Parczewski, A., 2010. Organic solvents in the pharmaceutical industry. Acta poloniae pharmaceutica 67, 3-12.

Grosvenor, M.P., 1991. The physico-mechanical properties of electrostatically deposited polymers for use in pharmaceutical powder coating. University of Bath.

Grosvenor, M.P., Staniforth, J.N., 1996. The Influence of Water on Electrostatic Charge Retention and Dissipation in Pharmaceutical Compacts for Powder Coating. Pharmaceutical research 13, 1725-1729.

Gupta, S.S., Meena, A., Parikh, T., Serajuddin, A.T., 2014. Investigation of thermal and viscoelastic properties of polymers relevant to hot melt extrusion, I: Polyvinylpyrrolidone and related polymers. Journal of Excipients and Food Chemicals 5, 32-45.

Guskov, S., 2002. Electrostatic phenomena in powder coating. Powder System Group Nordson Corporation.

Gutiérrez-Rocca, J., McGinity, J.W., 1994. Influence of water soluble and insoluble plasticizers on the physical and mechanical properties of acrylic resin copolymers. International Journal of Pharmaceutics 103, 293-301.

Gutierrez-Rocca, J.C., Mcginity, J.W., 1993. Influence of aging on the physical-mechanical properties of acrylic resin films cast from aqueous dispersions and organic solutions. Drug Development and Industrial Pharmacy 19, 315-332.

Haidopoulos, M., Turgeon, S., Sarra-Bournet, C., Laroche, G., Mantovani, D., 2006. Development of an optimized electrochemical process for subsequent coating of 316 stainless steel for stent applications. J Mater Sci: Mater Med 17, 647-657.

Han, Z., Tay, B., 2008. Electrical conductivity of poly (ethylene terephthalate) modified by titanium plasma. Journal of applied polymer science 107, 3332-3336.

Hao, T., Tukianen, J., Nivorozhkin, A., Landrau, N., 2013. Probing pharmaceutical powder blending uniformity with electrostatic charge measurements. Powder Technology 245, 64-69.

Harmuth, C.M., 1982. Melt-blending method of forming pigmented powder coatings. Google Patents.

Hassan, M., Lau, R., 2009. Effect of Particle Shape on Dry Particle Inhalation: Study of Flowability, Aerosolization, and Deposition Properties. AAPS PharmSciTech 10, 1252-1262.

Herling, U., Bill, W.S., 2000. Polyethylene glycol coating for electrostatic dry deposition of pharmaceuticals. WO2000035424.

Ho, C.Y., Chu, T., 1977. Electrical resistivity and thermal conductivity of nine selected AISI stainless steels. DTIC Document.

Hoburg, J.F., 1982. Charge density, electric field, and particle charging in electrostatic precipitation with back ionization. Industry Applications, IEEE Transactions on, 666-672.

Hoffmann, E.M., Breitenbach, A., Breitkreutz, J., 2011. Advances in orodispersible films for drug delivery. Expert opinion on drug delivery 8, 299-316.

Hogan, J.E., Page, T., Reeves, L., Staniforth, J.N., 1996. Powder coating composition for electrostatic coating of pharmaceutical substrates. Google Patents.

Hogan, J.E., Page, T., Reeves, L., Staniforth, J.N., 2002. Powder coating composition for electrostatic coating of pharmaceutical substrates. Phoqus Limited.

Hopkinson, I., Myatt, M., 2002. Phase Separation in Ternary Polymer Solutions Induced by Solvent Loss. Macromolecules 35, 5153-5160.

Huatan, H., Ross, R., 2011. Treatment of adrenal insufficiency.

Hughes, J., 1989. Powder coating technology. Journal of Electrostatics 23, 3-23.

Hughes, J.F., 1984. Electrostatic Powder Coating. DTIC Document.

Jensen, D., Morgan, L., 1991. Particle size as it relates to the minimum film formation temperature of latices. Journal of applied polymer science 42, 2845-2849.

Kablitz, C.D., Urbanetz, N.A., 2007. Characterization of the film formation of the dry coating process. European Journal of Pharmaceutics and Biopharmaceutics 67, 449-457.

Karner, S., Littringer, E.M., Urbanetz, N.A., 2014. Triboelectrics: The influence of particle surface roughness and shape on charge acquisition during aerosolization and the DPI performance. Powder Technology 262, 22-29.

Karner, S., Urbanetz, N.A., 2011. The impact of electrostatic charge in pharmaceutical powders with specific focus on inhalation-powders. Journal of Aerosol Science 42, 428-445.

Katz, G., Harchandani, B., Shah, B., 2015. Drug-Eluting Stents: the Past, Present, and Future. Curr Atheroscler Rep 17, 1-11.

Keddie, J.L., Routh, A.F., 2010. Particle Deformation, Fundamentals of Latex Film Formation: Processes and Properties. Springer Netherlands, Dordrecht, pp. 121-150.

Khan, H., Fell, J.T., Macleod, G.S., 2001. The influence of additives on the spreading coefficient and adhesion of a film coating formulation to a model tablet surface. International Journal of Pharmaceutics 227, 113-119.

Khan, W., Farah, S., Domb, A.J., 2012. Drug eluting stents: Developments and current status. Journal of Controlled Release 161, 703-712.

Khuathan, N., Pongjanyakul, T., 2014. Modification of quaternary polymethacrylate films using sodium alginate: Film characterization and drug permeability. International Journal of Pharmaceutics 460, 63-72.

Kianfar, F., Chowdhry, B.Z., Antonijevic, M.D., Boateng, J.S., 2012. Novel films for drug delivery via the buccal mucosa using model soluble and insoluble drugs. Drug Dev Ind Pharm 38, 1207-1220.

Kiefer, S.L., 2004. Powder coating material developments promise new opportunities for finishers. Metal Finishing 102, 35-37.

Kim, J.K., Kim, W.H., Lee, D.H., 2002. Adhesion properties of UV crosslinked polystyrene-block-polybutadiene-block-polystyrene copolymer and tackifier mixture. Polymer 43, 5005-5010.

Kinloch, A., 2012. Adhesion and adhesives: science and technology. Springer Science & Business Media.

Kinloch, A.J., 1980. The science of adhesion. J Mater Sci 15, 2141-2166.

Klar, F., Urbanetz, N.A., 2009. The role of capillary force promoters in dry coating procedures – Evaluation of acetylated monoglyceride, isopropyl myristate and palmitate. European Journal of Pharmaceutics and Biopharmaceutics 71, 124-129.

Koland, M., Sandeep, V.P., Charyulu, N.R., 2010. Fast Dissolving Sublingual Films of Ondansetron Hydrochloride: Effect of Additives on in vitro Drug Release and Mucosal Permeation. Journal of Young Pharmacists : JYP 2, 216-222.

Koleske, J.V., 2012. Paint and Coating Testing Manual: 15th Edition of the Gardner-Sward Handbook. ASTM International.

Kozma, L., Olefjord, I., 1987. Surface treatment of steel for structural adhesive bonding. Materials Science and Technology 3, 954-962.

Lacombe, R., 2005. Adhesion measurement methods: theory and practice. CRC Press.

Lam, J.K.W., Xu, Y., Worsley, A., Wong, I.C.K., 2014. Oral transmucosal drug delivery for pediatric use. Advanced Drug Delivery Reviews 73, 50-62.

Landauer, R., 1978. Electrical conductivity in inhomogeneous media, Electrical transport and optical properties of inhomogeneous media. AIP Publishing, pp. 2-45.

Lang, B., McGinity, J.W., Williams, R.O., 2014. Hot-melt extrusion – basic principles and pharmaceutical applications. Drug Development and Industrial Pharmacy 40, 1133-1155.

Lee, L.-H., 1991. Fundamentals of adhesion. Springer Science & Business Media.

Lee, S., 2006. Encyclopedia of chemical processing. Taylor & Francis, New York.

Lehtola, V.M., Heinämäki, J.T., Nikupaavo, P., Yliruusi, J.K., 1995. Effect of Some Excipjents and Compression Pressure on the Adhesion of Aqueous-Based Hydroxypropyl Methylcellulose Film Coatings to Tablet Surface. Drug Development and Industrial Pharmacy 21, 1365-1375.

Low, A.Q.J., Parmentier, J., Khong, Y.M., Chai, C.C.E., Tun, T.Y., Berania, J.E., Liu, X., Gokhale, R., Chan, S.Y., 2013. Effect of type and ratio of solubilising polymer on characteristics of hot-melt extruded orodispersible films. International Journal of Pharmaceutics 455, 138-147.

Luo, Y., Zhu, J., Ma, Y., Zhang, H., 2008. Dry coating, a novel coating technology for solid pharmaceutical dosage forms. International Journal of Pharmaceutics 358, 16-22.

Malik, P., Castro, M., Carrot, C., 2006. Thermal degradation during melt processing of poly(ethylene oxide), poly(vinylidenefluoride-co-hexafluoropropylene) and their blends in the presence of additives, for conducting applications. Polymer Degradation and Stability 91, 634-640.

Malik, S., Hossainy, S., 2005. Electrostatic loading of drugs on implantable medical devices. US20050273161.

Mallappa, A., Sinaii, N., Kumar, P., Whitaker, M.J., Daley, L.-A., Digweed, D., Eckland, D.J.A., Van Ryzin, C., Nieman, L.K., Arlt, W., Ross, R.J., Merke, D.P., 2014. A Phase 2 Study of Chronocort, a Modified-Release Formulation of Hydrocortisone, in the Treatment of Adults With Classic Congenital Adrenal Hyperplasia. The Journal of Clinical Endocrinology & Metabolism 100, 1137-1145.

Mani, G., Feldman, M.D., Patel, D., Agrawal, C.M., 2007. Coronary stents: A materials perspective. Biomaterials 28, 1689-1710.

Marshall, P., 1984. Austenitic stainless steels: microstructure and mechanical properties. Springer Science & Business Media.

Masuda, S., Mizuno, A., 1977. Initiation condition and mode of back discharge. Journal of Electrostatics 4, 35-52.

Masuda, S., Washizu, M., 1979. Ionic charging of a very high resistivity spherical particle. Journal of Electrostatics 6, 57-67.

Matsusaka, S., Maruyama, H., Matsuyama, T., Ghadiri, M., 2010. Triboelectric charging of powders: A review. Chemical Engineering Science 65, 5781-5807.

Mazumder, M.K., Sims, R.A., Biris, A.S., Srirama, P.K., Saini, D., Yurteri, C.U., Trigwell, S., De, S., Sharma, R., 2006. Twenty-first century research needs in electrostatic processes applied to industry and medicine. Chemical Engineering Science 61, 2192-2211.

Mazumder, M.K., Wankum, D.L., Sims, R.A., Mountain, J.R., Chen, H., Pettit, P., Chaser, T., 1997. Influence of powder properties on the performance of electrostatic coating process. Journal of Electrostatics 40–41, 369-374.

Mazumder, M.K., Ware, R.E., Yokoyama, T., Rubin, B.J., Kamp, D., 1991. Measurement of particle size and electrostatic charge distributions on toners using E-SPART analyzer. Industry Applications, IEEE Transactions on 27, 611-619.

Mazur, S., Beckerbauer, R., Buckholz, J., 1997. Particle Size Limits for Sintering Polymer Colloids without Viscous Flow. Langmuir 13, 4287-4294.

McGinity, J.W., Felton, L.A., 2008. Aqueous Polymeric Coatings for Pharmaceutical Dosage Forms, 3 ed. Informa Healthcare, New York.

McLean, K., 1988. Electrostatic precipitators. Physical Science, Measurement and Instrumentation, Management and Education-Reviews, IEE Proceedings A 135, 347-361.

Meng, X., 2009. Study on corona discharge and corona charging in electrostatic powder coating process. The University of Western Ontario (Canada), Ann Arbor, p. 347.

Meng, X., Zhang, H., Zhu, J., 2009a. Characterization of particle size evolution of the deposited layer during electrostatic powder coating processes. Powder Technology 195, 264-270.

Meng, X., Zhu, J., Zhang, H., 2009b. Influences of different powders on the characteristics of particle charging and deposition in powder coating processes. Journal of Electrostatics 67, 663-671.

Meng, X., Zhu, J.J., Zhang, H., 2009c. The characteristics of particle charging and deposition during powder coating processes with ultrafine powder. Journal of Physics D: Applied Physics 42, 065201.

Misev, T.A., van der Linde, R., 1998. Powder coatings technology: new developments at the turn of the century. Progress in Organic Coatings 34, 160-168.

Missaghi, S., Fassihi, R., 2004. A novel approach in the assessment of polymeric film formation and film adhesion on different pharmaceutical solid substrates. AAPS PharmSciTech 5, 32-39.

Mollereau, G., Mazel, V., Busignies, V., Tchoreloff, P., Mouveaux, F., Rivière, P., 2013. Image Analysis Quantification of Sticking and Picking Events of Pharmaceutical

Powders Compressed on a Rotary Tablet Press Simulator. Pharmaceutical research 30, 2303-2314.

Moore, R., Dunham, B., 2008. Zirconization™: The future of coating pretreatment processes: Alternative, phosphate-free, eco-friendly pretreatment procedure addresses energy and chemical consumption while improving product quality. Metal Finishing 106, 46-55.

Morales, J.O., McConville, J.T., 2011. Manufacture and characterization of mucoadhesive buccal films. European Journal of Pharmaceutics and Biopharmaceutics 77, 187-199.

Murtomaa, M., Savolainen, M., Christiansen, L., Rantanen, J., Laine, E., Yliruusi, J., 2004. Static electrification of powders during spray drying. Journal of Electrostatics 62, 63-72.

Myers, G.L., 2008a. High dose film compositions and methods of preparation. Monosol Rx, Llc.

Myers, R., 2008b. Process of Electrostatically Coating A Stent On a Catheter. US20080113084.

Nadkarni, P.D., Kildsig, D.O., Kramer, P.A., Banker, G.S., 1975. Effect of surface roughness and coating solvent on film adhesion to tablets. Journal of Pharmaceutical Sciences 64, 1554-1557.

Nesseem, D.I., Eid, S.F., El-Houseny, S.S., 2011. Development of novel transdermal self-adhesive films for tenoxicam, an anti-inflammatory drug. Life Sciences 89, 430-438.

Newell, H.E., Buckton, G., Butler, D.A., Thielmann, F., Williams, D.R., 2001. The Use of Inverse Phase Gas Chromatography to Measure the Surface Energy of Crystalline, Amorphous, and Recently Milled Lactose. Pharmaceutical research 18, 662-666.

Noonan, C.M., 1977. Thin film electrostatic epoxy coating powder. Google Patents.

Nukala, R., Boyapally, H., Slipper, I., Mendham, A., Douroumis, D., 2010. The Application of Electrostatic Dry Powder Deposition Technology to Coat Drug-Eluting Stents. Pharmaceutical research 27, 72-81.

O'Neill, B., Bright, A., 1978. A parametric study of electrostatic powder coating. Journal of Electrostatics 4, 325-334.

Obermeier, P., Kohr, T., Kramer, K.T., Klokkers, K., 2008. Oral, Quickly Disintegrating Film, which Cannot be Spit Out, for an Antiemetic or Antimigraine Agent.

Okhamafe, A.O., York, P., 1984. Effect of solids-polymer interactions on the properties of some aqueous-based tablet film coating formulations. II. Mechanical characteristics. International journal of pharmaceutics 22, 273-281.

Owens, D.K., Wendt, R., 1969. Estimation of the surface free energy of polymers. Journal of applied polymer science 13, 1741-1747.

Owusu-Nkwantabisah, S., Staudt, C., Lesser, A.J., 2016. Improving flame retardancy and melt processability of polyethersulfone using low molecular weight additives. Journal of Applied Polymer Science 133.

Paasi, J., Nurmi, S., Vuorinen, R., Strengell, S., Maijala, P., 2001. Performance of ESD protective materials at low relative humidity. Journal of Electrostatics 51–52, 429-434.

Packham, D.E., 2003. Surface energy, surface topography and adhesion. International Journal of Adhesion and Adhesives 23, 437-448.

Patel, V.F., Liu, F., Brown, M.B., 2011. Advances in oral transmucosal drug delivery. Journal of Controlled Release 153, 106-116.

Pearnchob, N., Bodmeier, R., 2003. Coating of pellets with micronized ethylcellulose particles by a dry powder coating technique. International Journal of Pharmaceutics 268, 1-11.

Peart, J., 2001. Powder electrostatics: theory, techniques and applications. KONA Powder and Particle Journal 19, 34-45.

Peña, M.A., Reíllo, A., Escalera, B., Bustamante, P., 2006. Solubility parameter of drugs for predicting the solubility profile type within a wide polarity range in solvent mixtures. International Journal of Pharmaceutics 321, 155-161.

Perumal, V., Govender, T., Lutchman, D., Mackraj, I., 2008. Investigating a new approach to film casting for enhanced drug content uniformity in polymeric films. Drug development and industrial pharmacy 34, 1036-1047.

Peterlin, A., 1975. Structural model of mechanical properties and failure of crystalline polymer solids with fibrous structure. International Journal of Fracture 11, 761-780.

Podczeck, F., 1998. Particle-particle adhesion in pharmaceutical powder handling. World Scientific.

Podczeck, F., 1999. Investigations into the reduction of powder adhesion to stainless steel surfaces by surface modification to aid capsule filling. International Journal of Pharmaceutics 178, 93-100.

Prasad, L.K., Keen, J.M., LaFountaine, J.S., Maincent, J., Williams Iii, R.O., McGinity, J.W., 2015. Electrostatic powder deposition to prepare films for drug delivery. Journal of Drug Delivery Science and Technology 30, Part B, 501-510.

Prasad, L.K., LaFountaine, J.S., Keen, J.M., McGinity, J.W., Williams III, R.O., 2016a. Influence of process parameters on the preparation of pharmaceutical films by

electrostatic powder deposition. International Journal of Pharmaceutics (Revision Submitted).

Prasad, L.K., McGinity, J.W., Williams Iii, R.O., 2016b. Electrostatic powder coating: Principles and pharmaceutical applications. International Journal of Pharmaceutics 505, 289-302.

Preis, M., 2015. Orally Disintegrating Films and Mini-Tablets—Innovative Dosage Forms of Choice for Pediatric Use. AAPS PharmSciTech 16, 234-241.

Preis, M., Knop, K., Breitkreutz, J., 2014a. Mechanical strength test for orodispersible and buccal films. International Journal of Pharmaceutics 461, 22-29.

Preis, M., Woertz, C., Schneider, K., Kukawka, J., Broscheit, J., Roewer, N., Breitkreutz, J., 2014b. Design and evaluation of bilayered buccal film preparations for local administration of lidocaine hydrochloride. European Journal of Pharmaceutics and Biopharmaceutics 86, 552-561.

Prodduturi, S., Urman, K., Otaigbe, J., Repka, M., 2007. Stabilization of hot-melt extrusion formulations containing solid solutions using polymer blends. AAPS PharmSciTech 8, E152-E161.

Pu, Y., Mazumder, M., Cooney, C., 2009. Effects of electrostatic charging on pharmaceutical powder blending homogeneity. Journal of Pharmaceutical Sciences 98, 2412-2421.

Pugh, E., 1932. Method of and apparatus for coating articles. US1855869.

Puig, M., Cabedo, L., Gracenea, J.J., Jiménez-Morales, A., Gámez-Pérez, J., Suay, J.J., 2014. Adhesion enhancement of powder coatings on galvanised steel by addition of organo-modified silica particles. Progress in Organic Coatings 77, 1309-1315.

Puri, V., Dantuluri, A.K., Kumar, M., Karar, N., Bansal, A.K., 2010. Wettability and surface chemistry of crystalline and amorphous forms of a poorly water soluble drug. European Journal of Pharmaceutical Sciences 40, 84-93.

Qiao, M., Luo, Y., Zhang, L., Ma, Y., Stephenson, T.S., Zhu, J., 2010a. Sustained release coating of tablets with Eudragit® RS/RL using a novel electrostatic dry powder coating process. International Journal of Pharmaceutics 399, 37-43.

Qiao, M., Zhang, L., Ma, Y., Zhu, J., Chow, K., 2010b. A novel electrostatic dry powder coating process for pharmaceutical dosage forms: Immediate release coatings for tablets. European Journal of Pharmaceutics and Biopharmaceutics 76, 304-310.

Qiao, M., Zhang, L., Ma, Y., Zhu, J., Xiao, W., 2013. A novel electrostatic dry coating process for enteric coating of tablets with Eudragit® L100-55. European Journal of Pharmaceutics and Biopharmaceutics 83, 293-300.

Radebaugh, G.W., Murtha, J.L., Julian, T.N., Bondi, J.N., 1988. Methods for evaluating the puncture and shear properties of pharmaceutical polymeric films. International Journal of Pharmaceutics 45, 39-46.

Radhakrishnan, S., Sonawane, N., Siju, C.R., 2009. Epoxy powder coatings containing polyaniline for enhanced corrosion protection. Progress in Organic Coatings 64, 383-386.

Ramarathnam, G., Libertucci, M., Sadowski, M., North, T., 1992a. Joining of polymers to metal. Welding Journal New York 71, 483-s.

Ramarathnam, G., Libertucci, M., Sadowski, M., North, T., 1992b. Joining of polymers to metal. WELDING JOURNAL-NEW YORK- 71, 483-s.

Ransburg, H.P., Green, H.J., 1941. Apparatus for spray coating articles. US2247963.

Ratanatriwong, P., Barringer, S., 2007. Particle size, cohesiveness and charging effects on electrostatic and nonelectrostatic powder coating. Journal of Electrostatics 65, 704-708.

Rohly, K., Istephanous, N., Belu, A., Untereker, D., Coscio, M., Heffelfinger, J., Thomas, R., Allen, J., Francis, R., Robinson, A., 2003. Effect of time, temperature, and solution composition on the passivation of 316L stainless steel for biomedical applications, Materials Science Forum. Trans Tech Publ, pp. 3017-3022.

Rowe, R., 1983. Modulus enhancement in pigmented tablet film coating formulations. International Journal of Pharmaceutics 14, 355-359.

Rowe, R., Roberts, R., 1992. Simulation of crack propagation in tablet film coatings containing pigments. International journal of pharmaceutics 78, 49-57.

Rowe, R.C., 1988. Adhesion of film coatings to tablet surfaces —a theoretical approach based on solubility parameters. International Journal of Pharmaceutics 41, 219-222.

Rowley, G., 2001. Quantifying electrostatic interactions in pharmaceutical solid systems. International Journal of Pharmaceutics 227, 47-55.

Sakata, Y., Yamaguchi, H., 2011. Improvement of sticking in tablet compaction for tocopherol acetate. Drug development and industrial pharmacy 37, 1049-1059.

Sastry, S.V., Nyshadham, J.R., Fix, J.A., 2000. Recent technological advances in oral drug delivery – a review. Pharmaceutical Science & Technology Today 3, 138-145.

Sauer, D., Cerea, M., DiNunzio, J., McGinity, J., 2013. Dry powder coating of pharmaceuticals: A review. International Journal of Pharmaceutics 457, 488-502.

Sauer, D., McGinity, J.W., 2009. Influence of additives on melt viscosity, surface tension, and film formation of dry powder coatings. Drug development and industrial pharmacy 35, 646-654.

Sauer, D., Watts, A.B., Coots, L.B., Zheng, W.C., McGinity, J.W., 2009. Influence of polymeric subcoats on the drug release properties of tablets powder-coated with pre-plasticized Eudragit® L 100-55. International journal of pharmaceutics 367, 20-28.

Sauer, D., Zheng, W., Coots, L.B., McGinity, J.W., 2007. Influence of processing parameters and formulation factors on the drug release from tablets powder-coated with Eudragit® L 100-55. European Journal of Pharmaceutics and Biopharmaceutics 67, 464-475.

Scheirs, J., Bigger, S.W., Delatycki, O., 1991. Characterizing the solid-state thermal oxidation of poly (ethylene oxide) powder. Polymer 32, 2014-2019.

Shah, U., Zhang, C., Zhu, J., 2006a. Comparison of electrostatic fine powder coating and coarse powder coating by numerical simulations. Journal of electrostatics 64, 345-354.

Shah, U., Zhu, J., Zhang, C., Nother, J., 2006b. Numerical investigation of coarse powder and air flow in an electrostatic powder coating process. Powder technology 164, 22-32.

Shakya, P., Madhav, N.V.S., Shakya, A.K., Singh, K., 2011. Palatal mucosa as a route for systemic drug delivery: A review. Journal of Controlled Release 151, 2-9.

Sharma, R., Trigwell, S., Biris, A.S., Sims, R.A., Mazumder, M.K., 2003. Effect of ambient relative humidity and surface modification on the charge decay properties of polymer powders in powder coating. Industry Applications, IEEE Transactions on 39, 87-95.

Shen, B.d., Shen, C.y., Yuan, X.d., Bai, J.x., Lv, Q.y., Xu, H., Dai, L., Yu, C., Han, J., Yuan, H.l., 2013. Development and characterization of an orodispersible film containing drug nanoparticles. European Journal of Pharmaceutics and Biopharmaceutics 85, 1348-1356.

Sievens-Figueroa, L., Bhakay, A., Jerez-Rozo, J.I., Pandya, N., Romañach, R.J., Michniak-Kohn, B., Iqbal, Z., Bilgili, E., Davé, R.N., 2012. Preparation and characterization of hydroxypropyl methyl cellulose films containing stable BCS Class II drug nanoparticles for pharmaceutical applications. International Journal of Pharmaceutics 423, 496-508.

Sims, R., Mazumder, M., Biris, A., Sharma, R., Kumar, D., 2000. Effect of electrical resistivity on the adhesion and thickness of electrostatically deposited powder layers, Industry Applications Conference, 2000. Conference Record of the 2000 IEEE. IEEE, pp. 820-823.

Sims, R., Mazumder, M., Liu, X., Chok, W., Mountain, J., Wankum, D., Pettit, P., Chasser, T., 2001. Electrostatic effects on first pass transfer efficiency in the application of powder coatings. Industry Applications, IEEE Transactions 37, 1610-1617.

Slavkova, M., Breitkreutz, J., 2015. Orodispersible drug formulations for children and elderly. European Journal of Pharmaceutical Sciences 75, 2-9.

Smikalla, M., Mescher, A., Walzel, P., Urbanetz, N.A., 2011. Impact of excipients on coating efficiency in dry powder coating. International Journal of Pharmaceutics 405, 122-131.

Sriamornsak, P., Kennedy, R.A., 2006. A novel gel formation method, microstructure and mechanical properties of calcium polysaccharide gel films. International Journal of Pharmaceutics 323, 72-80.

Staniforth, J.N., Grosvenor, M.P., 1992. Improvements in or relating to electrostatic coating of substrates of medicinal products. WO1992014451.

Staniforth, J.N., Grosvenor, M.P., 1995. Electrostatic coating of substrates of medicinal products. Google Patents.

Stark, J., Zhang, J., Sharma, R., Adams, A., Mazumder, M., 2008. Measurement of Electrostatic Charge and Aero-dynamic Diameter of Sub-Micron Particles by the ESPART Analyzer, Proc. ESA Annual Meeting on Electrostatics, pp. 1-6.

Stegemann, S., Ecker, F., Maio, M., Kraahs, P., Wohlfart, R., Breitkreutz, J., Zimmer, A., Bar-Shalom, D., Hettrich, P., Broegmann, B., 2010. Geriatric drug therapy: Neglecting the inevitable majority. Ageing Research Reviews 9, 384-398.

Stegemann, S., Gosch, M., Breitkreutz, J., 2012. Swallowing dysfunction and dysphagia is an unrecognized challenge for oral drug therapy. International Journal of Pharmaceutics 430, 197-206.

Subramanian, V., van Ooij, W.J., 1999. Silane based metal pretreatments as alternatives to chromating: Shortlisted. Surface Engineering 15, 168-172.

Sudhakar, Y., Kuotsu, K., Bandyopadhyay, A.K., 2006. Buccal bioadhesive drug delivery — A promising option for orally less efficient drugs. Journal of Controlled Release 114, 15-40.

Sun, Y., Bao, H.-D., Guo, Z.-X., Yu, J., 2009. Modeling of the Electrical Percolation of Mixed Carbon Fillers in Polymer-Based Composites. Macromolecules 42, 459-463.

Suwardie, H., Wang, P., Todd, D.B., Panchal, V., Yang, M., Gogos, C.G., 2011. Rheological study of the mixture of acetaminophen and polyethylene oxide for hot-melt extrusion application. European Journal of Pharmaceutics and Biopharmaceutics 78, 506-512.

Takizawa, C., Gemmell, E., Kenworthy, J., Speyer, R., 2016. A Systematic Review of the Prevalence of Oropharyngeal Dysphagia in Stroke, Parkinson's Disease, Alzheimer's Disease, Head Injury, and Pneumonia. Dysphagia 31, 434-441.

Terebesi, I., Bodmeier, R., 2010. Optimised process and formulation conditions for extended release dry polymer powder-coated pellets. European Journal of Pharmaceutics and Biopharmaceutics 75, 63-70.

Theodore, A., Labana, S., 1973. Powdered coating compositions containing glycidyl methacrylate copolymers with anhydride crosslinking agents and flow control agent. Google Patents.

Tousey, M.D., 2003. Sticking and picking: some causes and remedies. Tablets and capsules.

Tseng, D., Donahue, W., Parsons, B.A., 2002. Polymer coated stent. US6364903.

Tzafriri, A.R., Groothuis, A., Price, G.S., Edelman, E.R., 2012. Stent elution rate determines drug deposition and receptor-mediated effects. Journal of Controlled Release 161, 918-926.

Uhlmann, P., Grundke, K., Influence of additives on interfacial phenomena during film formation of powder coatings. Journal of Coatings Technology 73, 59-65.

Visser, J.C., Dohmen, W.M.C., Hinrichs, W.L.J., Breitkreutz, J., Frijlink, H.W., Woerdenbag, H.J., 2015. Quality by design approach for optimizing the formulation and physical properties of extemporaneously prepared orodispersible films. International Journal of Pharmaceutics 485, 70-76.

Waknis, V., Chu, E., Schlam, R., Sidorenko, A., Badawy, S., Yin, S., Narang, A.S., 2014. Molecular Basis of Crystal Morphology-Dependent Adhesion Behavior of Mefenamic Acid During Tableting. Pharmaceutical research 31, 160-172.

Wang, F., 2005. title. Ph.D., The University of Western Ontario (Canada), Ann Arbor.

Ward, I.M., Sweeney, J., 2012. Mechanical properties of solid polymers. John Wiley & Sons.

Watanabe, H., Ghadiri, M., Matsuyama, T., Ding, Y.L., Pitt, K.G., Maruyama, H., Matsusaka, S., Masuda, H., 2007. Triboelectrification of pharmaceutical powders by particle impact. International Journal of Pharmaceutics 334, 149-155.

Weiss, K.D., 1997. Paint and coatings: A mature industry in transition. Progress in Polymer Science 22, 203-245.

Whiteman, M., Hallett, M.D., Feather, D.H., Nelson, D.H., Gazza, J.M., 2006. Electrostatic application of powder material to solid dosage forms utilizing an electrically conductive shield. US7144597.

Wicks, Z.W., Jones, F.N., Pappas, S.P., Wicks, D.A., 2007. Organic coatings: science and technology, 3rd ed. Wiley-Interscience, Hoboken, N.J.

Wong, J., Chan, H.-K., Kwok, P.C.L., 2013. Electrostatics in pharmaceutical aerosols for inhalation. Therapeutic Delivery 4, 981-1002.

Wong, J., Kwok, P., Noakes, T., Fathi, A., Dehghani, F., Chan, H.-K., 2014. Effect of Crystallinity on Electrostatic Charging in Dry Powder Inhaler Formulations. Pharmaceutical research 31, 1656-1664.

Wong, J., Kwok, P.C.L., Chan, H.-K., 2015. Electrostatics in pharmaceutical solids. Chemical Engineering Science 125, 225-237.

Xi, J., Si, X., Longest, W., 2014. Electrostatic Charge Effects on Pharmaceutical Aerosol Deposition in Human Nasal–Laryngeal Airways. Pharmaceutics 6, 26-35.

Yang, M., Wang, P., Gogos, C., 2013. Prediction of acetaminophen's solubility in poly(ethylene oxide) at room temperature using the Flory–Huggins theory. Drug Development and Industrial Pharmacy 39, 102-108.

Yang, M., Wang, P., Huang, C.-Y., Ku, M.S., Liu, H., Gogos, C., 2010. Solid dispersion of acetaminophen and poly(ethylene oxide) prepared by hot-melt mixing. International Journal of Pharmaceutics 395, 53-61.

Yang, M., Wang, P., Suwardie, H., Gogos, C., 2011. Determination of acetaminophen's solubility in poly(ethylene oxide) by rheological, thermal and microscopic methods. International Journal of Pharmaceutics 403, 83-89.

Yang, Q., Ma, Y., Zhu, J., 2015. Applying a novel electrostatic dry powder coating technology to pellets. European Journal of Pharmaceutics and Biopharmaceutics 97, Part A, 118-124.

Young, T., 1805. An Essay on the Cohesion of Fluids. Philosophical Transactions of the Royal Society of London 95, 65-87.

Yousuf, S., Barringer, S.A., 2007. Modeling nonelectrostatic and electrostatic powder coating. Journal of Food Engineering 83, 550-561.

Yurteri, C.U., Mazumder, M.K., Grable, N., Ahuja, G., Trigwell, S., Biris, A.S., Sharma, R., Sims, R.A., 2002. Electrostatic Effects on Dispersion, Transport, and Deposition of Fine Pharmaceutical Powders: Development of an Experimental Method of Quantitative Analysis. Particulate Science & Technology 20, 59.

Zhang, H., Zhang, J., Streisand, J., 2002. Oral Mucosal Drug Delivery. Clin Pharmacokinet 41, 661-680.

Zhang, J., Ebbens, S., Chen, X., Jin, Z., Luk, S., Madden, C., Patel, N., Roberts, C.J., 2006. Determination of the Surface Free Energy of Crystalline and Amorphous Lactose by Atomic Force Microscopy Adhesion Measurement. Pharmaceutical research 23, 401-407.

Zhu, J., Luo, Y., Ma, Y., Zhang, H., 2007. Direct coating solid dosage forms using powdered materials. US20070128274.

Zografi, G., Tam, S.S., 1976. Wettability of Pharmaceutical Solids: Estimates of Solid Surface Polarity. Journal of Pharmaceutical Sciences 65, 1145-1149.